

Dissolved Carbon Dioxide Driven Repeated Batch Fermentation

A Thesis submitted to the College of Graduate Studies and Research in partial
fulfillment of the requirements for the degree of

Master of Science

In the Department of Chemical and Biological Engineering,
University of Saskatchewan,
Saskatoon, Saskatchewan

By

Sijing Feng

©Copyright Sijing Feng, November, 2014. All rights reserved

PERMISSION TO USE

I agree that the Libraries of University of Saskatchewan may make this thesis, which presented in partial fulfillment of the requirements for a Master of Science degree from this University, freely available for inspection. I further agree that the permission to copy this thesis, in whole or in part, for scholarly purposes only be granted by this thesis advisor. It is understood that any copying, publication or use of this thesis or part thereof for financial gain shall not be permitted without this thesis supervisor's written consent. It is also understood that due recognition shall be given to me as well as to the University of Saskatchewan for any scholarly use by using the materials in this thesis in whole or in part.

All requests for permission to use the materials in this thesis in whole or in part should be addressed to:

Head of the Department of Chemical & Biological Engineering

University of Saskatchewan

57 Campus Drive, Saskatoon, SK,

Saskatoon, SK, S7N 5A9

Canada

ABSTRACT

Dissolved carbon dioxide driven repeated batch fermentation has been performed under four glucose concentrations: ~ 150 , ~ 200 , ~ 250 and ~ 300 g glucose l^{-1} , with three dissolved carbon dioxide (DCO_2) control conditions: without DCO_2 control, with DCO_2 control at 750 and 1000 mg l^{-1} levels. No residual glucose was observed under all performed fermentation conditions, and the repeated batch fermentation system could be operated by a computer as self-cycling system. The collected fermentation results presented that, under the same feeding concentration, ethanol concentration in the presence of DCO_2 control was significantly lower than that in the absence of DCO_2 control; and a higher biomass concentration in the presence of control was observed in this comparison as well. A higher biomass concentration resulted in a shorter fermentation time, which contributed to a higher ethanol production rate. The highest final ethanol concentration was observed as 113.5 g l^{-1} at 1000 mg DCO_2 l^{-1} control level under ~ 300 g glucose l^{-1} condition, where the lowest ethanol production rate of 1.18 g $\text{l}^{-1} \text{ h}^{-1}$ was observed. The highest ethanol production rate was 4.57 g $\text{l}^{-1} \text{ h}^{-1}$ and its corresponding ethanol concentration was 66.7 g ethanol l^{-1} at 1000 mg l^{-1} DCO_2 control level under ~ 200 g glucose l^{-1} condition. For all fermentation conditions, the viabilities of yeast at the end of fermentation were maintained at near 90% where their corresponding final ethanol concentrations were lower than 100 g l^{-1} . As soon as the final ethanol concentration at the end of each cycle was greater than 110 g l^{-1} , its corresponding viability decreased to $\sim 70\%$. The ethanol conversion efficiency was maintained at $\sim 90\%$ and $\sim 65\%$ in the absence and presence of DCO_2 control, respectively. Based on the changing of biomass concentration profiles in the stabilized cycles, two cell growth phases could be identified in the absence of DCO_2 control, and only one cell growth phase was noticeable in the presence of DCO_2 control cases. Meanwhile, a sudden decline of DCO_2 readings at the end of fermentation was constantly observed in both of in the absence and in the presence of DCO_2 control cases, which resulted in developing two control algorithms to determine self-cycling time. Comparison of

carbon balance analysis between in the absence and in the presence of DCO₂ control suggested that the availability of DCO₂ control might alter the metabolic flow during fermentation; and the figure of ethanol concentration against fermentation time illustrated that the changing of DCO₂ control level did not affect fermentation results, significantly. Moreover, comparisons of ethanol production rate between different processes and different initial glucose concentrations concluded that the ethanol production rate in the presence of DCO₂ control was generally higher than that in the absence of DCO₂ control under the same glucose concentration; and the ethanol production rate was decreased with the increasing of glucose concentration under the same DCO₂ control condition. The experiment results were scaled up to 10⁶ L as a sample analysis in production scale, which suggested that the fermentation with ~200 g glucose l⁻¹ feeding concentration in the absence of DCO₂ controlled would provide best profits in the all fermentation conditions.

ACKNOWLEDGEMENT

First and foremost, I would like to express my gratitude to my thesis advisor, Dr. Yen-Han Lin, for his guidance and support throughout the course of my project. He has been supportive not only by providing a research assistantship since I was an undergraduate student, but also academically and emotionally inspire my interests in biochemical engineering study. I also would like to thank all my thesis committee: Dr. Mehdi Nemati, Dr. Jian Peng and Dr. Takuji Tanaka, for their encouragements, insightful comments and suggestions for my reports and presentations. I sincerely thank the staffs in the Department of Chemical and Biological Engineering, Mr. Rlee Prokopishyn, Mr. Richard Blondin and Ms. Heli Eunike, for their technical expertise.

The mutual discussions between lab partners provided me invaluable knowledge on different subjects, which were not only limited in my thesis project. I would not be able to accomplish my work without the help from these friends. Therefore, I also want to appreciate my lab partners: Shyam Srinivasan, Yun Bai and Shu-Jyuan Li. Thank you very much for keeping a happy lab culture throughout the course of my four years study.

Last but not the least, I would like to thank my parents for supporting my undergraduate as well as graduate study financially and mentally in the last six years. Without your help, it would be very difficult to reach current achievements in such a short time.

TABLE OF CONTENTS

PERMISSION TO USE.....	i
ABSTRACT.....	ii
ACKNOWLEDGEMENT	iv
TABLE OF CONTENTS.....	v
LIST OF TABLES	ix
LIST OF FIGURES	x
ABBREVIATION.....	xiii
NOMENCLATURE	xiv
CHAPTER 1 INTRODUCTION	1
1.1 Background	1
1.2 Thesis organization.....	2
CHAPTER 2 LITERATURE REIVEW	3
2.1 Review of Biofuel.....	3
2.2 Yeast Metabolism	5
2.2.1 Glycerol and trehalose metabolism	8
2.2.2 Roles of oxygen and carbon dioxide in ethanol fermentation.....	10
2.3 Review of Very-high-gravity fermentation	11
2.3.1 Very-high-gravity fermentation technology.....	11
2.3.2 The challenges of very-high-gravity fermentation.....	12
2.3 Fermentation process review	13
2.3.1 Batch process.....	13

2.3.2 Continuous process	15
2.3.3 Fed-batch process	16
2.3.4 Repeated-batch process	17
2.4 Online measurements and bioprocess optimization	19
2.4.1 Temperature, pH and dissolved oxygen online measurements	20
2.4.2 Redox potential online measurements	21
2.4.3 Carbon dioxide online measurements	22
2.5 Knowledge Gaps.....	24
2.6 Objectives	25
CHAPTER 3 EXPERIMENTAL MATERIALS AND METHODS	26
3.1 Experimental design	26
3.2 Strain and growth media.....	27
3.3 Repeated batch system.....	28
3.4 Fermentation and process control.....	31
3.4.1 Glucose feeding strategies.....	31
3.4.2 Fermentation conditions	31
3.4.3 Determination of repeated cycles	31
3.4.4 Control of DCO ₂ level.....	32
3.5 Online measurements and sample analysis	32
3.5.1 Online measurements	32
3.5.2 Sample analysis	33
CHAPTER 4 RESULTS AND DISSCUSION.....	34

4.1 Reproducibility of dissolved carbon dioxide driven repeated batch fermentation	34
4.1.1 Characteristics of dissolved carbon dioxide driven repeated batch in the absence of DCO ₂ control under high-gravity conditions	37
4.1.2 Characteristics of dissolved carbon dioxide driven repeated batch in the presence of DCO ₂ control under HG and VHG conditions	39
4.2 Mode of dissolved carbon dioxide driven repeated batch fermentation.....	41
4.2.1 Dissolved carbon dioxide profiles during repeated batch fermentation	42
4.2.2 Initiating a new cycle in the presence and absence of DCO ₂ control ..	46
4.3 Effects of DCO ₂ control availability and DCO ₂ control level on self-cycling period and fermentation results	49
4.3.1 Approximate analysis of DCO ₂ driven repeated batch fermentation in the absence and presence of DCO ₂ control	49
4.3.2 Effects of dissolved carbon dioxide levels on self-cycling period.....	54
4.4 Applicability of DCO ₂ -driven and DCO ₂ -controlled repeated batch fermentation	59
4.4.1 Comparison of ethanol production rate under high-gravity and very-high-gravity conditions	59
4.4.2 Evaluation and comparison of ethanol productivities in DCO ₂ driven and controlled repeated batch fermentation	62
CHAPTER 5 CONCLUSIONS	67
CHAPTER 6 RECOMMENDATIONS.....	69
CHAPTER 7 REFERENCE	71
APPENDIX A.....	84
A1-Raw experimental data figures	84

A2-Calibration curves.....	97
APPENDIX B	101

LIST OF TABLES

Table 3.1 Summary of experimental design	26
Table 3.2 Concentration and supply resources of stock solution	28
Table 4.1 Summary of repeated batch fermentation in the absence of DCO ₂ control .	37
Table 4.2 Summary of repeated batch fermentation in the presence of DCO ₂ control	39
Table 4.3 Comparison between fitted results from Eqn (7) and Eqn (8)	58
Table 4.4 Comparisons in ethanol production rate between different feeding glucose concentrations through batch and repeated batch processes	60
Table 4.5 Comparison in ethanol production rate between different feeding glucose concentrations through continuous process	61
Table 4.6 Glucose utilization, ethanol and biomass productivity among four initial glucose feeding concentrations in the absence and presence of DCO ₂ control	64
Table A1.1 Correlation between fermentation condition and figure number	84

LIST OF FIGURES

Figure 2.1 Glycolytic pathway in yeast. Adopted from Kresnowati et al.(2006)	7
Figure 2.2 Metabolic pathway for trehalose synthesis form glucose in yeast. Adopted from Kresnowati et al.(2006)	8
Figure 2.3 Metabolic pathway for glycerol synthesis form glucose in yeast. Adopted from Kresnowati et al.(2006)	9
Figure 3.1 Illustration of experimental set-up for repeated batch fermentation process	30
Figure 4.1 Profiles of glucose and ethanol concentration, DCO ₂ , and biomass concentration under ~200 g glucose l ⁻¹ a) in the absence of DCO ₂ control b) and in the presence of DCO ₂ control at 750 mg l ⁻¹ DCO ₂ control level	36
Figure 4.2 Profiles of glucose, ethanol, biomass and DCO ₂ concentration in the absence of DCO ₂ control of a) batch process and b) stablized cycle in repeated batch process for intital concentratiton of ~200 g glucose l ⁻¹	43
Figure 4.3 Profiles of glucose, ethanol, biomass and DCO ₂ concentration at 750 mg l ⁻¹ DCO ₂ control level of a) batch process and b) stablized cycle in repeated batch process for intital concentratiton of ~250 g glucose l ⁻¹	45
Figure 4.4 Profiles of glucose, ethanol, biomass and DCO ₂ concentration in the absence of DCO ₂ control in the one of stablized cycles through repeated batch process for intital concentratiton of ~200 g glucose l ⁻¹	46
Figure 4.5 Profiles of glucose, ethanol, biomass and DCO ₂ concentration at 750 mg DCO ₂ l ⁻¹ control level in the one of stablized cycles through repeated batch process for intital concentratiton of ~200 g glucose l ⁻¹	48
Figure 4.6 Comparsons of carbon mole numbers in produced ethanol, CO ₂ , biomass and other metabolites in the different femrentaiton conditions. Condition 1-3 were under ~150 g glucose l ⁻¹ in the absence of DCO ₂ control, contorl at 750 mg l ⁻¹ and at 1000 mg l ⁻¹ level, respectively. Condition 4-6 were under ~200 g glucose l ⁻¹ in the absence of DCO ₂ control, contorl at 750 mg l ⁻¹ and at 1000 mg l ⁻¹ level, respectively. Condition 7-8 were under ~250 g glucose l ⁻¹ contorl at 750 mg l ⁻¹ and at 1000 mg l ⁻¹ level, respectively. Condition 9-10 were under ~300 g glucose l ⁻¹ contorl at 750 mg l ⁻¹ and at 1000 mg l ⁻¹ level, respectively.	51

Figure 4.7 Profiles of final ethanol concentration of each cycle against its corresponding fermentation time during repeated batch fermentation in the presence of DCO ₂ control at 1000 mg l ⁻¹ and 750 mg l ⁻¹	55
Figure A1.1 Raw data of ~150 g glucose l ⁻¹ feeding concentration in the absence of DCO ₂ control by using independent feeding method	85
Figure A1.2 Raw data of ~150 g glucose l ⁻¹ feeding concentration DCO ₂ control at 1000 mg l ⁻¹ level by using independent feeding method	86
Figure A1.3 Raw data of ~150 g glucose l ⁻¹ feeding concentration DCO ₂ control at 750 mg l ⁻¹ level by using independent feeding method	87
Figure A1.4 Raw data of ~200 g glucose l ⁻¹ feeding concentration in the absence of DCO ₂ control by using independent feeding method	88
Figure A1.5 Raw data of ~200 g glucose l ⁻¹ feeding concentration DCO ₂ control at 1000 mg l ⁻¹ level by using independent feeding method	89
Figure A1.6 Raw data of ~200 g glucose l ⁻¹ feeding concentration DCO ₂ control at 750 mg l ⁻¹ level by using independent feeding method	90
Figure A1.7 Raw data of ~250 g glucose l ⁻¹ feeding concentration DCO ₂ control at 1000 mg l ⁻¹ level by using independent feeding method	91
Figure A1.8 Raw data of ~250 g glucose l ⁻¹ feeding concentration DCO ₂ control at 750 mg l ⁻¹ level by using independent feeding method	92
Figure A1.9 Raw data of ~300 g glucose l ⁻¹ feeding concentration DCO ₂ control at 1000 mg l ⁻¹ level by using independent feeding method	93
Figure A1.10 Raw data of ~300 g glucose l ⁻¹ feeding concentration DCO ₂ control at 750 mg l ⁻¹ level by using independent feeding method	94
Figure A1.11 Raw data of DCO ₂ control at 1000 mg l ⁻¹ level by using continuous feeding method	95
Figure A1.12 Raw data of DCO ₂ control at 750 mg l ⁻¹ level by using continuous feeding method	96
Figure A2.1 Calibration curve for biomass	96
Figure A2.2 Calibration curve for glucose	97
Figure A2.3 Calibration curve for ethanol	98

Figure A2.4 Calibration curve for glycerol	99
--	----

ABBREVIATION

CSTR	Continuous stirred-tank reactor
DCO ₂	Dissolved carbon dioxide
DAS	Data acquisition system
DO	Dissolved oxygen
HG	High gravity
MCCF	Multistage continuous culture fermentation technologies
Redox	Reduction-oxidation
SCF	Self-cycling fermentation
VHG	Very high gravity

NOMENCLATURE

B_p	Biomass (g)
C_b	Biomass concentration (g l^{-1})
C_e	Ethanol concentration (g l^{-1})
C_g	Glucose concentration (g l^{-1})
C_{gly}	Glycerol concentration (g l^{-1})
D	Dilution rate (h^{-1})
E_p	Ethanol (g)
G_c	Glucose (g)
M_{tcb}	Carbon mole utilization rate to produce biomass ($\text{mole h}^{-1} \text{l}^{-1}$)
M_{tcc}	Carbon mole utilization rate to produce carbon dioxide ($\text{mole h}^{-1} \text{l}^{-1}$)
M_{tce}	Carbon mole utilization rate to produce ethanol ($\text{mole h}^{-1} \text{l}^{-1}$)
M_{tcg}	Glucose carbon mole utilization rate ($\text{mole h}^{-1} \text{l}^{-1}$)
M_{tcgly}	Carbon mole utilization rate to produce glycerol ($\text{mole h}^{-1} \text{l}^{-1}$)
M_{to}	Carbon mole utilization rate to produce other metabolites ($\text{mole h}^{-1} \text{l}^{-1}$)
R_e	Ethanol production rate ($\text{g l}^{-1} \text{h}^{-1}$)
R_{Eb}	Ethanol production rate in batch process ($\text{g l}^{-1} \text{h}^{-1}$)
R_{Ec}	Ethanol production rate in continuous process ($\text{g l}^{-1} \text{h}^{-1}$)
R_{Er}	Ethanol production rate in repeated batch process ($\text{g l}^{-1} \text{h}^{-1}$)
T_d	Down time (h)
T_f	Fermentation time (h)
T_{sf1}	Calculated fermentation time from Eqn (8) (h)
T_{sf2}	Calculated fermentation time from Eqn (9) (h)
V_w	Working volume (l)

CHAPTER 1 INTRODUCTION

1.1 Background

In order to counter the finite of global crude oil reserve, the study of fossil fuel substitute has been initiated and continued since Arab oil embargos in 1970s. As one of renewable and environment friendly energy, biomass and biofuel, which were consisted as high potential replacements of crude oil in the future, have drawn attentions and enthusiasms from researchers as well as the public.

However, the developments of shale oil in the U.S. in the recent years dramatically changed the picture of energy market. According to “Annual energy outlook 2014” from U.S. Department of Energy (U.S. Energy Information Administration, 2014a), the production of shale oil, worldwide, was expected to increase from 2.40 million barrels per day in 2012 to 7.28 million barrels per day in 2040. Comparing with the worldwide predictions of biofuel production in the same report, as “liquids from renewable sources”, 1.34 million barrels biofuel was produced every day in 2012 and a production of 2.48 million barrels per day was expected in 2040. The predicated shale oil production was three times of the biofuel in 2040. With the considerations of over 2.9 trillion barrels of recoverable shale oil reserves being estimated in 2003 (Dyni, 2006), the shale oil was more prospective to be the solution of energy crisis instead of biofuel, temporarily.

On the other hand, there has been a lot of debate on environmental impacts of the shale oil industries (Brendow, 2003; Lu et al., 2014; Vidic, Brantley et al., 2013) and profitability in shale oil production (Johnson et al., 2004; Schmidt, 2003). Moreover, the estimated quantity of shale oil reserve has been challenged as well. The estimated amount of recoverable shale oil buried in the Monterey shale deposits has been slashed by 96% and reduced from 13.7 billion barrels to 600 million barrels in June, 2014 (U.S. Energy Information Administration, 2014b). The opinion about shale oil being the best replacement of crude oil turned to uncertain, due to the lasted updated

information from governments and institutions. Hence, it was difficult to propose that the shale oil was either a temporary bubble or an energy revolution that significantly changing the global energy outlook. Consequently, the biofuel study was still important and necessary for a long term sustainable energy development.

In this thesis, the development of a novel bioethanol fermentation process is presented. This process utilizes fermentation dissolved CO_2 to monitor the progress of fermentation and is subsequently used to control the fermentation operation under repeated batch operating mode. As a result, a self-cycling bioethanol fermentation process is developed.

1.2 Thesis organization

Chapter 1 was the introduction of the thesis, which provided background information of bio-energy, and a description of thesis's organization.

Chapter 2 presented the current literature review of biofuel ethanol production and bioprocess optimization. The review included biofuel, yeast metabolism, very-high-gravity fermentation technologies, fermentation processes and online measurements technologies in bioprocess optimization. The knowledge gaps as well as the objectives of this thesis were also presented in this chapter.

Chapter 3 stated the experimental design the materials and methodology used in this project.

Chapter 4 discussed the experimental results, an overall mathematical analysis and estimations of ethanol productivities under different fermentation conditions.

Chapter 5 drew the conclusions based on the experimental findings.

Chapter 6 provided recommendations toward improving ethanol production efficiency and tuning PID DCO_2 controller.

CHAPTER 2 LITERATURE REIVIEW

Six sections were presented in this Chapter, which included four review sections from 2.1 to 2.4, knowledge gap as Section 2.5 and Objectives as Section 2.6. While some background information and technologies of biofuel were reviewed in Section 2.1, a review of yeast metabolism was presented in Section 2.2. Meanwhile, the fermentation process and online measurements and bioprocess optimization were also reviewed in this Chapter as Section 2.3 and 2.4, respectively.

2.1 Review of Biofuel

As some good examples to provide background information related to biofuel, a short review about biogas, biodiesel and bioethanol was presented in the next several paragraphs.

Biogas was produced from wastes, residues, and energy corps through anaerobic digestion. It has successfully replaced fossil fuels in applications such as: cooking, heating, and generating electricity, worldwide. It was also considered as one of the most energy-efficient and environmental friendly bioenergy production technologies (Weiland, 2010). A significantly increasing of biogas production has been reported in Europe as well as China, such as: Europe produced over 12000 Ktoe (K tonne of oil equivalent toe) biogas electricity generation in 2013 (Ryan & Jiang, 2013), and in the same year more than 20 billion cubic meters biogas was produced in China as the resource for heat and power (Flach et al., 2014). The biogas was produced through methane fermentation, which was a complex process including four phases: hydrolysis, acidogenesis, acetogenesis/dehydrogenation, and methanation (Gerardi, 2003). Different microorganisms were carried out in the four individual degradation steps with a syntrophic interrelation and unique requirements on the environment (Angelidaki et al., 1993). Therefore, the biogas production process technology was much more complex than ethanol fermentation. Biogas production process could be classified as wet and dry process. While wet digestion was operated

with lower than 10% solids concentration through continuous process, dry digestion fermented up to 70% solids concentration by using energy crops through batch process (Weiland, 2010). Due to the complexity of methane fermentation process, the improvements of biogas production were still necessary. Several articles (Lindorfer et al., 2008; Michel et al., 2010; Peidong et al., 2009; Ward et al., 2008) suggested researchers should focus on the influence of microbial community on fermentation stability and also develop new technologies for process monitoring and control.

Biodiesel was an alternative of diesel fuel, which was produced from a transesterification reaction between alcohol and vegetable oils (Berchmans & Hirata, 2008; Kaya et al., 2009; Sahoo & Das, 2009), animal fats (Goodrum et al., 2003; Saraf & Thomas, 2007) or even used cooking oils (Issariyakul et al., 2008). The application of catalysis in transesterification reaction significantly reduced the temperature and pressure during the reaction and improved the reaction efficiency. While base-catalysis was widely applied in commercial biodiesel production (Gerpen, 2005), acid-catalysis (Nelson et al., 1996) and enzyme-catalysis (Nelson et al., 1996) were also proposed by several researchers. However, the low transesterification reaction rate by using acid-catalysis and the high price and low efficiency by using enzyme-catalysis limited their industrial applications. In the most typical industrial biodiesel production cases, alcohol reacted with oil by 3:1 ratio at 60 °C under 1 atm pressure. The excessed alcohol would be recycled into system for further production. The batch process was used in the smaller plants and the continuous process was selected by large plants, which had an annual productivity of 4 million liters (Ma & Hanna, 1999). The continuous process consisted of two continuous stirred-tank reactors or plug flow reactors. The first continuous reactor normally provided 80% efficiency and the second reactor completed reaction with over 99% efficiency (Leung et al., 2010).

Ethanol was one of most traditional fossil fuel replacements and its bio-production method has been fully studied and well developed over decades. Since the bioethanol production supplements were mainly from sugar and starch feedstocks (Bai et al., 2008), the criticism of bioethanol in feed, food, fuel and price has been made in recent years, which resulted in the

development of cellulosic ethanol, as second generation bioethanol (Lal, 2007). The differences of bioethanol production technologies between different feedstocks were only limited in pre-treatment processes. The pre-treatment process was used to convert the feedstock into glucose, as carbon resource, to supply yeast for ethanol fermentation (Hill et al., 2006; Wooley et al., 1999). Therefore, the study in fermentation process optimization, as proposed in this thesis, not only could use to improve bioethanol production by using food crops but also, was capable of applying in cellulosic ethanol production in the future.

2.2 Yeast Metabolism

Yeast metabolism was a circular process of all the physical and chemical reactions, where all rephrase metabolites were synthesized, maintained and degraded in order to complete energy conversion in the living cells. The cells' metabolism referred to two categories: catabolism and anabolism. While the catabolism was an oxidative process, where the energy was generated by degrading complex organic substances, the anabolism was a reductive process, where the energy was consumed in order to synthesize new molecules to maintain the function and structure of cells. Either degrading complex substances or synthesizing new molecules required electrons exchanging between metabolites, which was predominantly mediated by redox cofactors, such as: NAD^+ or NADH and NADP^+ or NADPH (Walker, 1998). The coenzyme system of NAD(H) was primarily observed in the catabolism with a ratio value of $\frac{\text{NAD}^+}{\text{NADH}}$ near 1000 to maintain the trend of metabolite oxidation. Meanwhile, the coenzyme system of NADP(H) was normally discovered in the anabolism. The favors of metabolite reduction in anabolism were sustained by 0.01 value of $\frac{\text{NADP}^+}{\text{NADHP}}$ ratio (Voet et al., 1999).

A simplified representation of glycolytic pathway, fermentative pathway, respiratory pathway, trehalose and glycerol metabolic pathways were shown in Figure 2.1. At the first stage of respiro-fermentative metabolism, yeast cells used glycolysis to convert glucose into pyruvate. In this

pathway, one mole of glucose produced two moles of ATP and two moles of NADH. Once pyruvate was produced, yeast could use different modes of metabolism to generate energy based on the availability of oxygen. Under aerobic condition, pyruvate was completely oxidized by oxygen, as an electron acceptor, to Acetyl-CoA and ended as carbon dioxide with ATP production through TCA cycle. The biomass production from ATP was prioritized over production of ethanol in aerobic route (Daoud & Searle, 1990). On the other hand, when the oxygen supplement was limited, pyruvate was converted to acetaldehyde and carbon dioxide first, and followed by electrons exchanging between NADH and NAD^+ , which resulted in ethanol as final product. Moreover, some metabolites, such as trehalose and glycerol, were also produced during the respiro-fermentative metabolism in response to the high level of osmotic pressure and ethanol toxicity (Ribeiro et al., 1999).

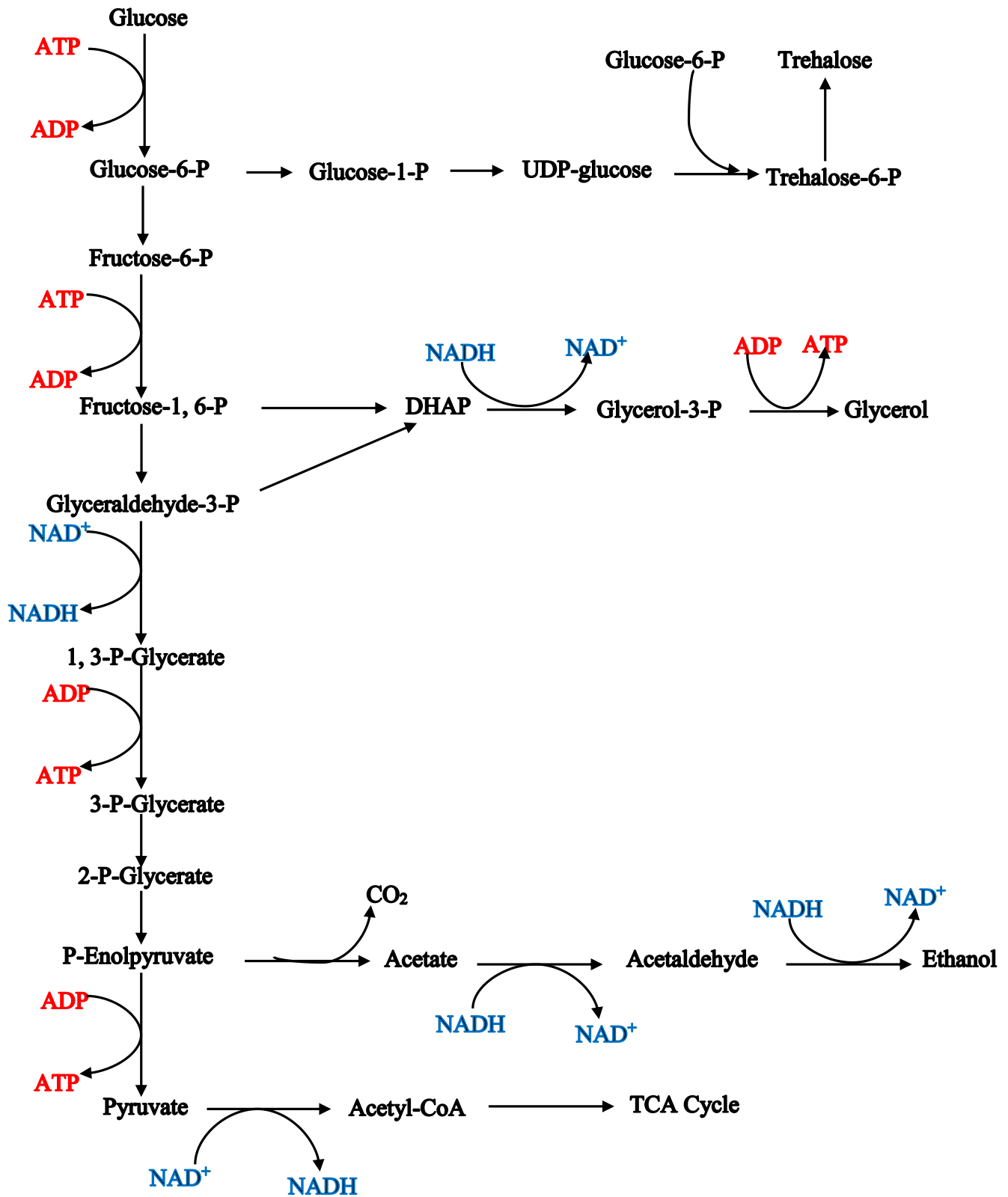


Figure 2.1 Glycolytic pathway in yeast. Adopted from Kresnowati et al.(2006)

2.2.1 Glycerol and trehalose metabolism

During the VHG ethanol fermentation, yeast produced glycerol and trehalose, as by-product, to balance redox potential inside the cells as well as to act as compatible solute to protect cells from high levels of osmotic stress and ethanol toxicity (Bell et al., 1998; Cronwright et al., 2002; Hounsa et al., 1998; Van Dijck et al., 1995). Figure 2.2 and 2.3 presented the trehalose and glycerol pathway, respectively.

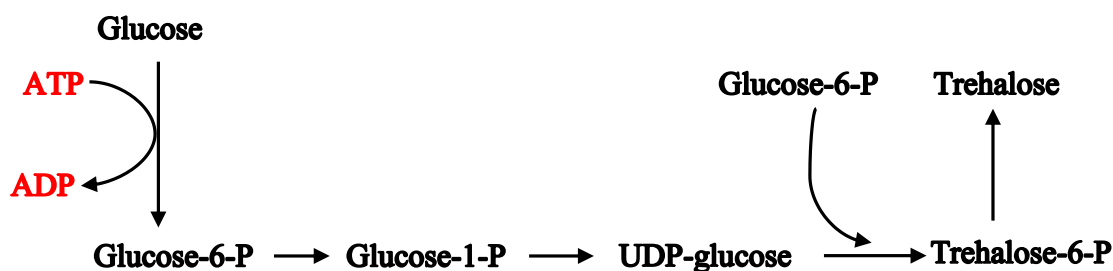


Figure 2.2 Metabolic pathway for trehalose synthesis from glucose in yeast. Adopted from Kresnowati et al.(2006)

As showing in Figure 2.2, trehalose was biosynthesized with a two-step process, which trehalose-6-P was converted from the reaction between UDP-glucose and glucose-6-P, and then trehalose-6-P reacted with water to synthesize trehalose (François & Parrou, 2001). Under the initial stages of VHG condition, the intercellular nutrient transporting through cell membranes was limited by osmosis effects, and the osmosis effects could be reduced by trehalose. Hence, trehalose was normally considered as an osmo-protectant under high osmotic stress (Bell et al., 1998; Hounsa et al., 1998; Van Dijck et al., 1995). While trehalose played a critical role to protect cells from different stress conditions in the most studies, some other publications also suggested an effect in glycolysis from trehalose biosynthesis. Hohmann et al. (1996) reported a restriction of influx of sugars into glycolysis by the inhibitions of trehalose-6-P on hexokinases.

The glycerol biosynthesis pathway was presented in Figure 2.3. In this pathway, the dihydroxyacetone phosphate (DHAP) was reduced to glycerol-3-P by glycerol-3-P dehydrogenase, which was a cytosolic NAD^+ enzyme; and then, glycerol-3-P is dephosphorlated to glycerol.

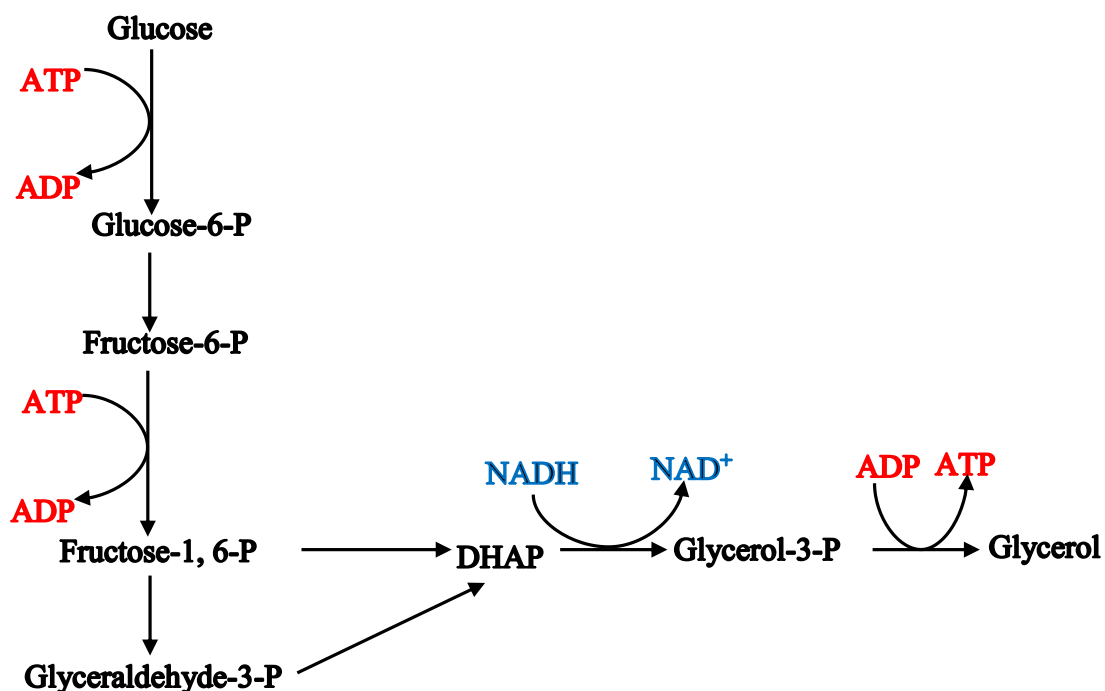


Figure 2.3 Metabolic pathway for glycerol synthesis from glucose in yeast. Adopted from Kresnowati et al.(2006)

NADH and NAD^+ were continuously recycled in the cells, while NADH was produced along with glucose to pyruvate, NADH was re-oxidized by the reduction of acetaldehyde to ethanol as well as glycerol production (Figure 2.1). In most cases, cytoplasmic redox was restored in the glycerol, which resulted in a high glycerol concentration indicating the oxidation stress in the fermentation media (Belo et al., 2003). As similar as trehalose, glycerol also played as a compatible solute when yeast cells were exposed under VHG condition. Glycerol was produced and accumulated to response stresses on the cells' membrane, and was also directly affected by the activity levels of glycerol-3-P dehydrogenase (Albertyn et al., 1994; Andre et al., 1991).

2.2.2 Roles of oxygen and carbon dioxide in ethanol fermentation

The oxygen availability in the broth determined either respiratory or fermentative pathway to produce energy during ethanol fermentation. While two moles of ATP were produced from each mole of glucose being utilized through fermentative route, 28 moles of ATP were generated when one mole of glucose was aerobically oxidized by oxygen (Daoud & Searle, 1990). As a result, more energy was released in aerobic environment in comparison to anaerobic condition. Since most energy was produced for cell growth and maintenance, higher biomass concentration and cells' viability were always observed in aerobic condition, which lowered fermentation time (Fornairon-Bonnefond et al., 2002; Verduyn et al., 1990). Moreover, some researchers also investigated the relationship between oxygen availability and cells viability. Verbelen et al. (2009) reported that the cells' viability was improved by the existence of ergosterol and sterols. While the ergosterol would increase the cells' structural integrity, sterols were used to make up the cell membranes. The biosynthesis of ergosterol and sterols was only observed when the medium was in the presence of oxygen. Therefore, an optimized oxygen concentration was critical to improve fermentation efficiency and the viability of cells. On the other hand, some researchers (Belo et al., 2003; Fornairon-Bonnefond et al., 2002) also concluded that the excess oxygen in the fermentation broth caused toxicity to the cells. A cell damage from the peroxidation of cell membrane was observed during a hyperbaric oxygen condition, which resulted in losing ethanol production.

Carbon dioxide was a major by-product of ethanol fermentation. The production of carbon dioxide was stoichiometrically related to glucose utilization and ethanol production. Moreover, the evolution of carbon dioxide was not only from fermentative pathway, but also was observed in the TCA cycle. Meanwhile, the TCA cycle also utilized carbon dioxide as substrate in carboxylation steps, such as succinic acid production (Ho et al., 1986; Song et al., 2007; Xi et al., 2011). Carbon dioxide in aqueous environments could be classified as three species: dissolved carbon dioxide (DCO_2), HCO_3^- and CO_3^{2-} . Since carbon dioxide exited as DCO_2 with minor concentrations of

HCO_3^- ions when the pH value of medium was in the range of 4-6. The carbon dioxide inhibition on cells was primarily from DCO_2 rather than HCO_3^- and CO_3^{2-} (Dixon & Kell, 1989; Frahm et al., 2002; Zosel et al., 2011). The current explanations of carbon dioxide inhibition were related to the change of cells membrane properties. As mentioned above, the cell membrane was primarily made up of sterols, lipids and unsaturated fatty acids, which could react with the absorbed DCO_2 molecules. The reactions modified the order and the fluidity of membrane, which resulted in the shifting of nutrition transport characteristics across the membrane (Dixon & Kell, 1989).

2.3 Review of Very-high-gravity fermentation

2.3.1 Very-high-gravity fermentation technology

Very-high-gravity (VHG) fermentation referred to the initial feedstock contained more than 270 grams mash per liter (Bayrock & Ingledew, 2001), which was equivalent to initial glucose concentration above 250 g l^{-1} (Devantier et al., 2005; Laopaiboon et al., 2009). Due to a lower water volume percentage under VHG condition, this technology was designed to reduce the energy cost from heating, cooling and evaporating water (Thomas et al., 1996). Moreover, since a high ethanol concentration was maintained during fermentation, the risk of bacterial contamination under VHG condition was much lower than other fermentation conditions.

VHG fermentation study has been carried by several groups with different feedstocks and various microorganisms since 1980s. Thomas et al., (1993) reported a 23.8% v/v ethanol productivity from 38% w/v wheat mash dissolved solids in a pilot plant scale. The same group also suggested multistage continuous culture fermentation technologies (MCCF) to improve the fuel ethanol production (Bayrock & Ingledew, 2001). In this study, 16.73% v/v ethanol was produced by MCCF from 32% w/v wheat mash dissolved solids solution. The authors also concluded that the continuous fermentation process improved the ethanol productivity comparing with batch process.

Recently, the investigations of sweet sorghum juice ethanol production also has been reported in several articles (Bvochora et al., 2000; Laopaiboon et al., 2009; Wu et al., 2010). Since only approximately 16 - 18% w/v fermentable sugar was contained in sweet sorghum juices (Wu et al., 2010), the juices was concentrated either by freeze-dried or by adding milled sorghum grain to obtain VHG level. Bvochora et al. (2000) successfully fermented the concentrated sweet sorghum juice, which involved 34% w/v dissolved solids, to produce 16.8% v/v ethanol through 96 h batch process. All these mentioned published results proved the high potential to apply VHG technology into bioethanol production scale.

2.3.2 The challenges of very-high-gravity fermentation

The challenges that limited the expanding of VHG fermentation in industrial environment, were not only the osmotic pressure in the beginning of the fermentation, but also included high level ethanol toxicity at the end of the process (Lin et al., 2011; Pratt et al., 2003). Since osmotic pressure was developed from the concentration differences between two solutions (Hohmann, 2002), exposing yeast cells into a concentrated solution would produce osmotic pressure on cellular functions and structures (Morris et al., 1986). Under VHG condition, yeast cells responded to hypertonic stress by losing turgor pressure, reducing cell size and wrinkling cell wall, which resulted in a decreasing of growth and fermentation rate (Beney, et al., 2001; De Maranon et al., 1996; Marechal & Gervais, 1994; Pratt et al., 2003).

Ethanol was a primary metabolic production in the yeast fermentative pathway. With the increasing of ethanol concentration in the media, the ethanol toxicity inhibited cells growth and declines viability, which resulted in yeast cells tending to stop fermentation routine (Lloyd et al., 1993). Therefore, the ethanol toxicity at the end of fermentation was one of the biggest challenges in most bioethanol production technologies, specifically, for VHG fermentation case (Hahn-Hägerdal et al., 2007). Although, the understanding of mode-of-action of ethanol was still limited, most researchers drew their attentions on plasma membrane (Attfield, 1997). As early as 1990s,

Alexandre et al.(1994) reported that yeast cells improved their ethanol tolerance by increasing proportion of ergosterol and unsaturated fatty acid levels and maintaining phospholipid biosynthesis. They also stressed that high membrane provided a close connection to ethanol tolerance. Moreover, some of recent articles (Dinh et al., 2008) also suggested that yeast cells adapted to high ethanol concentration environment by changing cell size and fatty acid content in cell membrane.

Media nutrient modification was one of most common methods to remove the effects from osmotic pressure and ethanol toxicity under VHGF fermentation condition. Casey et al. (1984) produced 16.2 % v/v ethanol from 31% w/v dissolved solids broth by adding nitrogen sources, ergosterol and oleic acid. Thomas et al.(1990) demonstrated the improvements of ethanol production rate by adding free amino nitrogen, which reduced fermentation time from 8 days to 3 days. Pereira et al. (2010) optimized a low-cost medium for VHGF ethanol fermentation, which resulted in 18.6% v/v ethanol production with a $2.4 \text{ g l}^{-1} \text{ h}^{-1}$ corresponding production rate. Moreover, the protective effect on yeast growth from ethanol toxicity by adding Mg^{2+} has been reported by several authors (D'amore & Stewart, 1987; D'amore et al., 1989; Walker, 1998). These studies indicated that the poor yeast viability and low yeast cell growth rate were not only contributed from high osmotic pressure and ethanol toxicity but also, were ascribed to the nutritional deficiency. Hence, a well-adjusted form of nutrition, such as: urea, amino acids, small peptides and ammonium ion, would significantly improve ethanol productivity under VHGF condition.

2.3 Fermentation process review

2.3.1 Batch process

Batch process was such a process that all ingredients were fed to the processing vessel in the beginning without addition and withdrawal of material during the operation. Since there was

neither addition nor withdrawal of materials during the batch process, it was known as the simplest process in the chemical and biochemical production. Due to the independence between sets in the batch process, the unexpected interference only affected on a single batch product. Consequently, the batch process was normally applied in high value and small volume chemical production, such as: medical and maquillage production (Keim, 1983). Moreover, the phenomenon through this process and final results was rarely influenced by external disturbance. Therefore, it was also considered as the first step in microbial study and developing new biotechnologies.

A typical industrial bioethanol batch production required 36 - 48 hours in order to completely utilize the substrate at $\sim 30^{\circ}\text{C}$ with ~ 4.5 initial pH value. The ethanol conversion efficiency of batch process usually lied in the range of 90 - 95%, which resulted in 10 – 16% v/v ethanol. Once the fermentation was completed, the fermented materials and produced microorganisms were pumped to a storage tank. The downtime, which was used for bioreactor filling, washing, sterilizing and recharging, was equal to 20% of overall batch operation. Therefore, in order to continuous feeding distillation system, several fermenters were usually operated in the batch process (Simpson & Sastry, 2013). Although, the ethanol conversion efficiency of batch process was the highest of all the processes. The longest downtime was not fitted to the requirement of high productivity from most bioethanol plants. Hence, the application of batch process normally only existed in small productivity scale plants. Moreover, batch process also has more priority in the early stage of new biotechnology developments. For instances, the VHG fermentation technology was tested through batch process first (Casey et al., 1984; O'Connor & Ingledew, 1989) and then followed by the studies of other processes.

The major strengths of batch system were low investment costs, its flexibility, and high conversion rate. As the simplest process, the process control system normally did not include in the batch process plants, which resulted in low investment costs for the plants. Meanwhile, the batch process was able to cope with seasonal, or shorter-term fluctuations in demand, due to the independent of each run. Moreover, the cultivation periods were easy to define in the batch

fermentation. Therefore, with an appropriate operating time a higher conversion level could be possible to obtain and the residue glucose could be completely depleted (Hill et al., 2006).

2.3.2 Continuous process

Continuous process was an open operation with ingredients continuously adding to the bioreactor, and the equivalent amount of harvest solution contained products and microorganisms simultaneously removing from the bioreactor. Due to the reduction of cost and downtime, which was associated with reactor filling, emptying and cleaning of the batch process, the high productivity was possible in this process (Simpson & Sastry, 2013).

Once the VHG continuous fermentation attained to steady state, the high glucose concentration from feeding media would be diluted by fermentation media, which removed the osmotic pressure effects in the process. However, the high residual glucose concentration in the harvest media was the biggest difficulty in VHG continuous process. As reported in Liu et al. (2011b), with 0.028 h^{-1} dilution rate, the residual glucose concentrations were ~189, 130 and 66 g glucose l^{-1} by using single fermenter with ~300, ~250 and ~200 g glucose l^{-1} feeding concentration, respectively. This high quantity of residual glucose would contribute to a low conversion level of ethanol production. In order to resolve the issue of residual glucose under VHG continuous process, several solutions were suggested by different groups. Bayrock et al. (2001) proposed a multistage continuous fermentation system to utilize residual glucose completely. Five continuous stirred-tank reactor (CSTR) were used in this study and all the glucose were depleted completely in the fifth fermenter with all five reported feeding glucose concentrations. The highest ethanol productivity was observed as ~17% v/v in the fifth fermenter by using 31.2% w/v dissolved solids feeding concentration with 0.05 h^{-1} dilution rate. However, the lowest biomass concentration and viability was also constantly observed in the same fermenter with the same condition, which was 5.92 g l^{-1} and 34%, respectively. Different from Bayrock et al. (2001) suggestions, Liu et al. (2011a; 2012) designed an ageing vessel system with reduction-oxidation (redox) potential control to

improve the ethanol production performance in VHG continuous process. One single fermenter coupled with several ageing vessels, which were used to completely convert glucose to ethanol, was required in this system design. Once the ageing system achieved the steady state, the ageing vessel continuously received influx from fermenter and operated as fed-batch process until the vessel was full. From this moment, the fermenter would connect to a new ageing vessel and the previous ageing vessel would operate as batch process to deplete all the residual glucose in the media. The highest ethanol concentration in the ageing vessel design was reported as 125.66 g/l with ~80 hours ageing time under -50 mv redox-potential control level by using ~300 g glucose l⁻¹ feeding concentration.

VHG continuous operation was benefited by low manpower and no unproductive down-time. Comparing with batch operation, the working volume of continuous fermenter was much lower and its harvest media kept a constant quality. Hence, this process always had a priority in the large scaled bioethanol plants (Keim, 1983; Simpson & Sastry, 2013). However, there were also some disadvantages in VHG continuous system. Due to a long operation time being required in order to reach steady state, continuous process normally had low flexibility on dilution rate, temperature and medium composition. Moreover, the high investment cost was also required for control and automation equipment (Pretreatment, 2011).

2.3.3 Fed-batch process

Fed-batch process was designed to maximize the productivity and the yield of desired products by feeding a growth-limiting nutrient to a culture (Yamanè & Shimizu, 1984). This process was widely used to produce primary and secondary metabolites, proteins and other biopolymers. A high cell density or high metabolites productivity could be obtained in fed-batch operation by changing feeding strategies to modify cells' metabolism pathway (Lee, 1996). Since the modifications of single or multiple nutrients were detrimental to cell growth and production, the feeding strategy optimization was critical in fed-batch cultivation. Moreover, the complexity

of bioprocess and unreliable devices caused the unstraightforward optimization work in fed-batch operation (Johnson, 1987).

Ethanol fermentation through fed-batch process also has been studied by several groups. Alfenore et al. (2002) reported up to 19% v/v ethanol in 45 hours in a fed-batch culture at 30 °C. Two feeding strategies were involved in their study: vitamin and glucose. While the glucose concentration during fermentation maintained at ~100 g l⁻¹ by feeding 700 g glucose l⁻¹ solution, the final ethanol concentration and yield of ethanol conversion level was improved by exponential feeding of vitamins. By using different feedstock, a ~120 g l⁻¹ ethanol productivity with ~94% ethanol conversion efficiency through fed-batch process was reported by Laopailboon et al. (2007). There were three feeding strategies involved in their experimental design: batch, one-time feeding and two-time feeding. The highest ethanol concentration was observed in the 75:25 one-time feeding strategy, which was filled 75% of working volume first and followed by refilled up to 100% of working volume after 49 hours. By comparing the results in three strategies, the authors suggested that fed-batch fermentation improved the ethanol conversion efficiency. A similar conclusion was also driven by Cheng et al. (2012) by using corncob hydrolysate as feedstock.

According to these mentioned literatures, fed-batch operation was able to remove osmotic effects in VHG fermentation by starting a low initial glucose concentration and diluting high glucose feeding solution with fermented medium. However, the unproductive down-time was normally unavoidable in this process, which was used to fill, discharge, clean and refill the fermenter. Meanwhile, more operating costs would be spent on process operators training, due to the complexity of the feeding strategies. Hence, the fed-batch process was rarely operated in fuel-ethanol production, and it was only practiced when low conversion efficiency was observed in batch process and it was impossible to run in continuous process.

2.3.4 Repeated-batch process

Repeated batch was a cyclic process operation that was in essence an oscillating process. In theory, cycles in a repeated batch operation were based on the metabolic rates of the fermenting

cell population thus taking into account the biochemical aspect of any bioprocess (Feng et al., 2012). The details of the repeated batch process have been discussed by several authors (Brown et al., 1999; Brown & Cooper, 1991). An automatically operating repeated batch process was proposed by Cooper's group. Since the process was on a feedback control strategy and there was no external parameter controlling the cyclic process, it was given the name as self-cycling fermentation (SCF). For a fermentation process to be self-cycling, a parameter that was representative of the state of the cells in the fermenter should be measured. According to these measurements, broth removal and fresh media feeding would be accomplished.

Previous SCF studies used dissolved oxygen (DO) concentrations or off-gas carbon dioxide evolution rates as the measured variables to perform feedback control strategy under aerobic conditions (Brown & Cooper, 1991; Hughes & Cooper, 1996). Meanwhile, the prior research in the area of SCF processes has been discussed for various bacteria and yeasts other than *Saccharomyces cerevisiae* (Brown et al., 1999; Brown & Cooper, 1991). Moreover, most of these studies, where the DO concentration has been used as a control variable to start SCF operation, were concerned with carbohydrate fermentation and lasted for a maximum of 40–50 h with cycle times in the range of 2.5–4 h (Brown et al., 1999; Brown & Cooper, 1991).

According to the characters of SCF technology, VHG fermentation would be significantly improved by removing osmotic pressure and increasing ethanol toxicity tolerance (Feng et al., 2012). However, the limitations of sensor design were the main reasons of the inoperability of a DO driven SCF process in an anoxic environment (Cortón et al., 1999; Janata, 2009; Zosel et al., 2011). Feng et al. (2012) used redox potential as the new internal parameter to perform SCF operation. The SCF could successfully operate at high-gravity (HG) condition, and the highest ethanol productivity was reported as $\sim 90 \text{ g l}^{-1}$ with ~ 14 hours fermentation time under $\sim 200 \text{ g glucose l}^{-1}$ feeding concentration. However, as soon as the feeding glucose concentration greater than 250 g l^{-1} , the depletion of glucose could not be observed at the end of each cycle, which resulted in a manually cycle period being settled as 36 hours.

2.4 Online measurements and bioprocess optimization

The products from biotechnology processes varied from primary and secondary metabolites to therapeutic proteins with different host cell systems, such as bacteria, fungi and plant cells. Consequently, the process optimizations to maximize production efficiency and to improve the product quality were required (Scheper et al., 1996; Scheper & Lammers, 1994). With the developments of bio-sensors, more parameters became available and apply for bioprocess monitoring, which resulted in a better understanding of the environmental effects on microorganism's growth. While temperature, pH and DO sensors have been widely applied into academic study as well as industrial production, some advanced technologies, such as: two-dimensional fluorescence spectra and NADH sensors, also were proposed by several authors in the recent years (D'Auria & Lakowicz, 2001; Ido et al., 2001; Navani & Li, 2006; Simon et al., 2000).

However, the challenges of the bioprocess online measurements were always presented and limited the expanding of sensors' application. For industrial sensors' application, the mixing issue was normally observed in a large working volume fermenter, which caused an inconstant concentration condition in the fermenter. In order to provide an accurate online measurements in large fermenter, the fermenter with large working volume always required multiple feeding zones along with different locations alongside the fermenter (Bylund et al., 2000; Lübbert & Bay Jørgensen, 2001). Different from traditional bioprocess sensors, the advanced online measurement technologies were only utilized in the laboratory systems and operated with a small working volume. For these advanced sensors' measurements, the readings were normally stable and accurate; however, the complex interferences and the overlaps between parameters resulted in difficulty to interpret the collected data (Simon et al., 2000; Wolf et al., 2001).

In situ and in-line monitoring were most common methods to perform online measurements. While *in situ* measurement was standard for placing sensors in the vessel directly, in-line

monitoring indicated a flow lines associate with monitoring system. A rapid measurement in chemical or physical parameters, such as: pH, DO, DCO₂, with high data acquisition rate were normally achieved by *in situ* measurement system, which resulted in being capable of performing real-time measurement and directly control. Several reported online measured parameters by using *in situ* sensors in VHG fermentation were briefly reviewed in following sections: temperature, pH and DO were organized together as the most common measurements, redox-potential, gas phase CO₂ and DCO₂ were also presented due to the strong connection to ethanol fermentation.

2.4.1 Temperature, pH and dissolved oxygen online measurements

Temperature was one of the well understood and controllable parameters in bioprocesses. It has been proved to provide a critical effect on cells growth and ethanol productivity in VHG ethanol fermentation (Jones & Ingledew, 1994). Jones et al. (1994) reported the investigations of ethanol concentration at temperature between 17 and 33 °C through 14.0 to 36.5% w/v solids %. While the highest ethanol concentration was observed as 17.8% v/v at either 20 or 24 °C, the fermentation time at 20 or 24 °C was 7 days longer than the time at 33 °C with 3.6% v/v ethanol productivity increasing. Therefore, Jones et al. suggested that 33 °C was the best temperature condition to maximize ethanol productivity in VHG condition.

The pH control during the VHG fermentation was used to avoid bacterial contaminations and to improve yeast cells growth (Pampulha & Loureiro-Dias, 1989). Due to acetic acid being a by-product of ethanol fermentation, the pH value decreased with the progress of fermentation. The effects of pH on yeast cells' activity, growth and fermentation productivity have been discussed by several authors (Hwang et al., 2004; Pampulha & Loureiro-Dias, 1989; Pradeep et al., 2012). By using response surface methodology, Pradeep et al. (2012) reported 4.8 as the optimized pH value for VHG ethanol fermentation.

Ethanol fermentation was always considered as anaerobic reaction, which requested a small DO concentration in the media. The low DO value resulted in inaccurate readings during ethanol fermentation. Hence, the online measurements of DO were not normally observed in ethanol

fermentation study (Lin & Tanaka, 2006). However, in all aerobic bioprocess study, DO was an essential control parameter to influence cells growth.

2.4.2 Redox potential online measurements

Redox potential was used to describe the momentary metabolic status of microorganisms during propagation. Either a positive, which indicated an oxidation state, or a negative, which reflected a reduction situation, redox potential value was investigated in the process. Several articles reported the redox potential profiles with cells' growth, which concluded that the changing of redox potential during the process was normally contributed by NADH and DO. While NADH served as the electron donor, the DO acted as electron acceptor (Harrison, 1972).

As early as 1970s, redox potential has been widely applied in microorganisms' production. Kjaergaard (1977) presented a detailed review related to theory and applications of redox potential in biotechnology. The developments of redox potential in microorganism growth and chemical production have been developed and discussed through different authors (Berovič, 1999; Cord-Ruwisch et al., 1988; Dave & Shah, 1998; Tengerdy, 1961). Most of these authors concluded that redox potential provided a much more accuracy online measurements to describe the cell's growth and activity in an anaerobic condition than DO. Therefore, as one of classical anaerobic reactions, redox potential was normally selected to monitor the process of ethanol fermentation (Nagodawithana et al., 1974).

The redox potential profiles in batch process under VHG ethanol fermentation was first investigated by Lin et al. (2010). Meanwhile, a correlation between redox potential profile and glucose utilization was also observed and reported in the same article. According to the redox potential readings during batch fermentation, a series of redox potential control schemes to improve ethanol productivity under VHG condition was developed and reported (Lin et al., 2011; Liu et al., 2011b). Besides of batch process, the study of redox potential monitored and controlled experiments were performed and reported by Liu et al. (2011a; 2011b; 2012). These publications

suggested a significantly ethanol productivity improvement could achieve by using redox potential controlled continuous process under VHG condition. In order to resolve the residual glucose in the continuous process, aging vessel system with redox potential control was developed (Liu et al., 2011a; Liu et al., 2012). Moreover, with the monitoring of redox potential, an automatically repeated batch system was developed and successfully operated under high gravity (HG) condition (Feng et al., 2012).

2.4.3 Carbon dioxide online measurements

Carbon dioxide could be either products from cells' respiration or reagents to supply metabolites biosynthesis. The monitoring of carbon dioxide could provide the detailed information related to cells' growth or metabolites production condition. For example: since glucose utilization, ethanol production and yeast cells growth had a direct stoichiometric relationship, the monitoring of CO₂ in ethanol fermentation was beneficial to evaluate microbial activity and ethanol productivity (Chen et al., 2008; Dahod, 1993; Daoud & Searle, 1990; El Haloui et al., 1988; Royce & Thornhill, 1991). Off-gas CO₂ and DCO₂ were two most common parameters in the fermentation process, which were used to measure CO₂ concentrations in the gas phase and liquid phase, respectively.

The monitoring of CO₂ in the off-gas stream was first proposed to determine its corresponding ethanol and glucose concentration by El Haloui et al. (1988). In this paper, a theoretical model was developed to convert the CO₂ volume in off-gas stream to DCO₂ concentration in the fermentation media. However, due to a unequilibrium condition between dissolved and off-gas CO₂ during the fermentation, the El Haloui's model failed to provide an accurate DCO₂ concentration from CO₂ volume in off-gas stream. Moreover, due to the technology limitations in CO₂ sensor, the investigations of CO₂ in the off-gas streams during the initial hours (0-12h) of fermentation could not be determined in the previous studies (Daoud & Searle, 1990; Golobič, et al., 1999).

The application of off-gas CO₂ online measurement was used in ethanol fermentation but also, applied to mammalian production. While the monitoring of off-gas CO₂ in ethanol fermentation helped to estimated ethanol production (Cortón et al., 1999; Ho et al., 1986; Zosel et al., 2011), the volume of purged off-gas CO₂ in mammalian culture media affected cells growth and secondary metabolites production, significantly (Aehle et al., 2011; Pattison, Swamy et al., 2000; Sieblist et al., 2011). As the fatty acid biosynthesis resources, CO₂ was required during the mammalian culturing. However, the large quantity of CO₂ could inhibit cells growth and reduce the production of metabolites. Hence, Aehle et al. (2011) and Pattison et al. (2000) suggested the purged CO₂ volume be maintained between 5% and 10% v/v of working volume during the cell culturing.

Dissolved carbon dioxide (DCO₂) was always observed at a high level during the course of fermentation. This was because of the low pH favors the presence of CO₂ as DCO₂ and high ethanol concentration environment increasing CO₂ solubility in the medium (Kruger et al., 1992; Kühbeck et al., 2007). When the fermentation was performed in the protein rich fermentation broths, more organic molecules were tending to bind CO₂ on the cell membrane and in the medium, which resulted in increasing of solubility of CO₂ (Kruger et al., 1992). Therefore, the measurements of DCO₂ concentration to monitor fermentation process were much more reliable than the measurements based on CO₂ volume in off-gas stream. Moreover, the solubility of CO₂ was more than 10 times greater than the solubility of O₂ in aqueous medium (Kawase et al., 1992; Schumpe & Deckwer, 1979; Schumpe et al., 1982), which resulted in a much more reliable online measurements of DCO₂ than that of DO. Consequently, several DCO₂ online measurement devices were proposed by several authors (Cortón et al., 1999; Shoda & Ishikawa, 1981; Sipior et al., 1996).

InPro 5000 by Mettler Toledo was the commercialized sensor to perform DCO₂ online measurements during the fermentation. It could be considered as the combination of DO probe and pH sensor. Theoretically, the DCO₂ concentration values were calculated from the changing of pH value, which were monitored by the pH sensor in InPro 5000. During the measurements, the sensor

was immersed into bicarbonate buffer, and the buffer was filled in a hydrophobic membrane made tube. The produced carbon dioxide gas molecules in fermentation media diffused through hydrophobic membrane to bicarbonate buffer and changed the pH value of bicarbonate buffer. By using pre-determined mathematical equations, the varying of pH value was directly connected to the dissolved carbon dioxide concentration in the media. Srinivasan et al. (2012) reported DCO₂ profiles and characteristics during HG and VHG fermentation by using InPro 5000 DCO₂ sensor. They also concluded that DCO₂ online measurement would provide much more accurate tendency of glucose utilization, ethanol production and yeast activities than redox potential online monitoring.

2.5 Knowledge Gaps

The earlier VHG fermentation studies were focused on media nutrition modifications and testifying VHG conditions through various processes (Bayrock & Ingledew, 2001a; Pereira et al., 2010; Wang et al., 2007). In recent years, the inhibitory effects from external parameters, such as: DO, pH and temperature, also have been discussed by several authors to optimize VHG fermentation results (Alfenore et al., 2004; Jones & Ingledew, 1994; O'Connor & Ingledew, 1989). However, only few of these studies reported the effects of internal parameters (Feng et al., 2012; Srinivasan et al., 2012), such as: redox-potential and DCO₂, on the efficacy of VHG fermentation.

Although, our group has successfully applied repeated batch process into ethanol fermentation under HG condition by using redox-potential as the feedback control signal (Feng et al., 2012); and also developed a new fermentation control technology driven by DCO₂ under batch process (Srinivasan et al., 2012). These priori observations and results suggested that repeated batch significantly improved the efficacy of VHG fermentation process, but failed to apply the repeated batch system with an automatically operation into VHG condition.

Moreover, redox-potential profiles of repeated batch fermentation would provide details about overall cells' physiology during the repeated batch process, but the descriptions of ethanol production during the process could not be estimated by using redox-potential profiles. Therefore, determining the DCO₂ profiles of repeated batch process could help to identify the relationship between cell growth, glucose concentration and CO₂ evolution, which could help in calculating ethanol production rate during in the process as well as determining DCO₂ process control schemes for complete utilization of glucose.

2.6 Objectives

Based on the knowledge gaps identified above, this project aimed at developing an automatically operating DCO₂ driven and controlled repeated batch system to produce ethanol under HG and VHG conditions. The proposed objectives of this project include:

- I. Performing HG and VHG fermentation without residual glucose through repeated batch process;
- II. determining different cycling strategies to develop automatically repeated batch fermentation in the absence and presence of DCO₂ control;
- III. exploring the characteristics and DCO₂ profiles of repeated batch fermentation in the absence and presence of DCO₂ control;
- IV. revealing the differences of fermentation results where DCO₂ was under control or without control;
- V. determining the effects of fermentation results by different DCO₂ control levels;
- VI. estimating the ethanol productivity among different fermentation conditions and processes.

CHAPTER 3 EXPERIMENTAL MATERIALS AND METHODS

3.1 Experimental design

Four glucose concentrations, ~150, ~200, ~250 and ~300 g l⁻¹, were chosen in this project. Different glucose concentrations were used to study the performance of DCO₂ driven repeated batch system. Two DCO₂ control levels were applied in the presence of DCO₂ control for all four feeding glucose concentrations in order to determine their effects on fermentation time. Additional, no DCO₂ control cases were chosen as references. Hence, there were 12 combinations of fermentation conditions (Table 3.1).

Table 3.1 Summary of experimental design

	HG Condition		VHG Condition	
	~150 g l ⁻¹	~200 g l ⁻¹	~250 g l ⁻¹	~300 g l ⁻¹
absence of DCO₂ control	√ ¹	√	- ²	-
DCO₂ controlled at 750 mg l⁻¹	√	√	√	√
DCO₂ controlled at 1000 mg l⁻¹	√	√	√	√

Note: ¹ performed, ² did not perform

Srinivasan et al. (2012) concluded that VHG fermentation could not be completed without residual glucose in the absence of DCO₂ control. Meanwhile, according to the previous reported results (Feng et al., 2012), the repeated batch system could not be automatically operated during VHG fermentation in the absence of redox-potential control. Hence, fermentation in the absence of DCO₂ control was only performed under HG condition. Consequently, ten sets of experimental conditions were carried out in this project (Table 3.1). For each experimental condition, at least 10 cycles were performed and recorded. Moreover, at least two independent trials under each respective condition were performed to confirm the reproducibility of experimental results.

3.2 Strain and growth media

Ethanol Red™ strain of *Saccharomyces cerevisiae* was used in this study. This strain was supplied by Lesaffre Yeast Corp (Milwaukee, MI, USA) in an active dry yeast form. The dry yeast was pre-cultured through rehydrating with 50 ml sterilized water, followed by culturing in YPD agar (10 g l⁻¹ yeast extract, 10 g l⁻¹ peptone, 20 g l⁻¹ dextrose and 20 g l⁻¹ agar) with two sub-culture steps. The harvest yeast cells were stored at 4 °C for future use.

With a total working volume of 100 ml, the pre-culture medium contained glucose 20% (w/v), yeast extract 1% (w/v), MgSO₄ 0.2% (v/v) and urea 0.5% (v/v). This medium was constituted by three portions of solution and proper amount of reverse osmosis (RO) water. Three portions of solution were steam sterilized separately at 121 °C for 15 minutes in an autoclave. After steam sterilization, these solutions were mixed in a 250 ml shake flask and cooled to room temperature aseptically. The yeast cell used for pre-culturing was collected from agar plate and pre-cultured at 32 °C in the prepared media with 120 rpm for 18 h until the mid-exponential phase was achieved.

The fermentation medium consisted of four portions (A, B, C and D). Each portion was sterilized independently in a steam sterilizer (ST75925 Sterilizer Harvey Sterilemax) under 121 °C for 15 minutes. After sterilization, each respective medium was allowed to cool to room temperature first, and then portion A, B and C were mixed aseptically in the fermenter, and at last the mixture of A, B and C was made up to the desired working volume using portion D. Portion A consisted of one of four desired glucose concentrations, which were 15%, 20%, 25% and 30% (w/v). Portion B consisted of yeast extract 1% (w/v) and L-(+)-Sodium Glutamate Monohydrate (glutamic acid) 0.1% (w/v). Portion C consisted of MgSO₄ 0.2% (v/v), Urea 0.5% (v/v), KH₂PO₄ 0.5% (v/v), (NH₄)₂SO₄ 0.1% (v/v) and each of H₃BO₃, Na₂MoO₄, MnSO₄ · H₂O, CuSO₄, KI, FeCl₃ · 6H₂O, CaCl₂ · 2H₂O and ZnSO₄ · 7H₂O 0.1% (v/v). Portion D was RO water.

Urea and mineral salts were prepared as stock solution. The concentration of each stock solution and their supply resources were presented in the Table 3.2. All the chemicals were of HPLC grade or higher purity. Yeast extract was received from HiMedia Laboratories (Mumbai, India) and L-(+)-Sodium Glutamate Monohydrate was provided from J. T. Baker (Phillipsburg, U.S.A).

Table 3.2 Concentration and supply resources of stock solution

<i>Media Constituent</i>	<i>Concentration (mM)</i>	<i>Supply Resources</i>
(NH ₄) ₂ SO ₄	1000	E.M. Science
CaCl ₂ .2H ₂ O	82	J. T. Baker
CuSO ₄	10	Fisher Science
FeCl ₃ .6H ₂ O	100	Fisher Science
H ₃ BO ₃	24	Fisher Science
MgSO ₄ .7H ₂ O	1000	AMRESCO
MnSO ₄ .H ₂ O	2	Fisher Science
KI	1.8	Fisher Science
KH ₂ PO ₄	735	E.M. Science
Na ₂ MoO ₄	1.5	Fisher Science
Urea	1600	E.M.D.
ZnSO ₄ .7H ₂ O	1000	Alfa Aesar

3.3 Repeated batch system

Ethanol production by *S. cerevisiae* from glucose substrates under VHG conditions was investigated by using repeated batch process. The process flow diagram was illustrated in Figure 2.1. Four parts were involved in the repeated batch system: feeding, fermentation, control and

harvest. While both of feeding and harvest systems were built by one vessel and a peristaltic pump, the fermentation apparatus was a jar fermenter (Model: Omni Culture, New York, NY, USA) with a 1.5 l working volume. A detachable stainless steel lid was placed on top of the jar to maintain sterility during the fermentation. Online measurements, such as temperature, DCO_2 , redox potential, were determined by using different electric sensors through the ports on the lid. Agitation during the fermentation was kept constant at 200 rpm through a six bladed impeller. The impeller was fixed under the stainless steel cover by mounting to the agitator shaft. Control system involved computer (Model: HP Envy 700), control box (Model: NI PCI-6013) and an air pump, which was used to determine the fermentation ending point in each cycle and to maintain the controlled DCO_2 levels during fermentation. Labview (Version 2013, National Instrument, Austin, TX, USA) was used to acquired and controlled fermenter DCO_2 at a desired level.

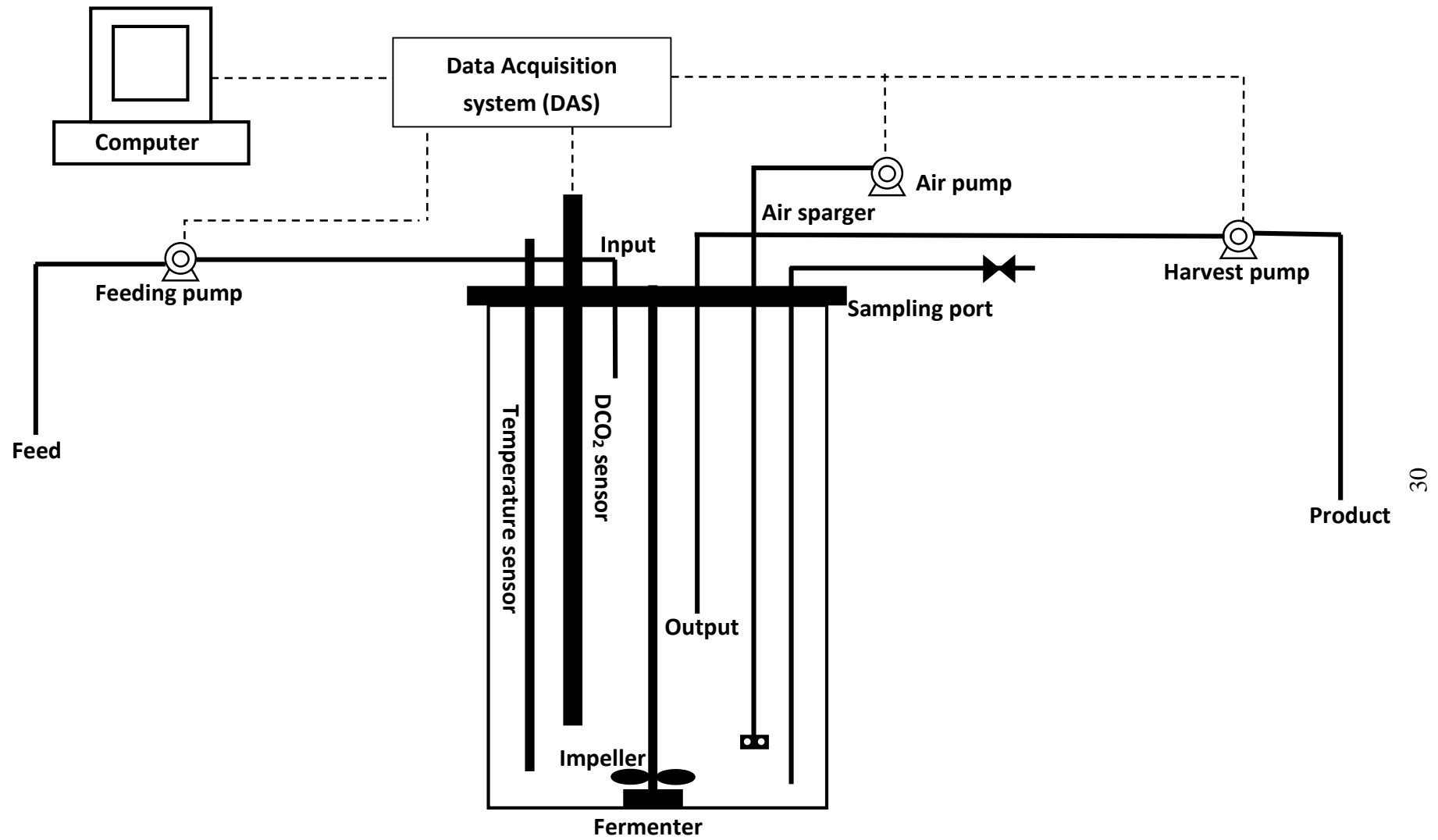


Figure 3.1 Illustration of experimental set-up for repeated batch fermentation process

3.4 Fermentation and process control

3.4.1 Glucose feeding strategies

Two glucose feeding strategies: independent feeding and continuous feeding, were implemented in this project. The former strategy indicated that the repeated batch fermentation experiment was independently performed at each glucose under three different DCO₂ control levels. The results of independent feeding strategy were presented and discussed in Sections 4.1 and 4.2. Feeding continuous strategy suggested that for each repeated batch fermentation experiment, four glucose concentrations, from ~150 g glucose l⁻¹ to ~300 g glucose l⁻¹, were continuously fed into fermenter under one of the two DCO₂ control conditions: with DCO₂ control at 750 mg l⁻¹ and 1000 mg l⁻¹. Section 4.3 presented and discussed the results and conclusions from continuous feeding strategy. Irrespective of which feeding strategy, the fermentation conditions (Table 3.1) were kept the same.

3.4.2 Fermentation conditions

The ethanol fermentation was performed in a steam-sterilized fermenter with 1.5 l working volume. The inoculated yeast was collected from pre-culture flask with 5% inoculum. The initial pitching rate of fermenter was adjusted to 10⁷ viable cells per ml for all the experiments. The fermentation temperature was kept at 32 °C by circulating water from a water bath. The fermentation medium was mixed by a six bladed impeller with 200 rpm agitation speed. The samples were collected in the beginning and at the end of each cycle. In some of cycles, the samples were taken every two hours for mathematical modeling study in the future.

3.4.3 Determination of repeated cycles

In reference to one of the previous publications (Srinivasan et al., 2012), the end point of fermentation could be determined by the variations of DCO₂ profile during the fermentation.

In the absence of DCO₂ control condition, a sudden drop of DCO₂ profile was observed at the end of fermentation. As a result, the cycling process was started as soon as a continuous decrease of DCO₂ slope was detected.

Meanwhile, in the presence of DCO₂ control cases, a sudden decrease of DCO₂ profile was also observed at the end of fermentation. However, due to the DCO₂ level was controlled by purging air through the process, which resulted in the failing of cycling determination by using above mentioned method. Hence, the cycling of a repeated batch system was triggered once the DCO₂ reading was lower than 500 mg l⁻¹ with a negative slope of DCO₂ profile for a certain period of time (more than ten minutes).

3.4.4 Control of DCO₂ level

Fermentator DCO₂ was controlled at a specific level during the course of fermentation by using membrane-sterile air. Two DCO₂ levels (750 and 1000 mg l⁻¹) were selected in the presence of DCO₂ control cases. The selected levels were based on the maximal solubility of CO₂ in the fermentation medium. Several articles reported the maximal CO₂ solubility value (Ho et al., 1986; Shoda & Ishikawa, 1981) and its influence factors, such as the concentration of organic and inorganic salts in the media (Kruger et al., 1992; Zosel et al., 2011). The details related to the selection of DCO₂ control levels have also been reviewed and discussed in the Mr. Srinivasan master thesis (2012, University of Saskatchewan).

3.5 Online measurements and sample analysis

3.5.1 Online measurements

A commercial autoclaveable DCO₂ sensor (InPro[®]5000, Mettler-Toledo, Bedford, MA, USA) was used to measure DCO₂ concentrations in the medium during the fermentation. The sensor required a one point calibration by using pH 9.21 buffer before steam sterilization. A serials of raw signal was collected as voltage version through the sensor every five seconds. The collected raw data was converted into DCO₂ concentration value by using an M400 controller (Mettler-Toledo, Bedford, MA, USA). The converted data was averaged and recorded as text file every five minutes by using Labview (Version 2013, National Instrument, Austin, TX, USA).

3.5.2 Sample analysis

The collected samples were analyzed for biomass, cell viability, pH, concentrations of sugar and organic acids. The biomass concentration was recorded as cell dry weight. A colorimeter (Klett™ Colorimeter, Belart, NJ, USA) was used to determine optical density (OD) of collected samples at 600 nm. All the samples were diluted 10 times before OD measurements. A calibration table of different OD values against cell dry weight of yeast was prepared before experiments and the table was used to obtain biomass concentration of samples. In order to calculate cell viabilities during the fermentation, methylene violet staining was used to stain death cell in the medium (Smart et al., 1999). The cell viabilities were then determined from total cell number and death cell number, which were counted under a microscope on a hemacytometer (Hausser Scientific, Horsham, PA, USA).

Two mls of collected sample were transferred to centrifuge for determining sugar and organic acids concentration. The transferred sample was centrifuged at $9000 \times g$ at $4\text{ }^{\circ}\text{C}$ for 10 minutes. The supernatant was diluted five times and then used to measure concentrations of sugar and organic acids by HPLC (Series 1100, Agilent Technologies, Mississauga, ON) equipped with a refractive index (RI) detector (HP 1047A, Hewlett Packard, Mississauga, ON), which was operated at $35\text{ }^{\circ}\text{C}$. An ion exclusion ION-300 column (Transgenomic, Inc., Omaha, NE, USA) was used to separate supernatant with 8.5 mM H_2SO_4 at 0.4 ml/min as mobile phase at $65\text{ }^{\circ}\text{C}$. Each sample was injected into the column at least two times with 10 μl injection volume.

CHAPTER 4 RESULTS AND DISSCUSION

The fermentation was performed either with DCO₂ or without DCO₂ control. Under DCO₂ control scenario, either 750 or 1000 mg l⁻¹ DCO₂ control level was chosen. Meanwhile, four glucose feeding concentrations at ~150, ~200, ~250 and ~300 g glucose l⁻¹ were involved in this project, which resulted in 12 combinations of fermentation conditions during repeated batch fermentation. When glucose feed concentration was greater than ~200 g l⁻¹, the residual glucose concentration at the end of fermentation would never be zero, which cannot satisfy the objectives of this project. Therefore, without DCO₂ control conditions were excluded in the experimental design. The concentration profiles of DCO₂, biomass, glucose and ethanol during repeated batch fermentation were collected and discussed in this chapter.

Section 4.1 presented the reproducibility of DCO₂ driven repeated batch fermentation. Sections 4.2 discussed characteristics of DCO₂ driven repeated batch fermentation. The determinations of time for self-cycling system in the absence and in the presence of DCO₂ control were also presented in this section. The effects of DCO₂ control on fermentation time under different fermentation conditions during repeated batch operations were discussed in Section 4.3. An equation based on these effects and relating fermentation time with final ethanol concentration has been concluded in Section 4.3 as well. Comparisons of ethanol productivity between different processes as well as the in the absence and in the presence of DCO₂ control were presented in section 4.4.

4.1 Reproducibility of dissolved carbon dioxide driven repeated batch fermentation

Repeated batch fermentation began with a batch experiment and followed by a series of batch operations. As soon as the current batch fermentation was completed, half of working volume of spent medium was withdrawn and then refilled with an equal volume of fresh medium into the fermenter. Since the batch operations would keep running once the process started, a single batch operation was also called one cycle operation during the repeated batch fermentation cycling. The cycling time between cycles could be determined either manually or

automatically. While the manual determination was an empirical decision, the automatic one running was based on the change of slope of DCO₂ concentration during the course of each respective repeated batch. The change of slope of DCO₂ indicated the depletion of glucose, which was affected by yeast cells activities and viabilities. Therefore, this automatically operating process was also named as self-cycling fermentation (SCF). It was important to note that the reported repeated batch processes in this project were all operated automatically based on the changing of DCO₂ concentrations profiles.

Typical profiles of glucose, ethanol, DCO₂ and biomass concentrations for ~200 g glucose l⁻¹ initial feeding concentration in the absence and with DCO₂ control at 750 mg l⁻¹ were presented in Figure 4.1. The observations of other experimental conditions as listed in Table 3.1 were similar to those shown in Figure 4.1. Therefore, the summary figures of all performed fermentation conditions were collectively illustrated in Appendix A1. As shown in Figure 4.1, the final biomass concentration was increased and stabilized after 4-5 cycles in both of with and without DCO₂ control cases, which indicated that the system required 4-5 cycles to reach the steady condition. The same experiment was duplicated, the average cycling time was 14.7±2.7 h and 7.3±0.2 h for in the absence of DCO₂ control and in the presence of DCO₂ control, respectively.

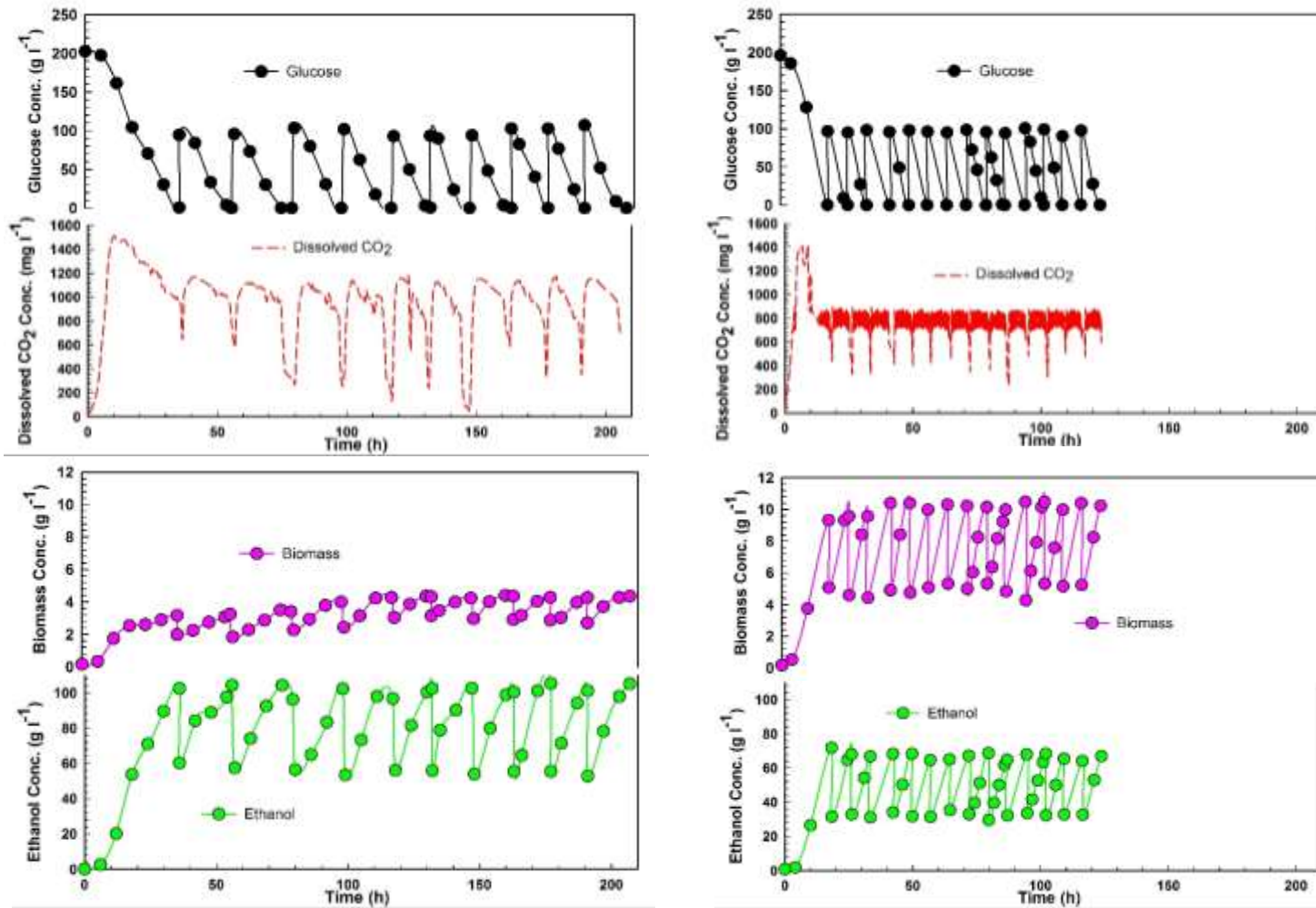


Figure 4.1 Profiles of glucose and ethanol concentration, DCO₂, and biomass concentration under ~200 g glucose l⁻¹ a) in the absence of DCO₂ control b) and in the presence of DCO₂ control at 750 mg l⁻¹ DCO₂ control level.

4.1.1 Characteristics of dissolved carbon dioxide driven repeated batch in the absence of DCO₂ control under high-gravity conditions

The repeated batch fermentation was designed to start a new cycle as soon as the previous cycle was completed. However, according to the previous observations during VHG fermentation (Lin et al., 2010; Srinivasan et al., 2012), the residual glucose would always remain at the end of fermentation making it difficult to determine cycling time of when to start repeated batch operation. Moreover, the reported observations from redox potential driven repeated batch fermentation with ~250 g glucose l⁻¹ feeding concentration in the absence of redox potential control (Feng et al., 2012) also provided a similar conclusion. Hence, the experiments of DCO₂ driven repeated batch fermentation in the absence of DCO₂ control were only performed under HG conditions resulting in complete glucose utilization. The summary of observations in the absence of DCO₂ condition was represented in Table 4.1.

Table 4.1 Summary of repeated batch fermentation in the absence of DCO₂ control

	~150 g glucose l ⁻¹	~200 g glucose l ⁻¹
Final ethanol, g l ⁻¹	74.6±2.2	102.5±2.5
Final biomass, g l ⁻¹	3.2±0.2	4.2±0.3
Stable cycle time, h	11.3±1.1	14.7±2.7
Production efficiency ¹	0.91±0.05	0.91±0.07
Viability	0.94±0.03	0.90±0.08

$$^1 \text{ production efficiency} = \frac{\text{ethanol concentration}}{\text{maximal attainable ethanol concentration}}$$

Note: The reported values were average numbers from at least 10 stabilized cycles. The stabilized cycles indicated the difference of cycle time, final ethanol and biomass concentrations between the cycles was lower than 5%.

As seen in Table 4.1, under ~150 g glucose l⁻¹ conditions, the constant concentrations of biomass and ethanol were obtained as 3.2±0.2 and 74.6±2.2 g l⁻¹, respectively. Meanwhile, the self-cycling period, the time period between two consecutive cycles, was stabilized at 11.3±1.1 h. Similarly, for the ~200 g glucose l⁻¹ case, the final concentrations of biomass and ethanol at the end of each cycle were 4.2±0.3 and 102.5±2.5 g l⁻¹, respectively. The self-cycling period

under this condition was stabilized as 14.7 ± 2.7 h. The viabilities of cells in these two glucose concentrations were greater than 90%, which indicating that cells' activities were maintained at high levels in the HG conditions. Moreover, the ethanol production efficiency was calculated as ~91% in both cases.

Initial glucose concentration and ethanol toxicity at the end of fermentation could both be the primary effect on yeast growth. Since glucose was the essential carbon resource to support cell growth, a higher glucose concentration provided more energy, which resulted in a higher biomass concentration (Ragauskas et al., 2006; Saxena, Adhikari, & Goyal, 2009). Meanwhile, high ethanol concentration could be reached from high feeding glucose condition, which resulted in inhibiting yeast growth by ethanol toxicity (Pampulha et al., 1989; Salgueiro et al., 1988).

As shown in Table 4.1, when fermentation was performed under HG condition, the final biomass concentration, 4.2 ± 0.3 g l⁻¹, under ~200 g glucose l⁻¹ was significantly higher than the concentration, 3.2 ± 0.3 g l⁻¹, under ~150 g glucose l⁻¹ feeding concentration. However, a similar observation as the final biomass concentration increasing with the growing of glucose concentration was not seen under the VHG condition. A final biomass concentration under ~250 g glucose l⁻¹ feeding concentration through repeated batch process was observed as 3.1 ± 0.1 g l⁻¹ (Feng et al., 2012), which was lower than the biomass concentration under ~200 g glucose l⁻¹ cases. Higher biomass concentration normally indicated better yeast cells growth (Ingledew & Lin, 2011; Liu et al., 2011b). Under HG condition, biomass increased with the increasing of feeding glucose, which indicated glucose concentration was the primary factor affecting yeast growth. On the other hand, as soon as the fermentation performing under VHG condition, the ethanol toxicity became the new major limitation on yeast growth. As the proof, the biomass concentration was decreasing with the increasing of glucose feeding concentration under VHG condition. For example, 3.1 ± 0.1 g l⁻¹ (Feng et al., 2012) as biomass concentration was observed under ~250 g glucose l⁻¹ feeding concentration, while 3.2 ± 0.3 g l⁻¹ biomass concentration was reported under ~200 g glucose l⁻¹ feeding concentration in this project.

4.1.2 Characteristics of dissolved carbon dioxide driven repeated batch in the presence of DCO₂ control under HG and VHG conditions

The fermentation in the presence of DCO₂ control under HG and VHG feeding condition was performed and the results were presented in Table 4.2.

Table 4.2 Summary of repeated batch fermentation in the presence of DCO₂ control

	~150 g glucose l ⁻¹		~200 g glucose l ⁻¹	
DCO ₂ control level	1000 mg l ⁻¹	750 mg l ⁻¹	1000 mg l ⁻¹	750 mg l ⁻¹
Final ethanol, g l ⁻¹	59.6±2.7	54.2±4.0	70.7±3.4	66.7±1.6
Final biomass, g l ⁻¹	10.7±0.2	10.1±0.3	10.9±0.2	10.1±0.3
Stable cycle time, h	6.6±0.3	6.2±0.2	8.7±0.5	7.3±0.2
Efficiency ¹	0.67 ±0.07	0.62±0.08	0.68±0.06	0.69±0.03
Viability	0.98±0.01	0.99±0.01	0.99±0.01	0.97±0.01
	~250 g glucose l ⁻¹		~300 g glucose l ⁻¹	
Final ethanol, g l ⁻¹	85.1±4.3	83.2±3.0	113.5±7.9	94.3±10.3
Final biomass, g l ⁻¹	9.9±0.7	9.9±0.2	7.4±1.0	8.8±1.5
Stable cycle time, h	14.9±1.9	12.1±1.1	31.5±7.0	21.7±6.0
Efficiency ¹	0.65±0.01	0.69±0.3	0.68±0.02	0.62±0.08
Viability	0.97±0.02	0.99±0.01	0.73±0.08	0.92±0.06

$$^1 \text{ production efficiency} = \frac{\text{ethanol concentration}}{\text{maximal attainable ethanol concentration}}$$

Note: The reported values were average numbers from at least 10 stabilized cycles. The stabilized cycles indicated the difference of cycle time, final ethanol and biomass concentrations between the cycles was lower than 5%.

As illustrated in Table 4.2, under ~150 g glucose l⁻¹ condition, the final ethanol concentration under DCO₂ controlled at 1000 mg l⁻¹ and 750 mg l⁻¹ level were 59.6±2.7 g l⁻¹ and 54.2±4.0 g l⁻¹, respectively. Meanwhile, the final biomass concentration was 10.7±0.2 g l⁻¹ under 1000 mg l⁻¹ DCO₂ control level, and 10.1±0.3 g l⁻¹ under 750 mg l⁻¹ DCO₂ control level. The fermentation time during repeated batch fermentation was 6.6±0.3 h under 1000 mg l⁻¹ DCO₂ control level and 6.2±0.2 h under 750 mg l⁻¹ DCO₂ control level. Similarly, under ~200 g glucose l⁻¹ condition, the final ethanol concentrations under DCO₂ control at 1000 mg l⁻¹ and 750 mg l⁻¹ level were 70.7±3.4 g l⁻¹ and 66.7±1.6 g l⁻¹, respectively. Meanwhile, the final biomass concentration was 10.9±0.2 g l⁻¹ under 1000 mg l⁻¹ DCO₂ control level, and 10.1±0.3

g l⁻¹ under 750 mg l⁻¹ DCO₂ control level. The fermentation time for each batch was 8.7 ± 0.5 h under 1000 mg l⁻¹ DCO₂ control level and 7.3 ± 0.2 h under 750 mg l⁻¹ DCO₂ control level.

Different from in the absence of DCO₂ control cases, the experiments in the presence of DCO₂ control were performed in both of HG and VH₂G fermentation. Under ~250 g glucose l⁻¹ condition, the final ethanol concentrations under DCO₂ control at 1000 mg l⁻¹ and 750 mg l⁻¹ level were 85.1 ± 4.3 g l⁻¹ and 83.2 ± 3.0 g l⁻¹, respectively. Meanwhile, the final biomass concentration was 9.9 ± 0.7 g l⁻¹ under 1000 mg l⁻¹ DCO₂ control level, and 9.9 ± 0.2 g l⁻¹ under 750 mg l⁻¹ DCO₂ control level. The fermentation time for one batch in repeated batch fermentation was 14.9 ± 1.9 h under 1000 mg l⁻¹ DCO₂ control level and 12.1 ± 1.1 h under 750 mg l⁻¹ DCO₂ control level. Similarly, under ~300 g glucose l⁻¹ condition, the stabilized final ethanol concentrations in the presence of DCO₂ control at 1000 mg l⁻¹ and 750 mg l⁻¹ level were 113.5 ± 7.9 g l⁻¹ and 94.3 ± 10.3 g l⁻¹, respectively. Meanwhile, the final biomass concentration was 7.4 ± 1.0 g l⁻¹ under 1000 mg l⁻¹ DCO₂ control level, and 8.8 ± 1.5 g l⁻¹ under 750 mg l⁻¹ DCO₂ control level. The fermentation time for one batch during repeated batch fermentation was 31.5 ± 7.0 h under 1000 mg l⁻¹ DCO₂ control level and 21.7 ± 6.0 h under 750 mg l⁻¹ DCO₂ control level.

As presented in Table 4.2, the ethanol concentration and cycling time in repeated batch process increased with the increasing of initial glucose concentration. Meanwhile, the biomass concentrations were 10.5 ± 0.4 g l⁻¹ in the HG condition and decreased as lowest as ~7.4 ± 1.0 g l⁻¹ under VH₂G condition. Moreover, while the ethanol conversion efficiencies were reported as ~72 ± 8% under HG and VH₂G conditions, the cell viabilities were maintained above ~97 ± 2% where ethanol concentration was lower than 100 g l⁻¹. The highest ethanol concentration, 113.5 ± 7.9 g l⁻¹, as well as the longest stabilized cycle time, 31.5 ± 7.0 hours, were observed with ~300 g glucose l⁻¹ feeding concentration at 1000 mg l⁻¹ DCO₂ control level, and its corresponding viability was 73 ± 8% as the lowest value in the all eight with DCO₂ control conditions.

When DCO₂ level was maintained during repeated batch fermentation process, a lower DCO₂ control level required more air, which resulted in higher DO concentration in the broth. As most studies suggested that more biomass would be produced under a higher DO

concentration in the medium, because of the biomass being prioritized over ethanol fermentation under aerobic condition (Daoud & Searle, 1990). Under ~ 300 g glucose l^{-1} feeding condition, 7.4 ± 1.0 g l^{-1} and 8.8 ± 1.5 g l^{-1} biomass concentrations were observed at 1000 mg l^{-1} and 750 mg l^{-1} DCO₂ control level, respectively, which agreed with the above mentioned conclusion. However, the opposite observations were also discovered in the ~ 150 and ~ 200 g glucose l^{-1} . Under ~ 150 g glucose l^{-1} feeding condition, the biomass concentration as 10.7 ± 1.0 g l^{-1} at 1000 mg l^{-1} DCO₂ control level was greater than that as 10.1 ± 0.3 g l^{-1} at 750 mg l^{-1} DCO₂ control level. Similarly, Under ~ 200 g glucose l^{-1} feeding condition, the biomass concentration as 10.9 ± 0.2 g l^{-1} at 1000 mg l^{-1} DCO₂ control level was greater than that as 10.1 ± 0.3 g l^{-1} at 750 mg l^{-1} DCO₂ control level. These opposite observations could be explained by the inhibition on cell from excess DO concentration in the medium, which was also known as excess oxygen toxicity (Belo et al., 2003; Fornairon-Bonnefond et al., 2002). Under ~ 300 g glucose l^{-1} feeding condition, yeast cells needed to produce ergosterol and sterols to respond ethanol toxicity from high ethanol concentration (Verbelen et al., 2009) by using extra DO in the medium, which resulted in no excess oxygen toxicity being observed under VHGF fermentation condition.

4.2 Mode of dissolved carbon dioxide driven repeated batch fermentation

Section 4.1 described that two fermentation modes were obtained depending on the availability of DCO₂ control. Since ethanol was directly converted from glucose, a higher initial glucose concentration resulted in a higher final ethanol concentration under the same DCO₂ control condition. However, a significant difference of final ethanol concentration between in the absence and presence of DCO₂ control with the same initial glucose concentration was observed in this study. This difference was contributed by purged air, which used to maintain DCO₂ under a control level in the presence of DCO₂ control conditions. While up to 10% of total glucose was being utilized for the formations of biomass and metabolic by-products in the absence of DCO₂ control, only $\sim 65\%$ of ethanol production efficiency was obtained in the presence of DCO₂ control.

4.2.1 Dissolved carbon dioxide profiles during repeated batch fermentation

The DCO₂ concentration profile for batch experiment in the absence of DCO₂ control under ~200 g glucose l⁻¹ condition during repeated batch fermentation was illustrated along with its corresponding biomass, glucose and ethanol concentrations against time in Figure 4.2 (a). Similarly, the DCO₂ concentration profile for single stabilized cycle under same experiment condition was plotted along with its corresponding biomass, glucose and ethanol concentrations against time and shown in Figure 4.2 (b).

Three distinct phases could be identified based on the biomass profile in batch experiment from Figure 4.2 (a). Lag phase, log phase and stationary phase were presented as A-I, A-II and A-III, respectively. Since the experiment was stopped when glucose was depleted and the ethanol concentration was not high enough to inhibit cell growth, death phase was not observed in Figure 4.2 (a). Meanwhile, only two phases, log growth phase as B-I and stationary phase as B-II, were observed in the biomass profile of repeated batch stabilized cycle from Figure 4.2 (b). The repeated batch process has improved the activities as well as ethanol tolerance of yeast, which resulted in removing lag phase and reducing stationary phase. After cycling process was engaged, the initial biomass concentration of each cycle was diluted to half of the stabilized concentration (~2.2 g l⁻¹), which was much higher than the initial biomass concentration in batch process. Therefore, the lag phase of stabilized cycle in repeated batch process could not be observed. While the removal of lag phase significantly reduced total fermentation cycle time, the reduction of stationary phase contributed to a higher ethanol production rate. A similar conclusion was also drawn from the ethanol fermentation experiments through redox-potential driven repeated batch process (Feng et al., 2012).

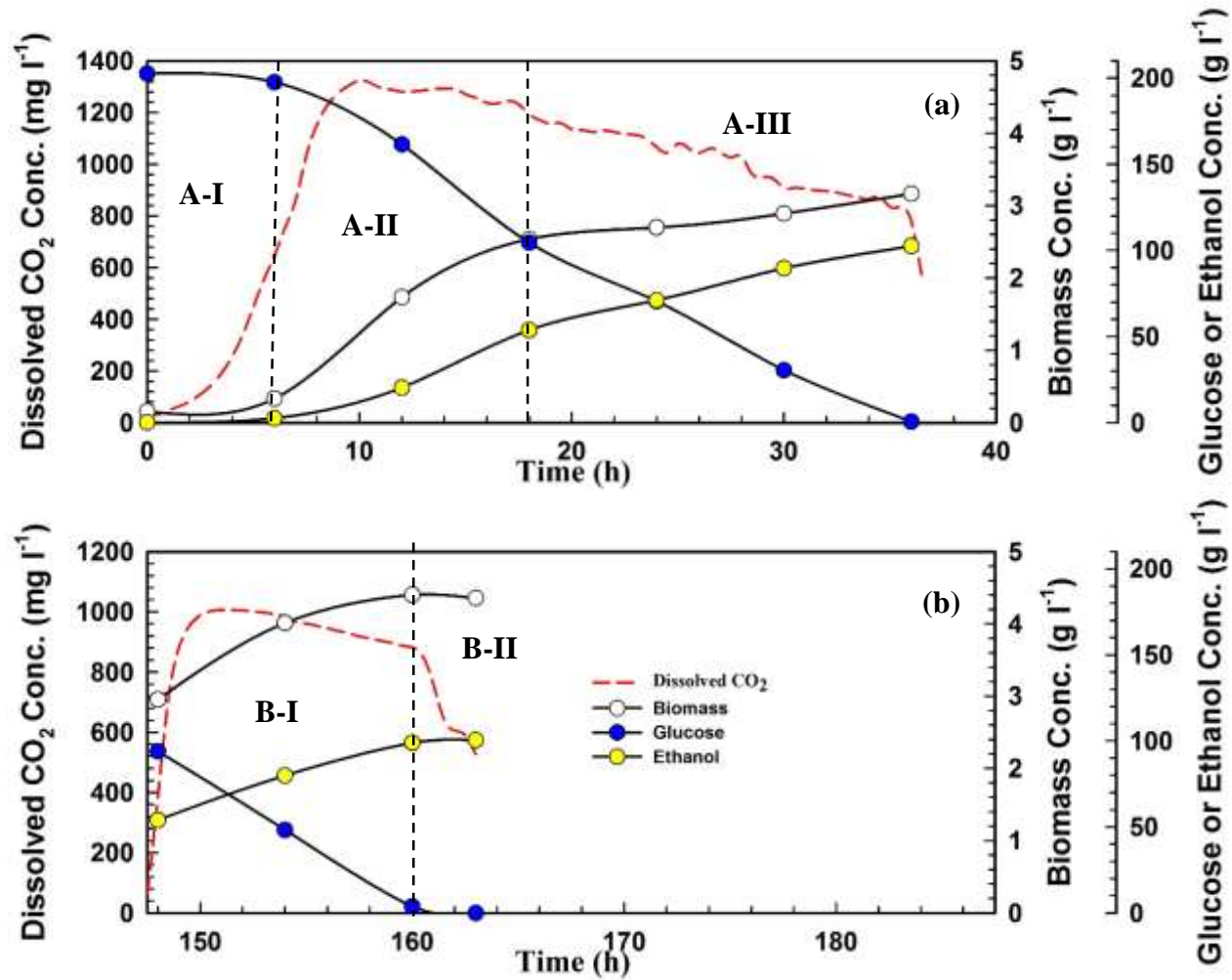


Figure 4.2 Profiles of glucose, ethanol, biomass and DCO₂ concentration in the absence of DCO₂ control of a) batch process and b) stablized cycle in repeated batch process for initial concentration of ~200 g glucose l⁻¹

The DCO₂ concentration profile for batch experiment in the presence of DCO₂ control at 750 mg l⁻¹ level under ~250 g glucose l⁻¹ feeding condition through repeated batch process was plotted along with its corresponding biomass, glucose and ethanol concentrations against time in Figure 4.3 (a). Similarly, the DCO₂ concentration profile for a single stabilized cycle under the same experiment condition was plotted along with its corresponding biomass, glucose and ethanol concentrations and compiled in Figure 4.3 (b).

According to Figure 4.3 (a), the identification of cells growth phase in batch process at 750 mg l⁻¹ DCO₂ control level was as the same as the case in Figure 4.2 (a). However, Figure 4.3 (b) recorded a different result of cells growth phase under 750 mg l⁻¹ DCO₂ control level in the stabilized cycle of repeated batch process comparing with that in the absence of DCO₂ control. Only single phase, log growth phase as B-I, was observed in the Figure 4.3 (b). While lag phase was not seen by repeated batch process, the growth log phase was prolonged by high DO concentration from DCO₂ control.

Moreover, as presented in Figure 4.2 and 4.3, in both absence and presence of DCO₂ control, the final biomass concentration of stabilized cycle in repeated batch process was higher than the concentration in batch process. A similar observation also reported by several authors by using different microorganisms under repeated batch process (Liu & Liu, 2004; Zhao et al., 2010). Liu et al. (2004) applied repeated batch process into glycerol fermentation production by using free *candida krusei*, which pointed out that the average final biomass concentration has been improved by 120.4% with cell cycling in comparison between repeated batch process and batch fermentation. Similarly, the maximal final biomass concentration in D-lactic acid production by *sporolactobacillus sp.* in using repeated batch process was increased from 1.5 g l⁻¹ in the first batch to 1.7 g l⁻¹ as average of last three cycles (Zhao et al., 2010).

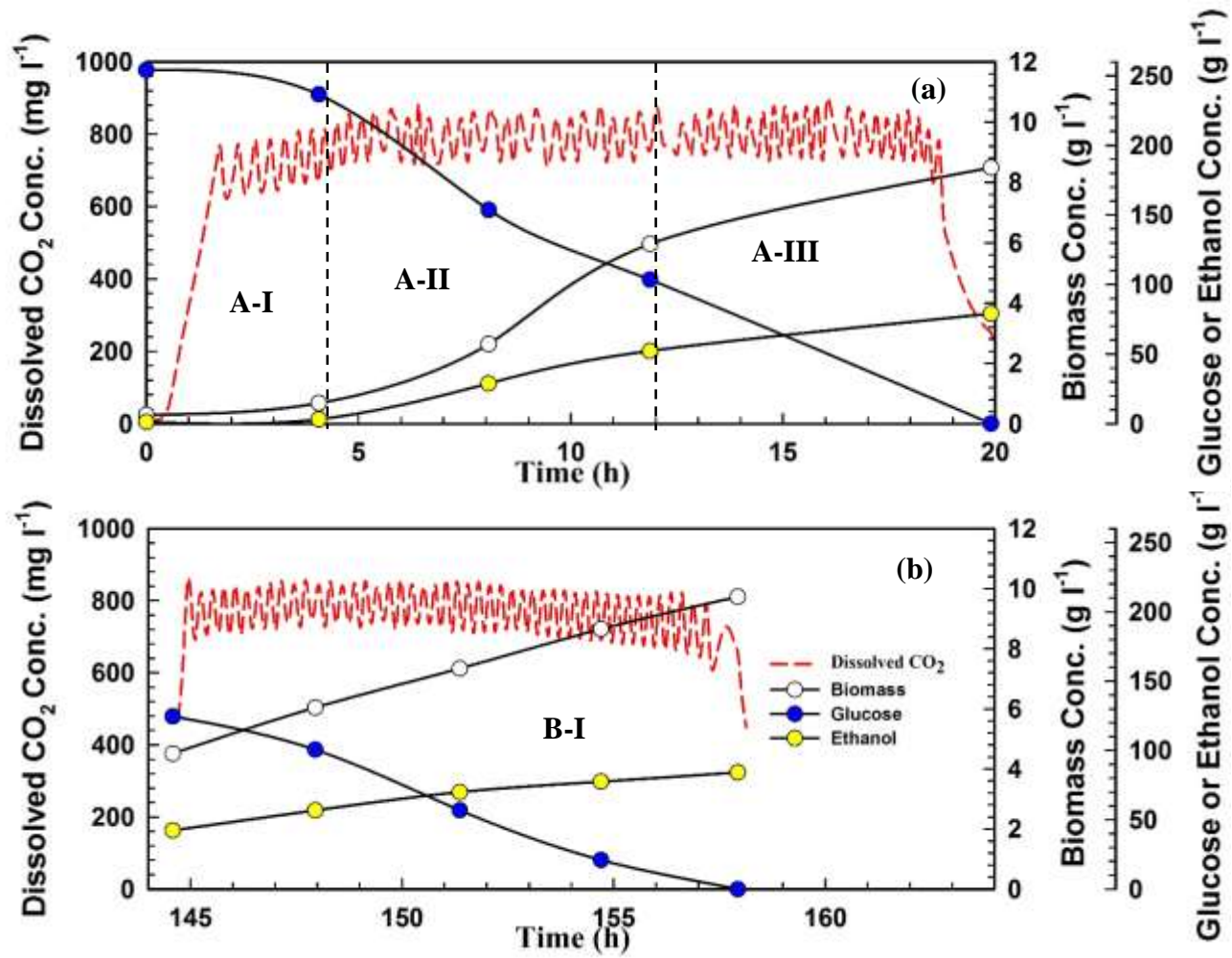


Figure 4.3 Profiles of glucose, ethanol, biomass and DCO₂ concentration at 750 mg l⁻¹ DCO₂ control level of a) batch process and b) stablized cycle in repeated batch process for initial concentration of ~250 g glucose l⁻¹

4.2.2 Initiating a new cycle in the presence and absence of DCO₂ control

Initiating a new cycle during repeated batch fermentation could be performed either manually or with computer. According to previous results (Feng et al., 2012), there were no residual glucose at the end of HG fermentation in the absence of redox potential control. Meanwhile, the cycling time in the repeated batch fermentation could be determined by the changing of redox-potential profiles. However, as soon as the fermentation changing into VHG condition, the residual glucose was always observed even after 72 h fermentation, and the changing of redox potential profile did not provide a clear correlation to glucose utilization. Hence, an empirical based cycle time was determined, such as 36 h under ~ 250 g glucose l⁻¹ case, in order to start a new cycle under VHG conditions (Feng et al., 2012).

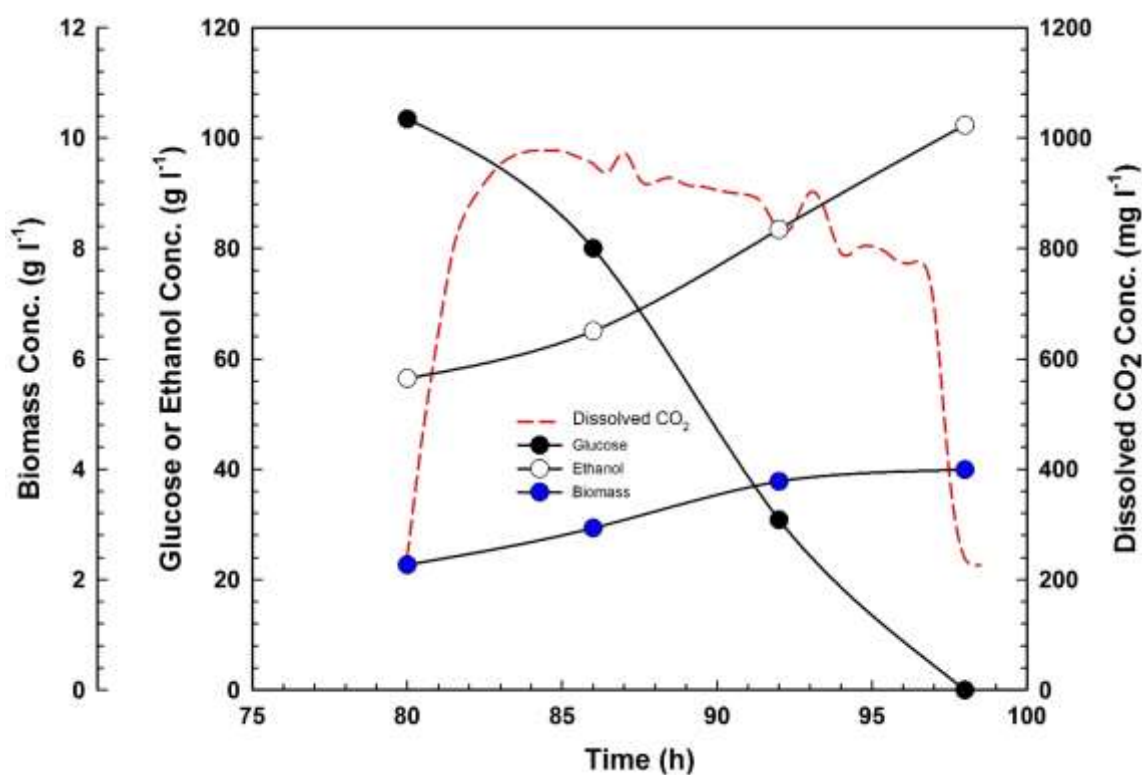


Figure 4.4 Profiles of glucose, ethanol, biomass and DCO₂ concentration in the absence of DCO₂ control in the one of stabilized cycles through repeated batch process for initial concentration of ~ 200 g glucose l⁻¹

As similar as the redox potential driven repeated batch system, in the absence of DCO₂ control, glucose has been completely utilized at the end of each cycle under HG fermentation. The DCO₂ concentration profile along with the glucose, ethanol and biomass concentrations were illustrated in Figure 4.4. As presented in Figure 4.4, the DCO₂ curve was increasing in the beginning of fermentation cycle first from ~80th to ~84th h, following with a slowly decreasing between ~84th and ~97th h, and completing with a sudden drop at ~98th h. In the early stage of fermentation, such as from ~80th to ~84th h in Figure 4.4, the DCO₂ concentration was cumulated with the fermentation progressing.

The DCO₂ concentration in the broth was determined by CO₂ production rate from fermentation and CO₂ evolution rate. When the DCO₂ concentration achieved the maximal CO₂ solubility, CO₂ started to release from aqueous solution to off-gas phase. In the beginning of the fermentation, the CO₂ production rate was higher than CO₂ evolution rate, which resulted in an increase of DCO₂ concentration in the medium. Meanwhile, the CO₂ evolution rate was increasing with the increasing of DCO₂ concentration in the medium, this resulted in the DCO₂ concentration decreasing from 84th to 97th h. As soon as the glucose being depleted, yeast fermentation was stopped and CO₂ production rate became zero. Since DCO₂ concentration was still much higher than CO₂ solubility, the CO₂ would continue to release from the medium. Therefore, a sudden drop of DCO₂ curve was observed at the end of fermentation, as showing at ~98th h in Figure 4.4.

As mentioned above, glucose could not be completely utilized under VHG condition through the repeated batch process. In order to completely exhaust glucose under VHG condition, repeated batch operation was performed in the presence of DCO₂ control. The DCO₂ control methods could be referred to Section 3.2.1. The DCO₂ concentration profile and its corresponding glucose, ethanol and biomass concentrations profiles were illustrated in Figure 4.5. As shown in the figure the DCO₂ profile was constantly oscillated around the set point, such as 750 mg l⁻¹.

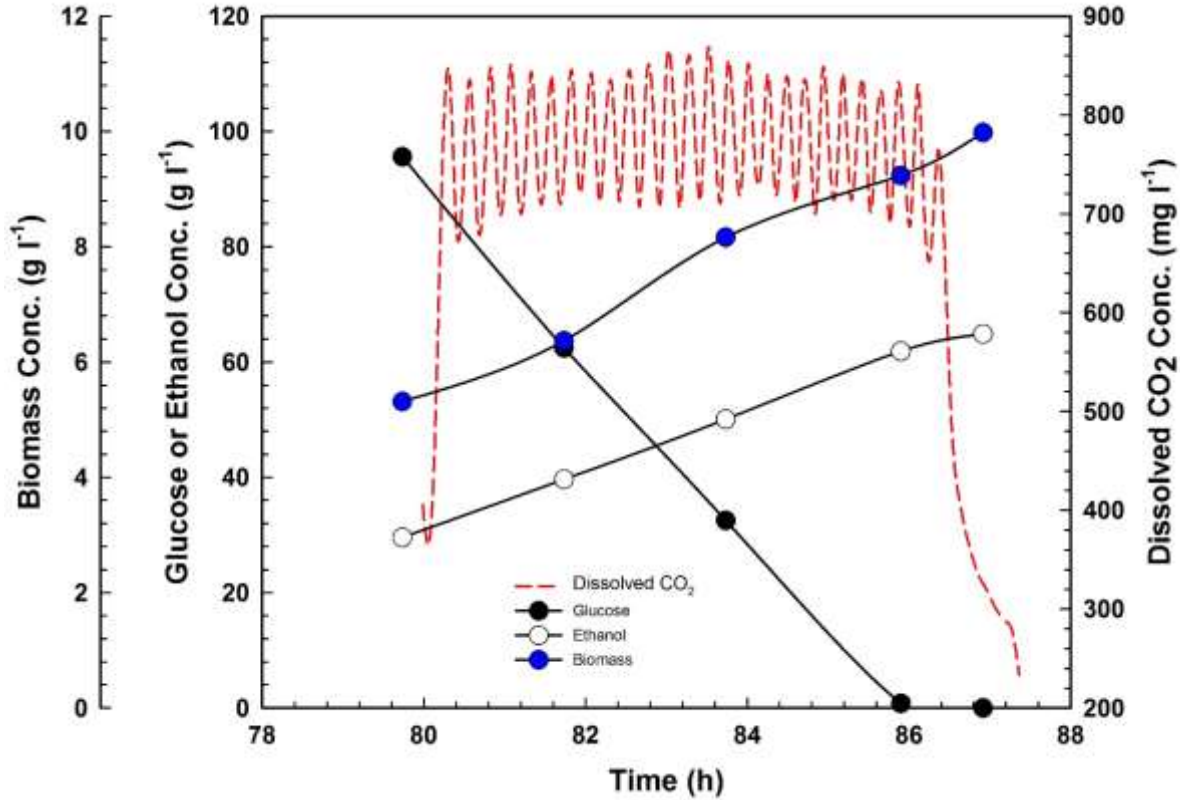


Figure 4.5 Profiles of glucose, ethanol, biomass and DCO_2 concentration at $750 \text{ mg DCO}_2 \text{ l}^{-1}$ control level in the one of stabilized cycles through repeated batch process for initial concentration of $\sim 200 \text{ g glucose l}^{-1}$

As similar as the absence of DCO_2 condition, a dramatically DCO_2 concentration decreasing was also observed when the glucose concentration turned to zero. The explanations about DCO_2 curve changing in Figure 4.5 were similar to the descriptions for Figure 4.4. The only difference of DCO_2 curve between two figures was identified during the DCO_2 control process, which was contributed by air purging to maintain DCO_2 level.

Since a sudden drop of DCO_2 profile was constantly observed when glucose was completely utilized, the process cycling determination was designed to depend on the of DCO_2 curve slope changing: when a series of DCO_2 curve slope decreasing was detected, glucose in the medium was considered as zero. Moreover, the cycling algorithm was also optimized for the absence and presence of DCO_2 control to prevent mis-determination from sensor noise. While the cycling

program was settled as five continuous decreasing of DCO₂ curve slope being recorded in the absence of DCO₂ control, the cycling determination for the presence of DCO₂ control was considered as a five continuous negative values of slope with their corresponding values being lower than 500 mg l⁻¹. Over 50 cycles of repeated batch process have been successfully determined cycling time by using above approach the programs in the absence as well as in the presence of DCO₂ control.

4.3 Effects of DCO₂ control availability and DCO₂ control level on self-cycling period and fermentation results

The fermentation time and results could be affected by several factors, such as: initial glucose concentration, fermentation condition, final ethanol concentration. While the influences on fermentation from initial glucose and final ethanol concentration were discussed in section 4.1 and 4.2, an approximately carbon balance under different fermentation conditions and effects on fermentation time and results from DCO₂ control levels were presented in this section as 4.3.1 and 4.3.2, respectively.

4.3.1 Approximate analysis of DCO₂ driven repeated batch fermentation in the absence and presence of DCO₂ control

The carbon mole utilization rate of initial glucose, produced ethanol, CO₂, glycerol, biomass and other metabolites of one cycle were calculated by Eqn (1) to (6), respectively:

$$M_{tcg} = \frac{C_g}{180 \text{ g mol}^{-1}} \times 6 \times \frac{1}{T_f} \quad (1)$$

$$M_{tce} = \frac{C_e}{46 \text{ g mol}^{-1}} \times 2 \times \frac{1}{2T_f} \quad (2)$$

$$M_{tcc} = \frac{C_e}{46 \text{ g mol}^{-1}} \times \frac{1}{2T_f} \quad (3)$$

$$M_{tcgly} = \frac{C_{gly}}{92 \text{ g mol}^{-1}} \times \frac{1}{2T_f} \quad (4)$$

$$M_{tcb} = \frac{C_b}{27.6 \text{ g mol}^{-1}} \times \frac{1}{2T_f} \quad (5)$$

$$M_{to} = M_{tcg} - M_{tce} - M_{tcc} - M_{tcgly} - M_{tcb} \quad (6)$$

It is important to note that the molecular weight of *Saccharomyces cerevisiae* in one carbon mole biomass was 26.7 h mol^{-1} , which was referred to Lange et al. (2001), and its average elemental composition was $\text{CH}_{1.748}\text{N}_{0.148}\text{O}_{0.596}\text{P}_{0.009}\text{S}_{0.0019}\text{M}_{0.018}$,

The calculated results were averaged from at least ten stabilized cycles under one of ten fermentation conditions, and the averaged values were presented in the Figure 4.6. In the Figure 4.6, the labeled percentage numbers were standard for the percentages of their corresponding metabolites: ethanol, CO_2 , glycerol, biomass or others of total carbon mole numbers in feeding carbon mole numbers from glucose.

As showing in Figure 4.6, 59.4% and 60.7% of total carbon moles from glucose were used to produce ethanol under ~ 150 and $\sim 200 \text{ g glucose l}^{-1}$ feeding concentrations in the absence of DCO_2 control, respectively. Around 45% of total carbon moles from glucose were converted to ethanol under both DCO_2 control levels with all four glucose concentrations. Moreover, the mole percentages of ethanol were slightly decreased with the increasing of glucose concentration under VH condition, 37.9% was recorded as lowest value in the ten conditions.

As mentioned in Subsection 2.2.1, glycerol was major by-product in yeast ethanol fermentation to response stresses on the cells' membrane (Albertyn et al., 1994; Andre et al., 1991). The lowest glycerol concentration in repeated batch fermentation was observed at $\sim 150 \text{ g glucose l}^{-1}$ concentration without DCO_2 control as 4.55 g l^{-1} , and the highest glycerol concentration value was recorded as 10.71 g l^{-1} in $\sim 300 \text{ g glucose l}^{-1}$ at 1000 mg l^{-1} DCO_2 control level. The increasing of glucose feeding concentration and purged air volume resulted in increasing of glycerol concentration at the end of fermentation. While higher glucose concentration contributed in higher osmotic stress level, larger volume of purged air resulted in higher DO concentration in the medium. In order to response to increase osmotic stress in the beginning of fermentation, more glycerol was produced through yeast ethanol fermentation (Albertyn et al., 1994). On the other hand, since glycerol was the major metabolite to restore cytoplasmic redox, the higher DO concentration in

the medium resulted in requiring more glycerol (Belo et al., 2003). As a result, higher glycerol concentration was observed in the presence of DCO₂ control cases than that under without DCO₂

control condition with the same feeding concentration.

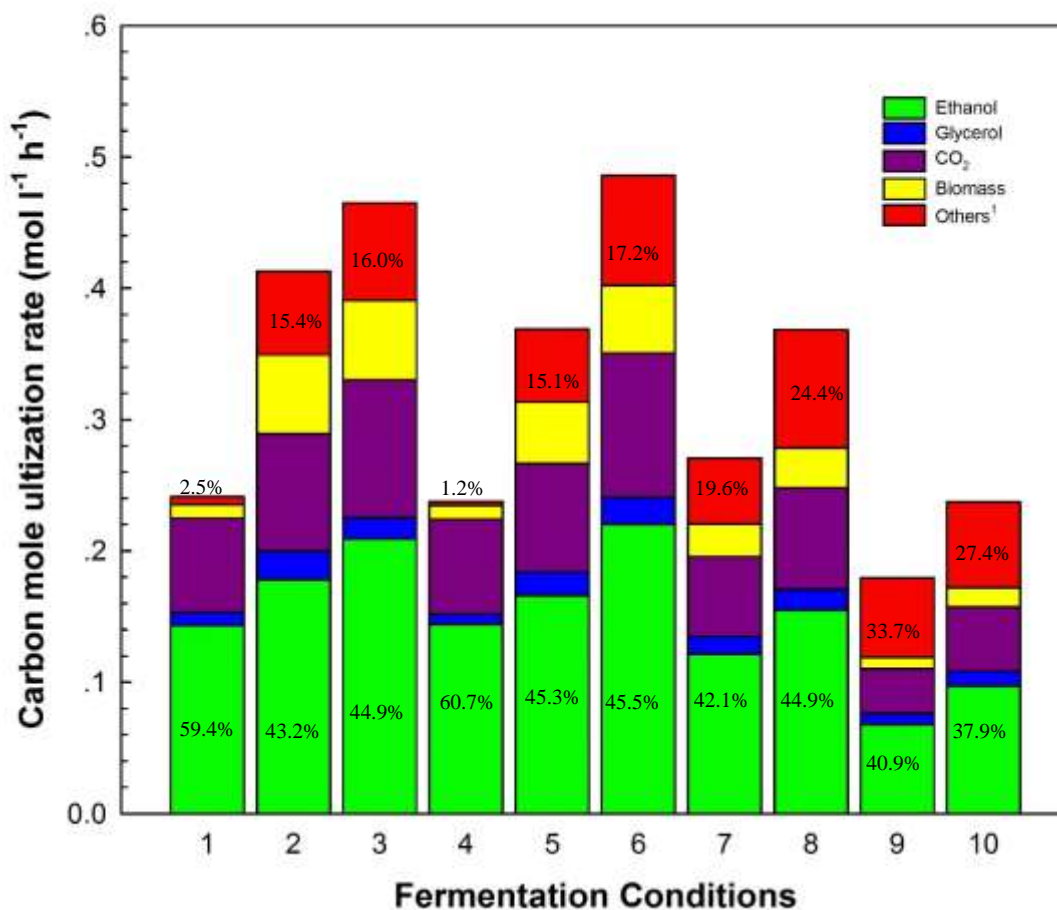


Figure 4.6 Comparisons of carbon mole numbers in produced ethanol, CO₂, biomass and other metabolites in the different fermentation conditions. Condition 1-3 were under ~150 g glucose l⁻¹ in the absence of DCO₂ control, control at 750 mg l⁻¹ and at 1000 mg l⁻¹ level, respectively. Condition 4-6 were under ~200 g glucose l⁻¹ in the absence of DCO₂ control, control at 750 mg l⁻¹ and at 1000 mg l⁻¹ level, respectively. Condition 7-8 were under ~250 g glucose l⁻¹ control at 750 mg l⁻¹ and at 1000 mg l⁻¹ level, respectively. Condition 9-10 were under ~300 g glucose l⁻¹ control at 750 mg l⁻¹ and at 1000 mg l⁻¹ level, respectively. Note: ¹ All the metabolites except glycerol, ethanol and CO₂. Glycerol carbon mole percentages were between 3.2% and 5.1% in ten fermentation conditions. The calculation of condition 1 was presented in Appendix B1.1 as sample calculation.

The reported values are average numbers from at least 10 stabilized cycles. The stabilized cycles indicated the difference of cycle time, final ethanol and biomass concentrations between the cycles was lower than 5%.

Although, the concentration of glycerol concentration showed a significantly difference between different fermentation conditions. The difference of carbon mole percentages of glycerol in total utilized carbon mole under different fermentation conditions was small. The smallest value was reported as 3.2% under ~ 200 g glucose l^{-1} feeding concentration without DCO_2 control, and the highest value was 5.1% under ~ 300 g glucose l^{-1} at 1000 mg l^{-1} DCO_2 control level, which presented only 2% difference between the highest and lowest value.

As mentioned in section 2.1 and 2.2, the yeast metabolic pathways could be altered by the varying of fermentation conditions, which resulted in different metabolites being produced through process. As presented in Figure 4.6, $\sim 4\%$ carbon was converted to biomass during the anaerobic environment, which indicated the ethanol production prioritizing over TCA cycle (Daoud & Searle, 1990). When the fermentation was performed in the presence of DCO_2 control, the carbon moles percentages of total glucose used in ethanol production were decreased to $\sim 45\%$ in all the four glucose concentrations and two DCO_2 control levels. More cells have been produced through the fermentation, due to a high DO concentration maintained during the process through DCO_2 control. Under VH condition, more carbon moles became available from high initial glucose concentration. Therefore, low carbon moles percentage of total glucose used in ethanol production in VH condition was not a necessary indication of a low ethanol concentration.

The highest carbon mole utilization rate was observed at 750 mg l^{-1} dCO_2 control level with 200 g glucose l^{-1} feeding concentration. Meanwhile, under HG condition, a higher ethanol carbon moles utilization rate was associated with a lower ethanol carbon moles percentage and a higher biomass carbon moles percentage, which indicated that higher carbon using in producing biomass would resulted in higher ethanol production rate.

Referring to Table 4.2, under VH condition, a lower biomass concentration was observed at higher glucose concentration, which pointed to a lower carbon moles percentage from glucose to produce biomass, theoretically. A similar observation was also presented in Figure 4.6. While biomass carbon percentage was 6.4% at 750 mg l^{-1} DCO_2 control level and biomass carbon moles

percentage was 4.8% at 1000 mg l⁻¹ level with ~300 g glucose l⁻¹ feeding condition, in ~250 g glucose l⁻¹ feeding condition 9.1% and 8.2% biomass carbon percentage were observed at 750 mg l⁻¹ and 1000 mg l⁻¹ control levels, respectively, which were significantly higher than previous cases.

Moreover, the highest carbon mole percentages in “others” were recorded in ~300 g glucose l⁻¹ conditions at 750 mg l⁻¹ dCO₂ control. Around ~30% carbon resources were used to produce other metabolites, due to the extra oxygen supplement and high ethanol concentration environment. This conclusion also has been discussed by several different authors (Bell et al., 1998; Cronwright et al., 2002; Hounsa et al., 1998; Van Dijck et al., 1995). From this project, a relative higher glycerol concentration, ~10.7 g l⁻¹, did observe at the end of cycle under VHG condition. A similar observation also reported by Lin et al. (2010) which was agreed with some of studies suggesting that yeast produced and intracellular accumulate glycerol to response high stresses environment (Albertyn et al., 1994; Andre et al., 1991).

4.3.2 Effects of dissolved carbon dioxide levels on self-cycling period

As discussed in the previous subsections, the availability of DCO₂ control significantly affected fermentation time and results in each cycle. In order to optimize DCO₂ control level to improve ethanol productivity, the influences from different DCO₂ control levels in fermentation time and results also needed to be identified. However, the current data failed to provide such an information, due to the volume of purged air varying with the changing of DCO₂ control levels. Therefore, a new experiment method was required to develop to detect the influence from DCO₂ levels. The details related to this new experiment method were presented in subsection 3.4.1, which was named as continuous feeding strategy. As presented in subsection 3.4.1, with the same DCO₂ control level, as soon as the repeated batch system being stabilized under one glucose concentration, a higher glucose concentration fed to fermenter until the system stabilized again. Since four glucose concentrations, from ~150 g glucose l⁻¹ to ~300 g glucose l⁻¹, were continuously fed under one DCO₂ control level, the final ethanol concentration between two adjacent glucose

concentrations was increased, incrementally. In order to determine the relationship between ethanol concentration, fermentation time and DCO₂ control levels, the fermentation time of one cycle was plotted against its corresponding final ethanol concentration as shown in Figure 4.7.

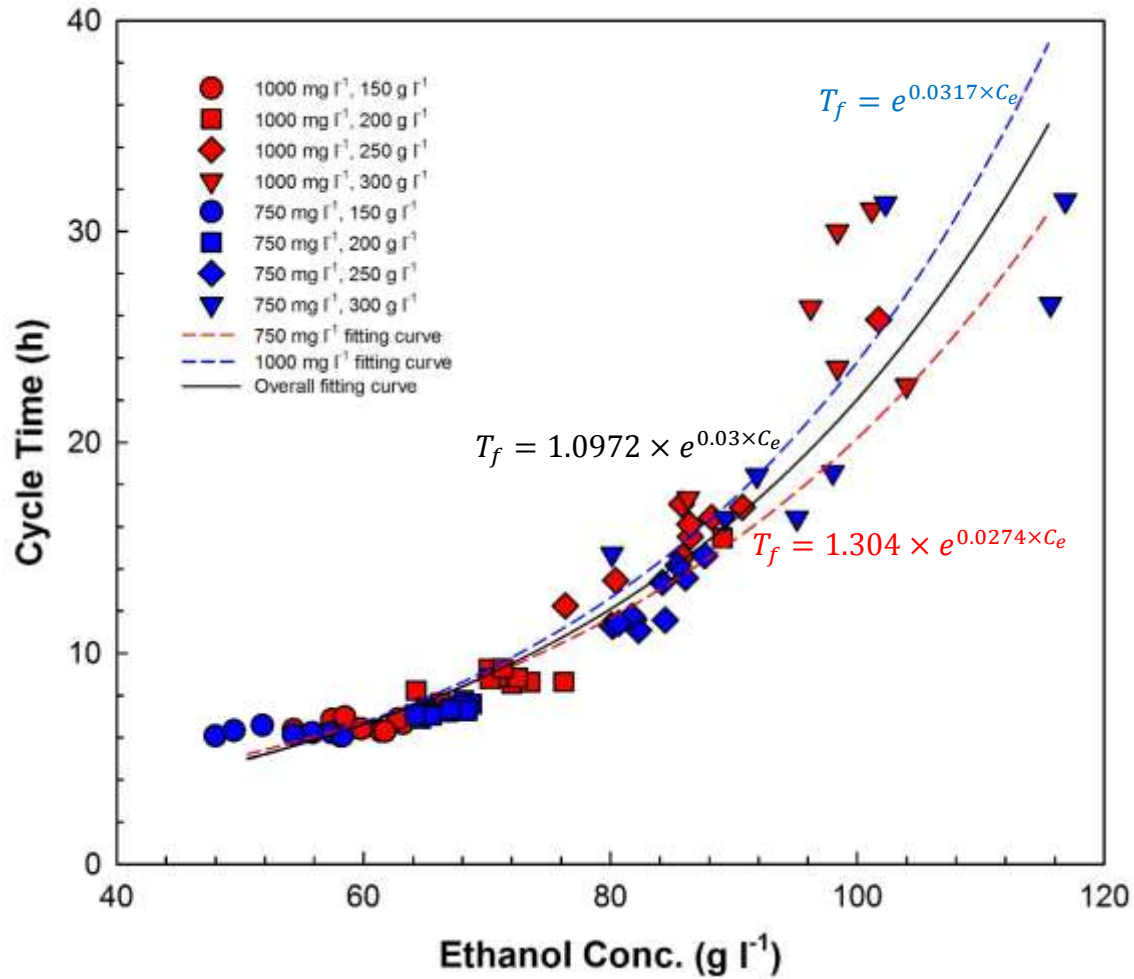


Figure 4.7 Profiles of final ethanol concentration of each cycle against its corresponding fermentation time during repeated batch fermentation in the presence of DCO₂ control at 1000 mg l⁻¹ and 750 mg l⁻¹

Since different feed glucose concentrations were continuously applied into the repeated batch system, the final ethanol concentration would be increased in the first 4-5 cycles and stabilized in the following 10 cycles. While the regions with ethanol concentration periodical increasing was given a name as a transition region, the districts of steady state ethanol concentration was called stabilized region. As shown in Figure 4.7, when the final ethanol concentration was lower than $\sim 90 \text{ g ethanol l}^{-1}$, the data points under the same fermentation condition were concentrated in the stabilized region. These data points indicated that the system reached a steady state after 4-5 cycles. This conclusion matched to the suggestions from biomass concentrations profiles in Figure 4.1. Meanwhile, as soon as the final ethanol concentration increased to above $\sim 90 \text{ g l}^{-1}$, the data points under the same ethanol concentration became scattered, which suggested that the system could not reach steady state at the high ethanol concentration. This observation also agreed with our previous observation: the maximal ethanol tolerance concentration was determined from ~ 85 to 90 g l^{-1} . Once the final ethanol concentration in each cycle was above the tolerance value, the cell's viability would dramatically decrease, which resulted in repeated batch system unstable in the high final ethanol concentration condition (above 90 g l^{-1} cases). Moreover, as shown in Figure 4.7, the slope of curves were significant increased when the ethanol concentration was above $\sim 75 \text{ g l}^{-1}$, which indicated a significantly decreasing of ethanol production rate (half reciprocal of slope of curve). Hence, the $\sim 75 \text{ g ethanol l}^{-1}$ was concluded as the target value for maximizing ethanol productivity.

The ethanol production rate was recognized as Eqn (7):

$$R_e = \frac{C_e}{2 \times T_f} \quad (7)$$

Due to half of working volume withdraw in the harvest process, half of final ethanol concentration was used to calculate ethanol production rate

According to the data shown in Figure 4.7, two equations could be drawn to describe the relationship between final ethanol concentration and its corresponding fermentation time under either 750 mg l^{-1} or 1000 mg l^{-1} DCO₂ control levels. While Eqn (8) was used to present correlation

at 750 mg l⁻¹ DCO₂ controlled case, the relationship at 1000 mg l⁻¹ DCO₂ control level condition was concluded in Eqn (9):

$$T_f = e^{0.0317 \times C_e} \quad (8)$$

$$T_f = 1.304 \times e^{0.0274 \times C_e} \quad (9)$$

Several different mathematical equations, such as power, polynomial and exponential equations, have been tried to fit the curve in Figure 4.7, and the exponential model provided the best fit among all tested equations in the both fitted equations. The coefficients of determination for two fitted equations were both above 90%, which were 92.77% and 94.59% for 750 mg l⁻¹ and 1000 mg l⁻¹ conditions, respectively. Since Eqn (8) and (9) have presented a same tendency and their parameters were close to each other, it was important to identify the difference between these two equations, which was used to determine the effects on fermentation time and results.

The difference between Eqn (8) and (9) was identified by calculating fermentation time under a same ethanol concentration. The settled ethanol concentration was increased from 30 to 90 g l⁻¹ with 5 g l⁻¹ difference. The calculated results and determined difference between two equations with their corresponding ethanol concentrations were presented in Table 4.3.

Table 4.3 Comparison between fitted results from Eqn (8) and Eqn (9)

Assumed ethanol concentration g l ⁻¹	T_{sf1} h	T_{sf2} h	¹ Difference %
² 30	2.59	2.97	12.75
35	3.03	3.40	10.86
40	3.55	3.90	8.92
45	4.16	4.47	6.94
50	4.88	5.13	4.92
55	5.72	5.89	2.85
60	6.70	6.75	0.74
65	7.85	7.74	1.40
70	9.20	8.88	3.49
75	10.78	10.18	5.55
80	12.63	11.67	7.56
85	14.80	13.39	9.52
90	17.34	15.35	11.45

¹Difference = $\frac{|T_{sf1} - T_{sf2}|}{\max(T_{sf1}, T_{sf2})}$; ² sample calculation as shown in Appendix B1.2

As shown in Table 4.3, lower than 10% difference between two fitted fermentation times from Eqn (8) and Eqn (9) was observed when final ethanol concentration was between 40 and 85 g l⁻¹. Due to the uniqueness of bio-reactions, these two results could be considered as identical. Therefore, we concluded that the effects from DCO₂ control levels on fermentation time and results were not significant. Consequently, two fitted equations were combined together as an overall condition as shown and represented by Eqn (10)

$$T_f = 1.0972 \times e^{0.03 \times C_e} \quad (10)$$

The coefficient of determination of Eqn (10) was 92.46%.

In reference to Table 4.1 and 4.2, the ethanol conversion efficiencies in the absence and presence of DCO₂ were kept around ~90% and ~65%, respectively. Hence, with known feeding glucose concentration, the final ethanol concentration in each cycle could be estimated if glucose concentration and its corresponding ethanol conversion efficiency were given. The fermentation time of this mentioned cycle could be concluded from one of Eqn (8) to (10).

4.4 Applicability of DCO₂-driven and DCO₂-controlled repeated batch fermentation

A comparison in ethanol production rate between different initial glucose concentrations and processes was shown and discussed in Subsection 4.4.1. In order to provide better understanding in the improvements from DCO₂ driven and DCO₂ controlled repeated batch fermentation, the applicability of this new process was evaluated in subsection 4.4.2. Since ethanol productivity in the small working volume was linear related to that in the large one, (Mosier et al., 2005; Ogbonna et al., 2001), the ethanol productivity in production scale could be estimated from the laboratory results by several mathematical equations directly.

4.4.1 Comparison of ethanol production rate under high-gravity and very-high-gravity conditions

Ethanol production rates under batch, repeated batch and continuous process were calculated by Eqn (11) to (13), respectively. All the calculated results were presented in Table 4.4 and Table 4.5. Their corresponding data resources were labeled and explained as footnotes.

$$R_{Eb} = \frac{C_e}{T_f} \quad (11)$$

$$R_{Er} = \frac{C_e}{2 \times T_f} \quad (12)$$

$$R_{Ec} = C_e \times D \quad (13)$$

While the calculated ethanol production rates through batch and repeated batch were shown in Table 4.4, the ethanol production rates through continuous process were presented in Table 4.5. As shown in Table 4.4, under batch and repeated batch process, the highest final ethanol concentration was observed from Thomas et al., (1990) as 187.30 g l⁻¹ with longest fermentation time as 130 hours. Meanwhile, the highest ethanol production rate was founded under ~200 g glucose l⁻¹ feeding concentration at 1000 mg l⁻¹ DCO₂ control level through repeated batch process as 4.57 g ethanol l⁻¹ h⁻¹, and the lowest ethanol production rate was reported in batch process with 379 g glucose l⁻¹ feeding concentration as 1.44 g l⁻¹ h⁻¹ (Thomas et al., 1990). As presented in Table

4.5, the highest ethanol production rate under continuous process was $17.39 \text{ g l}^{-1} \text{ h}^{-1}$ under $152 \text{ g glucose l}^{-1}$ feeding concentration with 0.34 h^{-1} dilution rate, and the lowest ethanol production rate was reported as $1.54 \text{ g l}^{-1} \text{ h}^{-1}$ with $303 \text{ g glucose l}^{-1}$ feeding concentration without redox potential control. For all three processes, ethanol production rate was constantly provided a lower value under VHG condition than that under HG condition subjected to same control, and the ethanol production rate in the presence of control was always higher than that without control.

Table 4.4 Comparisons in ethanol production rate between different feeding glucose concentrations through batch and repeated batch processes

Process	Availability of Control	Initial glucose con. (g l^{-1})	Residue glucose con. (g l^{-1})	Fermentation Time (h)	Ethanol con. (g l^{-1})	Ethanol production rate ($\text{g h}^{-1} \text{ l}^{-1}$)
¹ Batch	None	379	0	130	187.30	1.44^4
² Batch	None	201	0	24	89.27	3.72
² Batch	None	251	0	48	109.78	2.29
² Batch	None	280	17.97	48	116.3	2.42
² Batch	Redox potential	209	0	24	90.09	3.75
² Batch	Redox potential	201	0	24	88.25	3.68
² Batch	Redox potential	255	0	48	111.96	2.33
² Batch	Redox potential	252	0	48	116.96	2.44
² Batch	Redox potential	289	12.67	48	112.99	2.35
² Batch	Redox potential	293	12.53	48	131.25	2.73
Repeated batch	None	150	0	11.3	74.6	3.30^*
Repeated batch	None	200	0	14.7	102.5	3.49
³ Repeated batch	None	250	15.19	36	106.76	1.48
Repeated batch	DCO ₂	150	0	6.6	59.6	4.52
Repeated batch	DCO ₂	150	0	6.2	54.2	4.37
Repeated batch	DCO ₂	200	0	8.7	70.7	4.06
Repeated batch	DCO ₂	200	0	7.3	66.7	4.57
Repeated batch	DCO ₂	250	0	14.9	85.1	2.86
Repeated batch	DCO ₂	250	0	12.1	83.2	3.44
Repeated batch	DCO ₂	300	0	31.5	113.5	1.80
Repeated batch	DCO ₂	300	0	21.7	94.3	2.17

Note: ¹ data from Thomas et al., (1990); ² data from Lin et al., (2010); ³ data from Feng et al., (2012); ⁴ sample calculation as shown in Appendix B1.3

Table 4.5 Comparison in ethanol production rate between different feeding glucose concentrations through continuous process

Process	Availability of Control	Initial glucose con. (g l ⁻¹)	Residue glucose con. (g l ⁻¹)	Dilution Rate (h ⁻¹)	Ethanol con. (g l ⁻¹)	Ethanol production rate (g h ⁻¹ l ⁻¹)
¹ Continuous	None	152	0	0.34	51.15	17.39 ³
¹ Continuous	None	191	0	0.21	62.96	13.22
¹ Continuous	None	225	0	0.16	86.57	13.85
¹ Continuous	None	254	0	0.12	102.31	12.28
¹ Continuous	None	312	0	0.05	125.92	6.296
¹ Continuous	None	203	65.88	0.028	68.22	1.91
² Continuous	None	255	130.6	0.028	58.18	1.63
² Continuous	None	303	189.2	0.028	54.85	1.54
² Continuous	Redox potential	203	22.65	0.028	79.32	2.22
² Continuous	Redox potential	203	60.65	0.028	66.54	1.86
² Continuous	Redox potential	255	88.49	0.028	73.27	2.05
² Continuous	Redox potential	303	151.8	0.028	66.99	1.88

Note: ¹ data from Bayrock et al., (2001); ² data from Liu et al., (2012b); ³ sample calculation as shown in Appendix B1.4

Several researchers claimed that a higher ethanol production rate could be achieved through VHG technology rather than HG fermentation (Thomas et al., 1990; 1993; 1996; Bayrock et al., 2001). However, an opposite conclusion was drawn from Table 4.4 and Table 4.5. Although, a significantly higher final ethanol concentration was constantly observed during VHG fermentation comparing with HG counterpart. Due to the ethanol toxicity effects on yeast cells, this high ethanol concentration normally required much longer fermentation time, which resulted in a low ethanol production rate. Since ethanol production rate calculation did not involve downtime, the calculated rate through single stage continuous process was lower than that through batch process found in Table 4.4, which was against the most general beliefs that continuous process providing more ethanol productivity. With the considerations of downtime as 12 h between batches, the continuous process did provide higher productivity. Repeated batch fermentation, as the proposed method in this project, provided a higher ethanol production rate than batch as well as continuous process.

Even with downtime considerations, 2 hours cycling time between cycles did not reduce the ethanol productivity, significantly. Hence, the repeated batch process was considered as the best fitted method in ethanol fermentation.

According to the reported values in Table 4.4 and Table 4.5, it was safe to conclude that HG fermentation provides higher ethanol productivity than VHG fermentation in the absence of process control condition. The VHG technology requires process control, either redox potential or DCO₂, to improve cells activities and viabilities at the end of fermentation, which resulted in higher ethanol production rate. Moreover, a better fermentation result was constantly observed in the repeated batch process than batch and continuous process, which made this method have high potential to apply into industrial production to testify the conclusions from laboratory study.

4.4.2 Evaluation and comparison of ethanol productivities in DCO₂ driven and controlled repeated batch fermentation

It was important to note that: the working volume of fermenter was settled as 10⁵ L and the working time was equal to 7290 hours for all the equations in this section. In the repeated batch fermentation, the glucose utilization was estimated by Eqn. (14), and the biomass and ethanol productivities were calculated by Eqn. (15).

$$G_c = \frac{T_w}{T_f + T_d} \times V_w \times C_g \quad (14)$$

$$B_p(E_p) = \frac{T_w}{T_f + T_d} \times \frac{V_w}{2} \times C_b(C_e) \quad (15)$$

As presented in Subsection 3.3, half of working volume was withdraw to harvest vessel, when one cycle ethanol fermentation was completed. Therefore, only half of working volume was applied in the Eqn. (15). Meanwhile, the downtime between cycles was settled to 2 hours during repeated batch fermentation. All the calculated results in the absence and presence of DCO₂ control under HG and VHG fermentation conditions were presented in Table 4.6.

As illustrated in Table 4.6, for HG fermentation with $\sim 150 \text{ g l}^{-1}$ glucose concentration, $2221 \times 10^6 \text{ g}$ ethanol and $96 \times 10^6 \text{ g}$ biomass was produced from $4895 \times 10^6 \text{ g}$ glucose utilization in the absence of DCO_2 control. Similarly, with the same feeding glucose concentration in the presence of DCO_2 control, $2759 \times 10^6 \text{ g}$ and $2609 \times 10^6 \text{ g}$ ethanol with $497 \times 10^6 \text{ g}$ and $488 \times 10^6 \text{ g}$ biomass was produced from $7994 \times 10^6 \text{ g}$ and $7930 \times 10^6 \text{ g}$ glucose utilization at 1000 mg l^{-1} and 750 mg l^{-1} DCO_2 control level, respectively. With $\sim 200 \text{ g l}^{-1}$ feeding glucose $2228 \times 10^6 \text{ g}$ ethanol and $90 \times 10^6 \text{ g}$ biomass was produced from $4298 \times 10^6 \text{ g}$ glucose utilization in the absence of DCO_2 control. Similarly, with the same feeding glucose concentration in the presence of DCO_2 control, $2625 \times 10^6 \text{ g}$ and $2833 \times 10^6 \text{ g}$ ethanol with $406 \times 10^6 \text{ g}$ and $431 \times 10^6 \text{ g}$ biomass was produced from $7849 \times 10^6 \text{ g}$ and $8189 \times 10^6 \text{ g}$ glucose utilization at 1000 mg l^{-1} and 750 mg l^{-1} DCO_2 control level, respectively. For the VHG fermentation, with $\sim 250 \text{ g l}^{-1}$ feeding glucose concentration in the presence of DCO_2 control, $1994 \times 10^6 \text{ g}$ and $2337 \times 10^6 \text{ g}$ ethanol with $232 \times 10^6 \text{ g}$ and $278 \times 10^6 \text{ g}$ biomass was produced from $6273 \times 10^6 \text{ g}$ and $6801 \times 10^6 \text{ g}$ glucose utilization at 1000 mg l^{-1} and 750 mg l^{-1} DCO_2 control level, respectively. With $\sim 300 \text{ g l}^{-1}$ feeding glucose in the presence of DCO_2 control, $1342 \times 10^6 \text{ g}$ and $1576 \times 10^6 \text{ g}$ ethanol with $87 \times 10^6 \text{ g}$ and $147 \times 10^6 \text{ g}$ biomass was produced from $4014 \times 10^6 \text{ g}$ and $5167 \times 10^6 \text{ g}$ glucose utilization at 1000 mg l^{-1} and 750 mg l^{-1} DCO_2 control level, respectively.

Table 4.6 Glucose ultziation, ethanol and biomass productivity among four initial glucose feeding concentraiton in the absence and presence of DCO₂ control

	Glucose (10 ⁶ g)	Ethanol (10 ⁶ g)	Biomass (10 ⁶ g)	Glucose (10 ⁶ g)	Ethanol (10 ⁶ g)	Biomass (10 ⁶ g)
	~150 g glucose l ⁻¹			~200 g glucose l ⁻¹		
No control ¹	4895	2221	96	4298	2228	90
1000 (mg l ⁻¹)	7994	2759	497	7849	2625	406
750 (mg l ⁻¹)	7930	2609	488	8189	2833	431
	~250 g glucose l ⁻¹			~300 g glucose l ⁻¹		
1000 (mg l ⁻¹)	6273	1994	232	4014	1342	87
750 (mg l ⁻¹)	6801	2337	278	5167	1576	147

Note: ¹sample calculation as shown in Appendix B1.5

According to Table 4.6, for all ten simulated fermentation conditions, the maximal glucose utilization and ethanol productivity were observed at 750 mg l⁻¹ DCO₂ control with ~200 g glucose l⁻¹ feeding concentration, and the maximal biomass productivity was presented at 1000 mg l⁻¹ DCO₂ controlled under ~150 g glucose l⁻¹ feeding concentration. While the glucose utilization in the presence of DCO₂ control was much higher than that without DCO₂ control under the HG condition, the glucose utilization, biomass and ethanol productivities were decreased with the increasing of glucose concentration under VHG condition.

Glucose utilization, biomass and ethanol productivity were determined by their corresponding concentration and fermentation time in each cycle. Higher biomass concentration contributed to higher glucose utilization rate and ethanol production rate with shorter fermentation time, but it also resulted in lower final ethanol concentration. Hence, biomass productivity and glucose utilization was much higher in the presence of DCO₂ control than that in the absence of control; and the ethanol productivities in these two conditions were close to each other. As discussed in the Chapter 2, osmotic pressure in the beginning and ethanol toxicity at the end of fermentation were two major challenges during VHG fermentation. Although, the osmotic pressure has been removed by using repeated batch process in this project, the inhibitions of ethanol toxicity to cell growth still existed under VHG condition. The decrease of biomass concentration with the increasing of glucose concentration indicated that the cell growth was reduced by high ethanol concentration at the end of fermentation, which also resulted in prolonging fermentation time. The longer fermentation time caused fewer cycles, which led to lower annual ethanol productivity even with a high final ethanol concentration per batch.

The profits in bioethanol production were not only determined by production rate but also, affected by the unit price of corn/wheat, biomass and ethanol. Although, the maximal ethanol productivity was observed at 750 mg l⁻¹ DCO₂ control level under 200 g glucose l⁻¹ condition, the ethanol productivity in the absence of DCO₂ control was only ~20% fewer than the maximal value with half of glucose utilization. Due to a high unit price of corn/wheat and low price of biomass

and ethanol, the fermentation in the absence of DCO₂ control under ~200 g glucose l⁻¹ provided higher profits than the presence of DCO₂ control counterpart.

CHAPTER 5 CONCLUSIONS

Dissolved carbon dioxide driven repeated batch system has been successfully applied into the HG and VHG fermentation in the absence and in the presence of DCO₂ control. There were a total of ten sets fermentation conditions conducted in this project, and residual glucose was not observed under any of the performed fermentation conditions. Moreover, in all ten sets of fermentation conditions, the repeated batch fermentation cycling time was determined by labview program as presented in Section 3.4.3.

In summary, the ethanol concentration under DCO₂ control at both of 750 and 1000 mg l⁻¹ control level was significantly lower than that without DCO₂ control under the same feeding glucose concentration. Meanwhile, a lower biomass concentration in the without DCO₂ control condition was observed in this comparison as well. A higher biomass concentration resulted in a shorter fermentation time, which also contributed to a higher ethanol production rate in the presence of DCO₂ control cases. While the highest final ethanol concentration was observed as 113.5 g ethanol l⁻¹ at 1000 mg l⁻¹ DCO₂ controlled with ~300 g glucose l⁻¹ feeding concentration, the lowest ethanol production rate was recorded as 1.18 g l⁻¹ h⁻¹ at the same condition. The highest ethanol production rate was observed as 4.57 g l⁻¹ h⁻¹ and its corresponding ethanol concentration was 66.7 g ethanol l⁻¹ at 1000 mg l⁻¹ DCO₂ control level under ~200 g l⁻¹ glucose feeding concentration. The viabilities of yeast at the end of fermentation were maintained ~90% when their corresponding final ethanol concentrations were lower than 100 g l⁻¹. As soon as the final ethanol concentration at the end of cycle was increased to over ~110 g ethanol l⁻¹, its corresponding viability was decreased to ~70% as shown in the case of controlled at 1000 mg l⁻¹ DCO₂ control level with ~300 g glucose l⁻¹ feeding concentration. The ethanol conversion efficiency was maintained at ~90% and ~65% in the absence and presence of DCO₂ control, respectively.

The dissolved carbon dioxide profiles during repeated batch fermentation were reported in this project. Two cell growth phases, log growth phase and stationary phase, could be identified from DCO₂ profiles in the absence of DCO₂ control through repeated batch process, and only one cell growth phase, log growth phase, was shown in the presence of DCO₂ control. Meanwhile, a sudden decline of DCO₂ profile at the end of each fermentation cycle was constantly observed in both of the absence and the presence of DCO₂ control cases. According to these observations, two algorithms were developed and applied into repeated batch fermentation to determine cycling time under the absence and presence of DCO₂ control conditions.

Carbon balance analysis between the absence and presence of DCO₂ control through repeated batch process postulated that the availability of DCO₂ control would result in different metabolic pathways of the yeast during the fermentation process. Moreover, in the subsection 4.3.2, the comparison and the plotted figure of ethanol concentration against fermentation time suggested an insignificantly effects in fermentation results and cells activities from different DCO₂ control levels. Meanwhile, ~90 g ethanol l⁻¹ as maximal ethanol tolerance concentration and ~75 g ethanol l⁻¹ as maximal ethanol concentration to maximize ethanol production rate were also noticed from Figure 4.7.

Last not the least, comparisons of ethanol production rate between different processes and different initial feeding glucose concentrations concluded that the ethanol production rate in the presence of DCO₂ control was generally higher than that in the absence of DCO₂ control under the same feeding glucose concentration; and the ethanol production rate was decreased with the increasing of feeding glucose concentration under the same DCO₂ control condition. The collected data from this project was also simulated to a production working volume, as 10⁶ L, with 7290 working hours. The calculated values suggested that the fermentation with ~200 g glucose l⁻¹ feeding concentration in the absence of DCO₂ control would provide the best results among all investigated conditions.

CHAPTER 6 RECOMMENDATIONS

The recommendations and suggestions for further improvements of repeated batch process under VHG condition were presented in this section:

As showing in section 4.1.1 and 4.1.2, while the ethanol conversion efficiency in the presence of DCO₂ control fermentation condition was lower than 70%, the conversion efficiency in the absence of DCO₂ control was record as ~90%. As a result, the low ethanol conversion efficiency in the presence of DCO₂ control was the primary concern during the DCO₂ controlled fermentation process. Since DCO₂ level was maintained by purging air into the fermentation broth, excessive oxygen was purged into the medium, which resulted in low ethanol conversion. Consequently, different methods rather than purging air were required to perform DCO₂ level control in the future experiments.

In order to reduce the effects from oxygen in the fermentation process, purging nitrogen was an alternative option to maintain DCO₂ level. However, the dissolved oxygen in the broth may also be removed with the nitrogen purging, which results in inhibiting of cells growth and ethanol production. Hence, redox potential online measurement and control was required with DCO₂ monitoring and control. According to previous study, the redox potential was associate with dissolved oxygen concentration in the medium. The dissolved oxygen concentration could be maintained through redox potential control by using air purging. Moreover, the new proposed system with two parameters could also assist to decouple the effects on cells growth from dissolved oxygen supplement and DCO₂ removal during fermentation process, which was failed to achieved in this project.

As presented in Figure 4.3 and 4.5, an oscillation of DCO₂ profile was constantly observed during repeated batch fermentation in the presence of DCO₂ control, which resulted in failing to perform detailed analysis between purging air quantity and DCO₂ removal. Therefore, tuning of PID controller parameters for DCO₂ level control was required in the future study. The current

PID controller parameters were recorded as following: while proportional term value was 10, both of integral and derivative terms values were 0. The oscillation curves of DCO_2 indicated a decreasing of proportional term and increasing of integral term.

A mathematical model, which was based on fermentation online monitoring of DCO_2 to estimate corresponding ethanol concentration, could also be developed as a future target. As discussed in section 3.2.3, this proposed equation was directly connected to fermentation pH as well as CO_2 concentration in off-gas phase. Therefore, pH and off-gas carbon dioxide online monitoring was required in the new experiments.

CHAPTER 7 REFERENCE

- Aehle, M., Kuprijanov, A., Schaepe, S., Simutis, R., & Lübbert, A. (2011). Simplified off-gas analyses in animal cell cultures for process monitoring and control purposes. *Biotechnology Letters*, 33(11), 2103-2110.
- Albertyn, J., Hohmann, S., & Prior, B. A. (1994). Characterization of the osmotic-stress response in *Saccharomyces cerevisiae*: Osmotic stress and glucose repression regulate glycerol-3-phosphate dehydrogenase independently. *Current Genetics*, 25(1), 12-18.
- Alexandre, H., Rousseaux, I., & Charpentier, C. (1994). Relationship between ethanol tolerance, lipid composition and plasma membrane fluidity in *saccharomyces cerevisiae* and *kloeckera apiculata*. *FEMS Microbiology Letters*, 124(1), 17-22.
- Alfenore, S., Cameleyre, X., Benbadis, L., Bideaux, C., Uribe Larrea, J., Goma, G., Guillouet, S. (2004). Aeration strategy: A need for very high ethanol performance in *saccharomyces cerevisiae* fed-batch process. *Applied Microbiology and Biotechnology*, 63(5), 537-542.
- Alfenore, S., Molina-Jouve, C., Guillouet, S., Uribe Larrea, J., Goma, G., & Benbadis, L. (2002). Improving ethanol production and viability of *saccharomyces cerevisiae* by a vitamin feeding strategy during fed-batch process. *Applied Microbiology and Biotechnology*, 60(1-2), 67-72.
- Andre, L., Hemming, A., & Adler, L. (1991). Osmoregulation in *saccharomyces cerevisiae* studies on the osmotic induction of glycerol production and glycerol 3-phosphate dehydrogenase (NAD⁺). *FEBS Letters*, 286(1), 13-17.
- Angelidaki, I., Ellegaard, L., & Ahring, B. K. (1993). A mathematical model for dynamic simulation of anaerobic digestion of complex substrates: Focusing on ammonia inhibition. *Biotechnology and Bioengineering*, 42(2), 159-166.
- Attfield, P. V. (1997). Stress tolerance: The key to effective strains of industrial baker's yeast. *Nature Biotechnology*, 15(13), 1351-1357.
- Bai, F., Anderson, W., & Moo-Young, M. (2008). Ethanol fermentation technologies from sugar and starch feedstocks. *Biotechnology Advances*, 26(1), 89-105.
- Bayrock, D., & Ingledew, W. M. (2001). Application of multistage continuous fermentation for production of fuel alcohol by very-high-gravity fermentation technology. *Journal of Industrial Microbiology and Biotechnology*, 27(2), 87-93.

- Bell, W., Sun, W., Hohmann, S., Wera, S., Reinders, A., De Virgilio, C., Thevelein, J. M. (1998). Composition and functional analysis of the *saccharomyces cerevisiae* trehalose synthase complex. *The Journal of Biological Chemistry*, 273(50), 33311-33319.
- Belo, I., Pinheiro, R., & Mota, M. (2003). Fed-Batch cultivation of *saccharomyces cerevisiae* in a hyperbaric bioreactor. *Biotechnology Progress*, 19(2), 665-671.
- Beney, L., Marechal, P., & Gervais, P. (2001). Coupling effects of osmotic pressure and temperature on the viability of *saccharomyces cerevisiae*. *Applied Microbiology and Biotechnology*, 56(3-4), 513-516.
- Berchmans, H. J., & Hirata, S. (2008). Biodiesel production from crude *jatropha curcas* L. seed oil with a high content of free fatty acids. *Bioresource Technology*, 99(6), 1716-1721.
- Berovič, M. (1999). Scale-up of citric acid fermentation by redox potential control. *Biotechnology and Bioengineering*, 64(5), 552-557.
- Brendow, K. (2003). Global oil shale issues and perspectives (synthesis of the symposium on oil shale held in tallinn (estonia) on 18 and 19 November 2002). *Oil Shale*, 20(1), 81-92.
- Brown, W. A., Cooper, D. G., & Liss, S. N. (1999). Adapting the self-cycling fermentor to anoxic conditions. *Environmental Science & Technology*, 33(9), 1458-1463.
- Brown, W. A., & Cooper, D. G. (1991). Self-cycling fermentation applied to *acinetobacter calcoaceticus* RAG-1. *Applied and Environmental Microbiology*, 57(10), 2901-2906.
- Bvochora, J., Read, J., & Zvauya, R. (2000). Application of very high gravity technology to the cofermentation of sweet stem sorghum juice and sorghum grain. *Industrial Crops and Products*, 11(1), 11-17.
- Bylund, F., Castan, A., Mikkola, R., Veide, A., & Larsson, G. (2000). Influence of scale-up on the quality of recombinant human growth hormone. *Biotechnology and Bioengineering*, 69(2), 119-128.
- Casey, G. P., Magnus, C. A., & Ingledew, W. M. (1984). High-gravity brewing: Effects of nutrition on yeast composition, fermentative ability, and alcohol production. *Applied and Environmental Microbiology*, 48(3), 639-646.
- Chang, Y., Chang, K., Huang, C., Hsu, C., & Jang, H. (2012). Comparison of batch and fed-batch fermentations using corncob hydrolysate for bioethanol production. *Fuel*, 97, 166-173.

Chen, Y., Krol, J., Huang, W., Cino, J. P., Vyas, R., Mirro, R., & Vaillancourt, B. (2008). DCO₂ on-line measurement used in rapamycin fed-batch fermentation process. *Process Biochemistry*, 43(4), 351-355.

Cord-Ruwisch, R., Seitz, H., & Conrad, R. (1988). The capacity of hydrogenotrophic anaerobic bacteria to compete for traces of hydrogen depends on the redox potential of the terminal electron acceptor. *Archives of Microbiology*, 149(4), 350-357.

Cortón, E., Haim, L., Locascio, G., Galagosky, L., & Kocmur, S. (1999). CO₂-potentiometric determination and electrode construction, a hands-on approach. *Journal of Chemical Education*, 76(9), 1253.

Cronwright, G. R., Rohwer, J. M., & Prior, B. A. (2002). Metabolic control analysis of glycerol synthesis in *saccharomyces cerevisiae*. *Applied and Environmental Microbiology*, 68(9), 4448-4456.

Dahod, S. K. (1993). Dissolved carbon dioxide measurement and its correlation with operating parameters in fermentation processes. *Biotechnology Progress*, 9(6), 655-660.

D'amore, T., Panchal, C. J., Russell, I., & Stewart, G. (1989). A study of ethanol tolerance in yeast. *Critical Reviews in Biotechnology*, 9(4), 287-304.

D'Amore, T., & Stewart, G. G. (1987). Ethanol tolerance of yeast. *Enzyme and Microbial Technology*, 9(6), 322-330.

Daoud, I., & Searle, B. (1990). On-line monitoring of brewery fermentation by measurement of CO₂ evolution rate. *Journal of the Institute of Brewing*, 96(5), 297-302.

D'Auria, S., & Lakowicz, J. R. (2001). Enzyme fluorescence as a sensing tool: New perspectives in biotechnology. *Current Opinion in Biotechnology*, 12(1), 99-104.

Dave, R., & Shah, N. (1998). Ingredient supplementation effects on viability of probiotic bacteria in yogurt. *Journal of Dairy Science*, 81(11), 2804-2816.

De Maranon, I., Marechal, P., & Gervais, P. (1996). Passive response of *saccharomyces cerevisiae* to osmotic shifts: Cell volume variations depending on the physiological state. *Biochemical and Biophysical Research Communications*, 227, 519-523.

Devantier, R., Pedersen, S., & Olsson, L. (2005). Characterization of very high gravity ethanol fermentation of corn mash. effect of glucoamylase dosage, pre-saccharification and yeast strain. *Applied Microbiology and Biotechnology*, 68(5), 622-629.

- Dinh, T. N., Nagahisa, K., Hirasawa, T., Furusawa, C., & Shimizu, H. (2008). Adaptation of *saccharomyces cerevisiae* cells to high ethanol concentration and changes in fatty acid composition of membrane and cell size. *PLoS One*, 3(7), 2623.
- Dixon, N. M., & Kell, D. B. (1989). The inhibition by CO₂ of the growth and metabolism of micro-organisms. *Journal of Applied Bacteriology*, 67(2), 109-136.
- Dyni, J. R. (2006). *Geology and resources of some world oil-shale deposits* US Department of The Interior, US Geological Survey.
- El Haloui, N., Picque, D., & Corrieu, G. (1988). Alcoholic fermentation in winemaking: On-line measurement of density and carbon dioxide evolution. *Journal of Food Engineering*, 8(1), 17-30.
- Feng, S., Srinivasan, S., & Lin, Y.-H. (2012). Redox potential-driven repeated batch ethanol fermentation under very-high-gravity conditions. *Process Biochemistry*, 47(3), 523-527.
- Flach, B., Bendz, K., & Lieberz, S. (2014). *EU-28 biofuels annual EU biofuels annual 2014*. Hague: U.S.D.A Foreign Agricultural Service.
- Fornairon-Bonnefond, C., Demaretz, V., Rosenfeld, E., & Salmon, J. (2002). Oxygen addition and sterol synthesis in *saccharomyces cerevisiae* during enological fermentation. *Journal of Bioscience and Bioengineering*, 93(2), 176-182.
- Frahm, B., Blank, H., Cornand, P., Oelßner, W., Guth, U., Lane, P., Pörtner, R. (2002). Determination of dissolved CO₂ concentration and CO₂ production rate of mammalian cell suspension culture based on off-gas measurement. *Journal of Biotechnology*, 99(2), 133-148.
- François, J., & Parrou, J. L. (2001). Reserve carbohydrates metabolism in the yeast *saccharomyces cerevisiae*. *FEMS Microbiology Reviews*, 25(1), 125-145.
- Gerardi, M. H. (2003). *The microbiology of anaerobic digesters* John Wiley & Sons.
- Gerpen, J. V. (2005). Biodiesel processing and production. *Fuel Processing Technology*, 86(10), 1097-1107.
- Golobič, I., Gjerkeš, H., & Malenšek, J. (1999). On-line estimation of the specific growth rate in the bacitracin fermentation process. *AIChE Journal*, 45(12), 2550-2556.
- Goodrum, J. W., Geller, D. P., & Adams, T. T. (2003). Rheological characterization of animal fats and their mixtures with # 2 fuel oil. *Biomass and Bioenergy*, 24(3), 249-256.

- Hahn-Hägerdal, B., Karhumäki, K., Fonseca, C., Spencer-Martins, I., & Gorwa-Grauslund, M. F. (2007). Towards industrial pentose-fermenting yeast strains. *Applied Microbiology and Biotechnology*, 74(5), 937-953.
- Harrison, D. (1972). Physiological effects of dissolved oxygen tension and redox potential on growing populations of micro-organisms. *Journal of Applied Chemistry and Biotechnology*, 22(3), 417-440.
- Hill, J., Nelson, E., Tilman, D., Polasky, S., & Tiffany, D. (2006). Environmental, economic, and energetic costs and benefits of biodiesel and ethanol biofuels. *Proceedings of the National Academy of Sciences of the United States of America*, 103(30), 11206-11210.
- Ho, C. S., Shanahan, J. F., & Mou, D. (1986). Carbon dioxide transfer in bioreactors. *Critical Reviews in Biotechnology*, 4(2), 185-252.
- Hohmann, S., Bell, W., Neves, M. J., Valckx, D., & Thevelein, J. M. (1996). Evidence for trehalose-6-phosphate dependent and independent mechanisms in the control of sugar influx into yeast glycolysis. *Molecular Microbiology*, 20(5), 981-991.
- Hohmann, S. (2002). Osmotic stress signaling and osmoadaptation in yeasts. *Microbiology and Molecular Biology Reviews: MMBR*, 66(2), 300-372.
- Hounsai, C. G., Brandt, E. V., Thevelein, J., Hohmann, S., & Prior, B. A. (1998). Role of trehalose in survival of *saccharomyces cerevisiae* under osmotic stress. *Microbiology (Reading, England)*, 144 (Pt 3), 671-680.
- Hughes, S., & Cooper, D. (1996). Biodegradation of phenol using the self-cycling fermentation (SCF) process. *Biotechnology and Bioengineering*, 51(1), 112-119.
- Hwang, M. H., Jang, N. J., Hyun, S. H., & Kim, I. S. (2004). Anaerobic bio-hydrogen production from ethanol fermentation: The role of pH. *Journal of Biotechnology*, 111(3), 297-309.
- Ido, Y., Chang, K., Woolsey, T. A., & Williamson, J. R. (2001). NADH: Sensor of blood flow need in brain, muscle, and other tissues. *FASEB Journal: Official Publication of the Federation of American Societies for Experimental Biology*, 15(8), 1419-1421.
- Inglede, W. M. M., & Lin, Y.-H. (2011). 3.05 - ethanol from starch-based feedstocks. In M. Moo-Young (Ed.), *Comprehensive biotechnology (second edition)* (pp. 37-49). Burlington: Academic Press.

Issariyakul, T., Kulkarni, M. G., Meher, L. C., Dalai, A. K., & Bakhshi, N. N. (2008). Biodiesel production from mixtures of canola oil and used cooking oil. *Chemical Engineering Journal*, 140(1), 77-85.

Janata, J. (2009). *Principles of chemical sensors* Springer.

Johnson, H. R., Crawford, P. M., & Bunger, J. W. (2004). Strategic significance of america's oil shale resource: Volume 2--oil shale resources technology and economics.

Johnson, A. (1987). The control of fed-batch fermentation processes-a survey. *Automatica*, 23(6), 691-705.

Jones, A. M., & Ingledew, W. (1994). Fuel alcohol production: Appraisal of nitrogenous yeast foods for very high gravity wheat mash fermentation. *Process Biochemistry*, 29(6), 483-488.

Kawase, Y., Halard, B., & Moo - Young, M. (1992). Liquid-Phase mass transfer coefficients in bioreactors. *Biotechnology and Bioengineering*, 39(11), 1133-1140.

Kaya, C., Hamamci, C., Baysal, A., Akba, O., Erdogan, S., & Saydut, A. (2009). Methyl ester of peanut (*arachis hypogea L*) seed oil as a potential feedstock for biodiesel production. *Renewable Energy*, 34(5), 1257-1260.

Keim, C. R. (1983). Technology and economics of fermentation alcohol-an update. *Enzyme and Microbial Technology*, 5(2), 103-114.

Kjaergaard, L. (1977). The redox potential: Its use and control in biotechnology. *Advances in biochemical engineering, volume 7* (pp. 131-150) Springer.

Kruger, L., Pickerell, A., & Axccl, B. (1992). The sensitivity of different brewing yeast strains to carbon dioxide inhibition: fermentation and production of flavour-active volatile compounds. *Journal of the Institute of Brewing*, 98(2), 133-138.

Kühbeck, F., Müller, M., Back, W., Kurz, T., & Krottenthaler, M. (2007). Effect of hot trub and particle addition on fermentation performance of *saccharomyces cerevisiae*. *Enzyme and Microbial Technology*, 41(6), 711-720.

Lal, R. (2007). Cellulosic ethanol biofuel researchers prepare to reap a new harvest. *Science*, 314, 1488, 1491.

Lange, H.C., & Heijnen, J.J. (2001). Statistical reconciliation of the elemental and molecular biomass composition of *Saccharomyces cerevisiae*. *Biotechnology and bioengineering* 75(3), 334-344.

Laopaiboon, L., Nuanpeng, S., Srinophakun, P., Klanrit, P., & Laopaiboon, P. (2009). Ethanol production from sweet sorghum juice using very high gravity technology: Effects of carbon and nitrogen supplementations. *Bioresource Technology*, 100(18), 4176-4182.

Laopaiboon, L., Thanonkeo, P., Jaisil, P., & Laopaiboon, P. (2007). Ethanol production from sweet sorghum juice in batch and fed-batch fermentations by *saccharomyces cerevisiae*. *World Journal of Microbiology and Biotechnology*, 23(10), 1497-1501.

Lee, S. Y. (1996). High cell-density culture of *escherichia coli*. *Trends in Biotechnology*, 14(3), 98-105.

Leung, D. Y., Wu, X., & Leung, M. (2010). A review on biodiesel production using catalyzed transesterification. *Applied Energy*, 87(4), 1083-1095.

Lin, Y.-H., & Tanaka, S. (2006). Ethanol fermentation from biomass resources: Current state and prospects. *Applied Microbiology and Biotechnology*, 69(6), 627-642.

Lin, Y.-H., Chien, W., Duan, K., & Chang, P. R. (2011). Effect of aeration timing and interval during very-high-gravity ethanol fermentation. *Process Biochemistry*, 46(4), 1025-1028.

Lin, Y.-H., Chien, W., & Duan, K. (2010). Correlations between reduction–oxidation potential profiles and growth patterns of *saccharomyces cerevisiae* during very-high-gravity fermentation. *Process Biochemistry*, 45(5), 765-770.

Lindorfer, H., Waltenberger, R., Köllner, K., Braun, R., & Kirchmayr, R. (2008). New data on temperature optimum and temperature changes in energy crop digesters. *Bioresource Technology*, 99(15), 7011-7019.

Liu, Y., & Liu, D. (2004). Kinetic study on glycerol production by repeated batch fermentation using free *candida krusei*. *Process Biochemistry*, 39(11), 1507-1510.

Liu, C., Lin, Y.-H., & Bai, F. (2011a). Ageing vessel configuration for continuous redox potential-controlled very-high-gravity fermentation. *Journal of Bioscience and Bioengineering*, 111(1), 61-66.

Liu, C., Lin, Y.-H., & Bai, F. (2011b). Development of redox potential-controlled schemes for very-high-gravity ethanol fermentation. *Journal of Biotechnology*, 153(1–2), 42-47.

- Liu, C., Lin, Y.-H., & Bai, F. (2012). Ageing vessel design and optimization for continuous very-high-gravity ethanol fermentation processes. *Process Biochemistry*, 47(1), 57-61.
- Lloyd, D., Morrell, S., Carlsen, H. N., Degn, H., James, P. E., & Rowlands, C. C. (1993). Effects of growth with ethanol on fermentation and membrane fluidity of *saccharomyces cerevisiae*. *Yeast*, 9(8), 825-833.
- Lu, P., Yuan, T., Feng, Q., & Sun, Y. (2014). Environmental concerns of shale gas production in China. *Energy Sources, Part A: Recovery, Utilization, and Environmental Effects*, 36(6), 638-642.
- Lübbert, A., & Bay Jørgensen, S. (2001). Bioreactor performance: A more scientific approach for practice. *Journal of Biotechnology*, 85(2), 187-212.
- Ma, F., & Hanna, M. A. (1999). Biodiesel production: A review. *Bioresource Technology*, 70(1), 1-15.
- Marechal, P., & Gervais, P. (1994). Yeast viability related to water potential variation: Influence of the transient phase. *Applied Microbiology and Biotechnology*, 42(4), 617-622.
- Michel, J., Weiske, A., & Möller, K. (2010). The effect of biogas digestion on the environmental impact and energy balances in organic cropping systems using the life-cycle assessment methodology. *Renewable Agriculture and Food Systems*, 25(03), 204-218.
- Morimura, S., Ling, Z. Y., & Kida, K. (1997). Ethanol production by repeated-batch fermentation at high temperature in a molasses medium containing a high concentration of total sugar by a thermotolerant flocculating yeast with improved salt-tolerance. *Journal of Fermentation and Bioengineering*, 83(3), 271-274.
- Morris, G. J., Winters, L., Coulson, G. E., & Clarke, K. J. (1986). Effect of osmotic stress on the ultrastructure and viability of the yeast *saccharomyces cerevisiae*. *Journal of General Microbiology*, 132(7), 2023-2034.
- Mosier, N. S., Hendrickson, R., Brewer, M., Ho, N., Sedlak, M., Dreshel, R., Ladisch, M. R. (2005). Industrial scale-up of pH-controlled liquid hot water pretreatment of corn fiber for fuel ethanol production. *Applied Biochemistry and Biotechnology*, 125(2), 77-97.
- Nagodawithana, T. W., Castellano, C., & Steinkraus, K. H. (1974). Effect of dissolved oxygen, temperature, initial cell count, and sugar concentration on the viability of *saccharomyces cerevisiae* in rapid fermentations. *Applied Microbiology*, 28(3), 383-391.

- Navani, N. K., & Li, Y. (2006). Nucleic acid aptamers and enzymes as sensors. *Current Opinion in Chemical Biology*, 10(3), 272-281.
- Nelson, L. A., Foglia, T. A., & Marmer, W. N. (1996). Lipase-catalyzed production of biodiesel. *Journal of the American Oil Chemists' Society*, 73(9), 1191-1195.
- O'CONNOR, E., & Ingledew, W. (1989). Effect of the timing of oxygenation on very high gravity brewing fermentations. *Journal of the American Society of Brewing Chemists*, 48(1), 26-32.
- Ogbonna, J. C., Mashima, H., & Tanaka, H. (2001). Scale up of fuel ethanol production from sugar beet juice using loofa sponge immobilized bioreactor. *Bioresource Technology*, 76(1), 1-8.
- Pampulha, M., & Loureiro-Dias, M. (1989). Combined effect of acetic acid, pH and ethanol on intracellular pH of fermenting yeast. *Applied Microbiology and Biotechnology*, 31(5-6), 547-550.
- Pattison, R. N., Swamy, J., Mendenhall, B., Hwang, C., & Frohlich, B. T. (2000). Measurement and control of dissolved carbon dioxide in mammalian cell culture processes using an in situ fiber optic chemical sensor. *Biotechnology Progress*, 16(5), 769-774.
- Peidong, Z., Yanli, Y., Yongsheng, T., Xutong, Y., Yongkai, Z., Yonghong, Z., & Lisheng, W. (2009). Bioenergy industries development in china: Dilemma and solution. *Renewable and Sustainable Energy Reviews*, 13(9), 2571-2579.
- Pereira, F. B., Guimarães, P. M. R., Teixeira, J. A., & Domingues, L. (2010). Optimization of low-cost medium for very high gravity ethanol fermentations by *saccharomyces cerevisiae* using statistical experimental designs. *Bioresource Technology*, 101(20), 7856-7863.
- Pradeep, P., Reddy, O. V. S., Mohan, P. R., & Ko, S. (2012). Process optimization for ethanol production from very high gravity (VHG) finger millet medium using response surface methodology. *Iranian Journal of Biotechnology*, 10(3)
- Pratt, P. L., Bryce, J. H., & Stewart, G. G. (2003). The effects of osmotic pressure and ethanol on yeast viability and morphology. *Journal of the Institute of Brewing*, 109(3), 218-228.
- Pretreatment, D. (2011). Process design and economics for biochemical conversion of lignocellulosic biomass to ethanol. *Contract*, 303, 275-3000.
- Ragauskas, A. J., Williams, C. K., Davison, B. H., Britovsek, G., Cairney, J., Eckert, C. A., Tschaplinski, T. (2006). The path forward for biofuels and biomaterials. *Science (New York, N.Y.)*, 311(5760), 484-489.

- Ribeiro, M. J., Le ão, L. S., Morais, P. B., Rosa, C. A., & Panek, A. D. (1999). Trehalose accumulation by tropical yeast strains submitted to stress conditions. *Antonie Van Leeuwenhoek*, 75(3), 245-251.
- Royce, P. N., & Thornhill, N. F. (1991). Estimation of dissolved carbon dioxide concentrations in aerobic fermentations. *AIChE Journal*, 37(11), 1680-1686.
- Ryan, S., & Jiang, Y. (2013). *China-peoples republic of biofuels annual 2014*. Beijing: U.S.D.A Foreign Agricultural Service.
- Sahoo, P., & Das, L. (2009). Process optimization for biodiesel production from *jatropha*, *karanja* and polanga oils. *Fuel*, 88(9), 1588-1594.
- Salgueiro, S. P., Sa-Correia, I., & Novais, J. M. (1988). Ethanol-induced leakage in *saccharomyces cerevisiae*: Kinetics and relationship to yeast ethanol tolerance and alcohol fermentation productivity. *Applied and Environmental Microbiology*, 54(4), 903-909.
- Saraf, S., & Thomas, B. (2007). Influence of feedstock and process chemistry on biodiesel quality. *Process Safety and Environmental Protection*, 85(5), 360-364.
- Saxena, R., Adhikari, D., & Goyal, H. (2009). Biomass-based energy fuel through biochemical routes: A review. *Renewable and Sustainable Energy Reviews*, 13(1), 167-178.
- Scheper, T., Hilmer, J., Lammers, F., Müller, C., & Reinecke, M. (1996). Biosensors in bioprocess monitoring. *Journal of Chromatography A*, 725(1), 3-12.
- Scheper, T., & Lammers, F. (1994). Fermentation monitoring and process control. *Current Opinion in Biotechnology*, 5(2), 187-191.
- Schmidt, S. J. (2003). New directions for shale oil: Path to a secure new oil supply well into this century. *Oil Shale*, 20(3), 333-346.
- Schumpe, A., & Deckwer, W. (1979). Estimation of O₂ and CO₂ solubilities in fermentation media. *Biotechnology and Bioengineering*, 21(6), 1075-1078.
- Schumpe, A., Quicker, G., & Deckwer, W. (1982). Gas solubilities in microbial culture media. *Reaction engineering* (pp. 1-38) Springer.
- Sheppard, J. D., & Cooper, D. G. (1990). Development of computerized feedback control for the continuous phasing of *bacillus subtilis*. *Biotechnology and Bioengineering*, 36(5), 539-545.

- Shoda, M., & Ishikawa, Y. (1981). Carbon dioxide sensor for fermentation systems. *Biotechnology and Bioengineering*, 23(2), 461-466.
- Sieblist, C., Jenzsch, M., Pohlscheidt, M., & Luebbert, A. (2011). Underlying principles-bioreactor fluid dynamics. *Comprehensive Biotechnology*, 2, 47-62.
- Simon, D., Müller, R., Große, H., Bley, T., & Babel, W. (2000). Response of *ralstonia eutropha JMP 134* to long-term exposure to toxic substrates in nutristat cultivation as indicated by on-line fluorescence measurements. *Bioprocess Engineering*, 23(1), 1-10.
- Simpson, R., & Sastry, S. (2013). *Chemical and bioprocess engineering* Springer.
- Sipior, J., Randers-Eichhorn, L., Lakowicz, J. R., Carter, G. M., & Rao, G. (1996). Phase fluorometric optical carbon dioxide gas sensor for fermentation Off - Gas monitoring. *Biotechnology Progress*, 12(2), 266-271.
- Smart, K. A., Chambers, K. M., Lambert, I., Jenkins, C., & Smart, C. A. (1999). Use of methylene violet staining procedures to determine yeast viability and vitality. *Journal of the American Society of Brewing Chemists*, 57(1), 18-23.
- Song, H., Lee, J. W., Choi, S., You, J. K., Hong, W. H., & Lee, S. Y. (2007). Effects of dissolved CO₂ levels on the growth of *mannheimia succiniciproducens* and succinic acid production. *Biotechnology and Bioengineering*, 98(6), 1296-1304.
- Srinivasan, S., Feng, S., & Lin, Y.-H. (2012). Dissolved carbon dioxide concentration profiles during very-high-gravity ethanol fermentation. *Biochemical Engineering Journal*, 69(0), 41-47.
- Tengerdy, R. P. (1961). Redox potential changes in the 2-keto-L-gulonic acid fermentation—I. correlation between redox potential and dissolved oxygen concentration. *Journal of Biochemical and Microbiological Technology and Engineering*, 3(3), 241-253.
- Thomas, K., Hynes, S., & Ingledew, W. (1996). Practical and theoretical considerations in the production of high concentrations of alcohol by fermentation. *Process Biochemistry*, 31(4), 321-331.
- Thomas, K., Hynes, S., Jones, A., & Ingledew, W. (1993). Production of fuel alcohol from wheat by VHG technology. *Applied Biochemistry and Biotechnology*, 43(3), 211-226.
- Thomas, K. C., Hynes, S. H., & Ingledew, W. M. (1994). Effects of particulate materials and osmoprotectants on very-high-gravity ethanolic fermentation by *saccharomyces cerevisiae*. *Applied and Environmental Microbiology*, 60(5), 1519-1524.

- Thomas, K. C., & Ingledew, W. M. (1990). Fuel alcohol production: Effects of free amino nitrogen on fermentation of very-high-gravity wheat mash. *Applied and Environmental Microbiology*, 56(7), 2046-2050.
- U.S. Energy Information Administration. (2014a). *Annual energy outlook 2014 with projections to 2040*. Washington DC: U. S. Department of Energy.
- U.S. Energy Information Administration. (2014b). *Review of emerging resources: U. S. shale gas and shale oil plays*. Washington DC: U.S. Department of Energy.
- Van Dijck, P., Colavizza, D., Smet, P., & Thevelein, J. M. (1995). Differential importance of trehalose in stress resistance in fermenting and nonfermenting *saccharomyces cerevisiae* cells. *Applied and Environmental Microbiology*, 61(1), 109-115.
- Verbelen, P., Saerens, S., Van Mulders, S., Delvaux, F., & Delvaux, F. (2009). The role of oxygen in yeast metabolism during high cell density brewery fermentations. *Applied Microbiology and Biotechnology*, 82(6), 1143-1156.
- Verduyn, C., Postma, E., Scheffers, W. A., & van Dijken, J. P. (1990). Physiology of *saccharomyces cerevisiae* in anaerobic glucose-limited chemostat cultures. *Journal of General Microbiology*, 136(3), 395-403.
- Vidic, R. D., Brantley, S. L., Vandenbossche, J. M., Yoxtheimer, D., & Abad, J. D. (2013). Impact of shale gas development on regional water quality. *Science (New York, N.Y.)*, 340(6134), 1235009.
- Voet, D., Voet, J. G., & Pratt, C. W. (1999). *Fundamentals of biochemistry*. John Wiley: New York.
- Walker, G. M. (1998). *Yeast physiology and biotechnology* John Wiley & Sons.
- Wang, F., Gao, C., Yang, C., & Xu, P. (2007). Optimization of an ethanol production medium in very high gravity fermentation. *Biotechnology Letters*, 29(2), 233-236.
- Ward, A. J., Hobbs, P. J., Holliman, P. J., & Jones, D. L. (2008). Optimization of the anaerobic digestion of agricultural resources. *Bioresource Technology*, 99(17), 7928-7940.
- Weiland, P. (2010). Biogas production: Current state and perspectives. *Applied Microbiology and Biotechnology*, 85(4), 849-860.

- Wolf, G., Almeida, J. S., Pinheiro, C., Correia, V., Rodrigues, C., Reis, M. A., & Crespo, J. G. (2001). Two-dimensional fluorometry coupled with artificial neural networks: A novel method for on-line monitoring of complex biological processes. *Biotechnology and Bioengineering*, 72(3), 297-306.
- Wooley, R., Ruth, M., Glassner, D., & Sheehan, J. (1999). Process design and costing of bioethanol technology: A tool for determining the status and direction of research and development. *Biotechnology Progress*, 15(5), 794-803.
- Wu, X., Staggenborg, S., Prophet, J. L., Rooney, W. L., Yu, J., & Wang, D. (2010). Features of sweet sorghum juice and their performance in ethanol fermentation. *Industrial Crops and Products*, 31(1), 164-170.
- Xi, Y., Chen, K., Li, J., Fang, X., Zheng, X., Sui, S., Wei, P. (2011). Optimization of culture conditions in CO₂ fixation for succinic acid production using *actinobacillus succinogenes*. *Journal of Industrial Microbiology & Biotechnology*, 38(9), 1605-1612.
- Yaman, T., & Shimizu, S. (1984). *Fed-batch techniques in microbial processes* Springer.
- Yang, X., Wang, B., Cui, F., & Tan, T. (2005). Production of lipase by repeated batch fermentation with immobilized *rhizopus arrhizus*. *Process Biochemistry*, 40(6), 2095-2103.
- Zhao, B., Wang, L., Li, F., Hua, D., Ma, C., Ma, Y., & Xu, P. (2010). Kinetics of d-lactic acid production by *sporolactobacillus sp.* strain CASD using repeated batch fermentation. *Bioresource Technology*, 101(16), 6499-6505.
- Zosel, J., Oelßner, W., Decker, M., Gerlach, G., & Guth, U. (2011). The measurement of dissolved and gaseous carbon dioxide concentration. *Measurement Science and Technology*, 22(7), 072001 (45pp).

APPENDIX A

A1-Raw experimental data figures

The raw experimental data of DCO₂, glucose, biomass and ethanol concentrations in ten fermentation conditions by using independently feeding method was plotted in Figures A1.1-A1.10. The correlation between fermentation conditions and figure numbers was labeled in Table A1.1. Moreover, the summary of each fermentation condition in the absence and the presence of DCO₂ was presented in Table 4.1 and 4.2, respectively. Meanwhile, the raw experimental data of DCO₂, glucose, biomass and ethanol concentrations at 1000 mg l⁻¹ and 750 mg l⁻¹ by using continuously feeding method was plotted in Figures A1.11 and A1.12, respectively.

Table A1.1 Correlation between fermentation condition and figure number

Glucose con. (g l ⁻¹)	DCO ₂ control level (mg l ⁻¹)	Figure no.
150	without control	A1.1
150	1000	A1.2
150	750	A1.3
200	without control	A1.4
200	1000	A1.5
200	750	A1.6
250	1000	A1.7
250	750	A1.8
300	1000	A1.9
300	750	A1.10

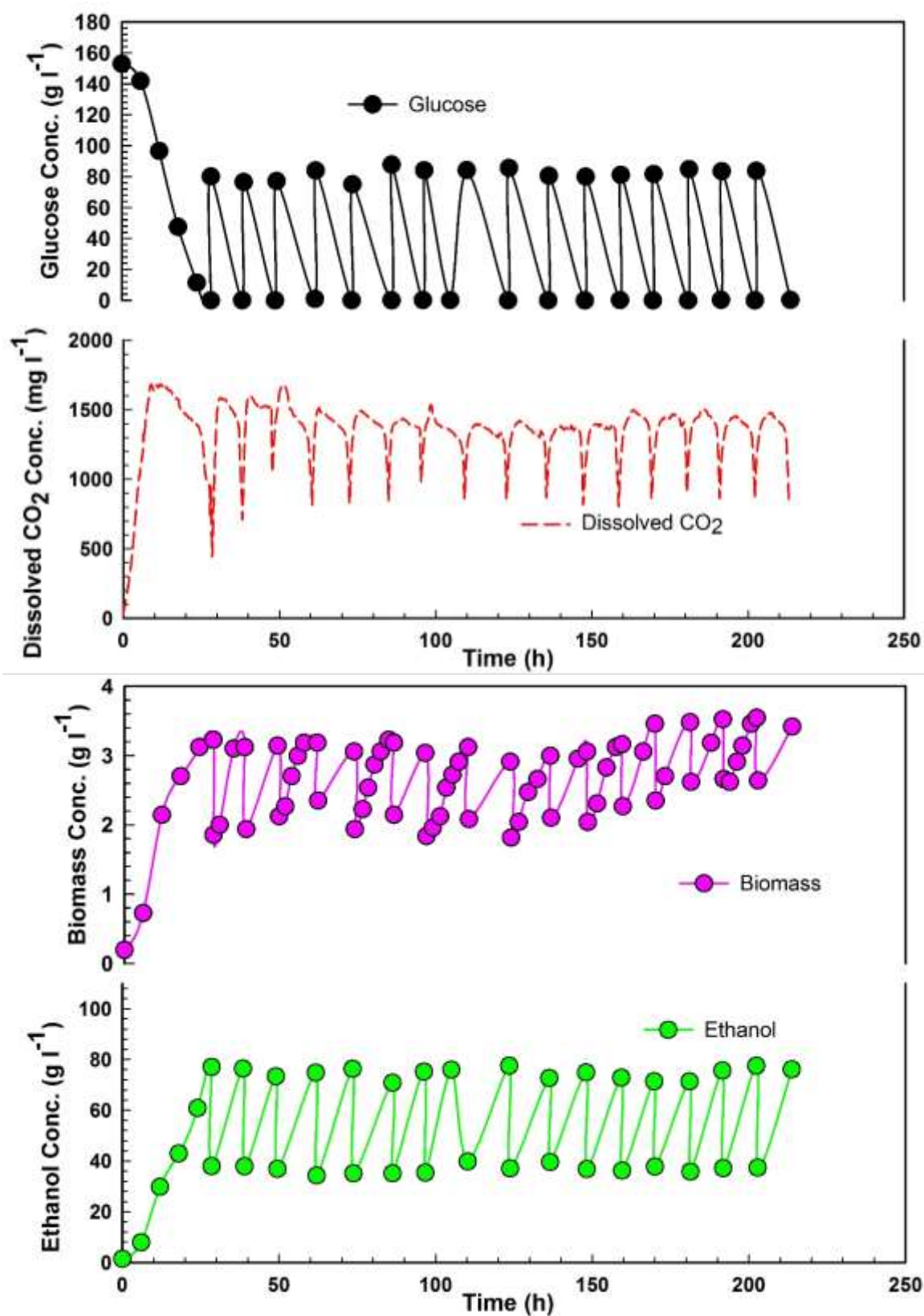


Figure A1.1 Raw data of $\sim 150 \text{ g glucose l}^{-1}$ feeding concentration in the absence of DCO_2 control by using independent feeding method

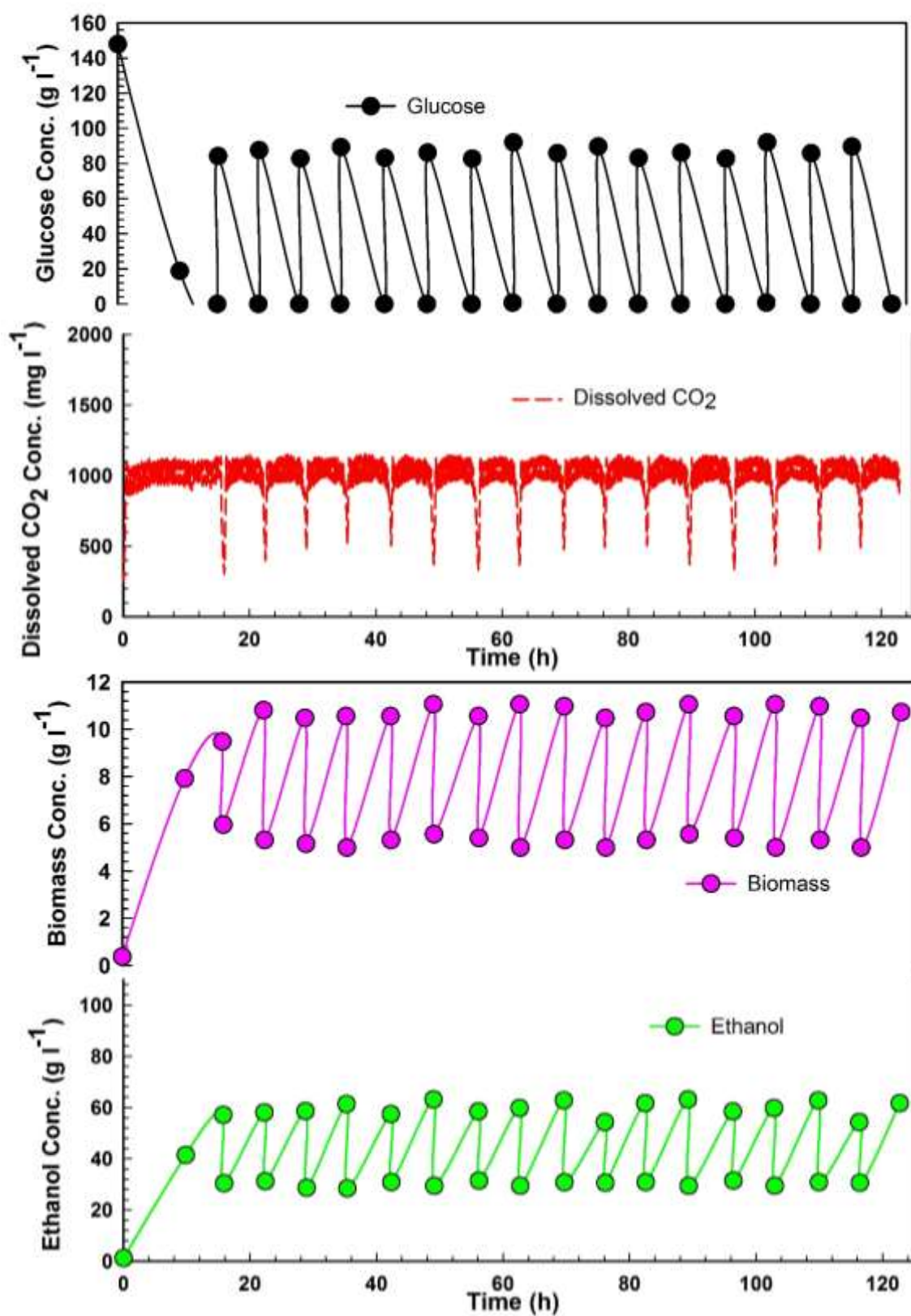


Figure A1.2 Raw data of $\sim 150 \text{ g glucose l}^{-1}$ feeding concentration DCO_2 control at 1000 mg l^{-1} level by using independent feeding method

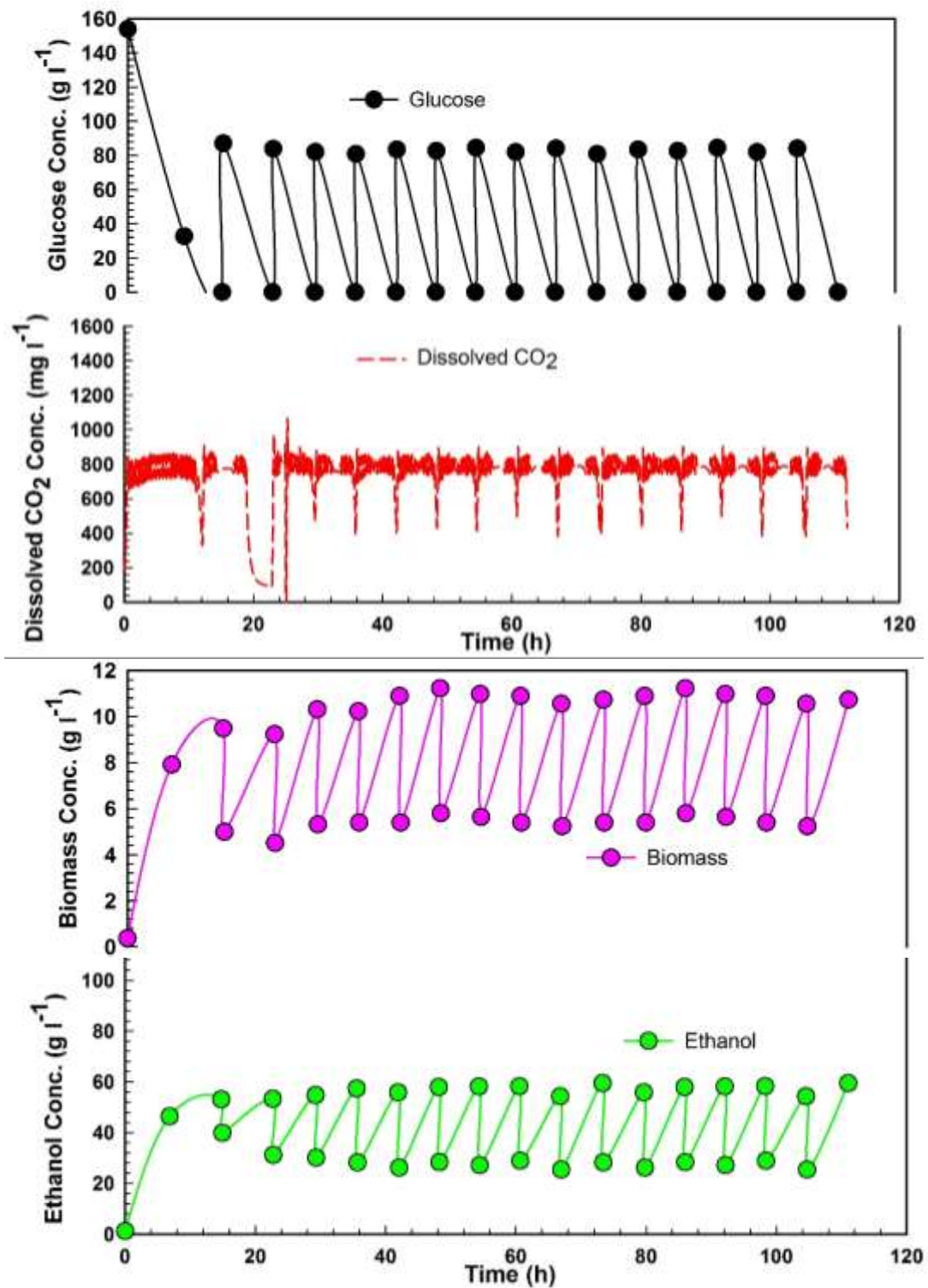


Figure A1.3 Raw data of $\sim 150 \text{ g glucose l}^{-1}$ feeding concentration DCO_2 control at 750 mg l^{-1} level by using independent feeding method

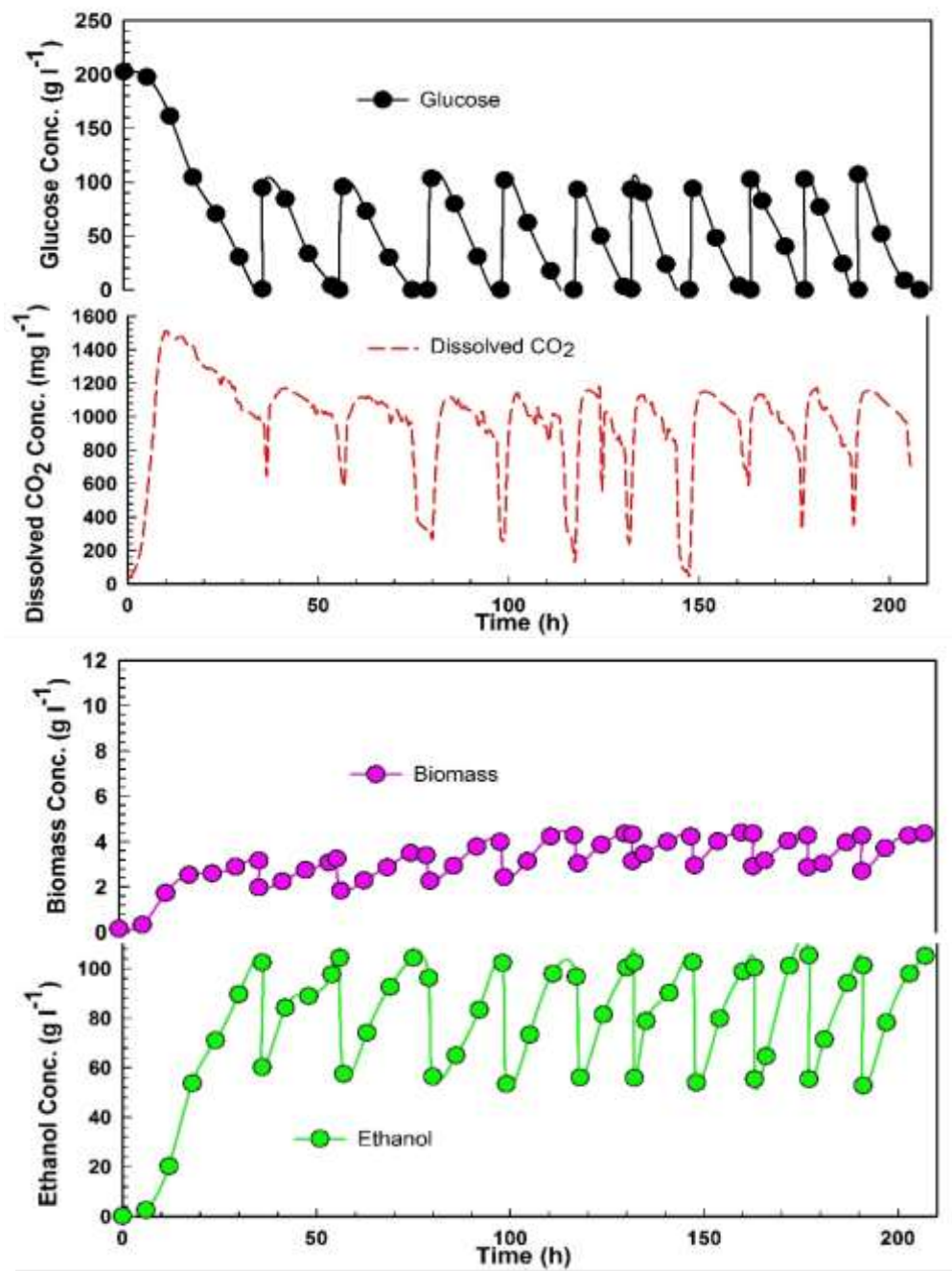


Figure A1.4 Raw data of ~200 g glucose l⁻¹ feeding concentration in the absence of DCO₂ control by using independent feeding method

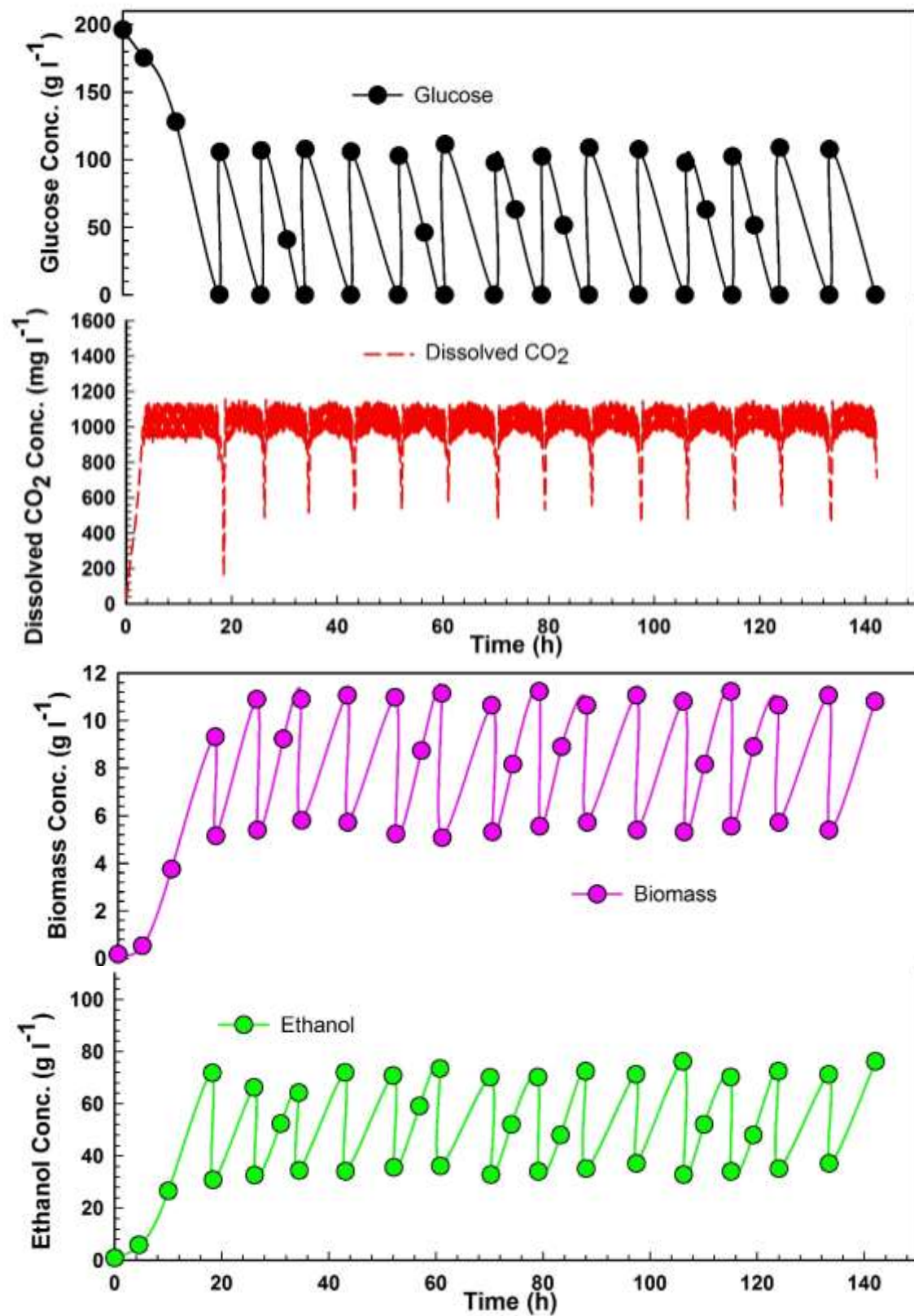


Figure A1.5 Raw data of $\sim 200 \text{ g glucose l}^{-1}$ feeding concentration DCO_2 control at 1000 mg l^{-1} level by using independent feeding method

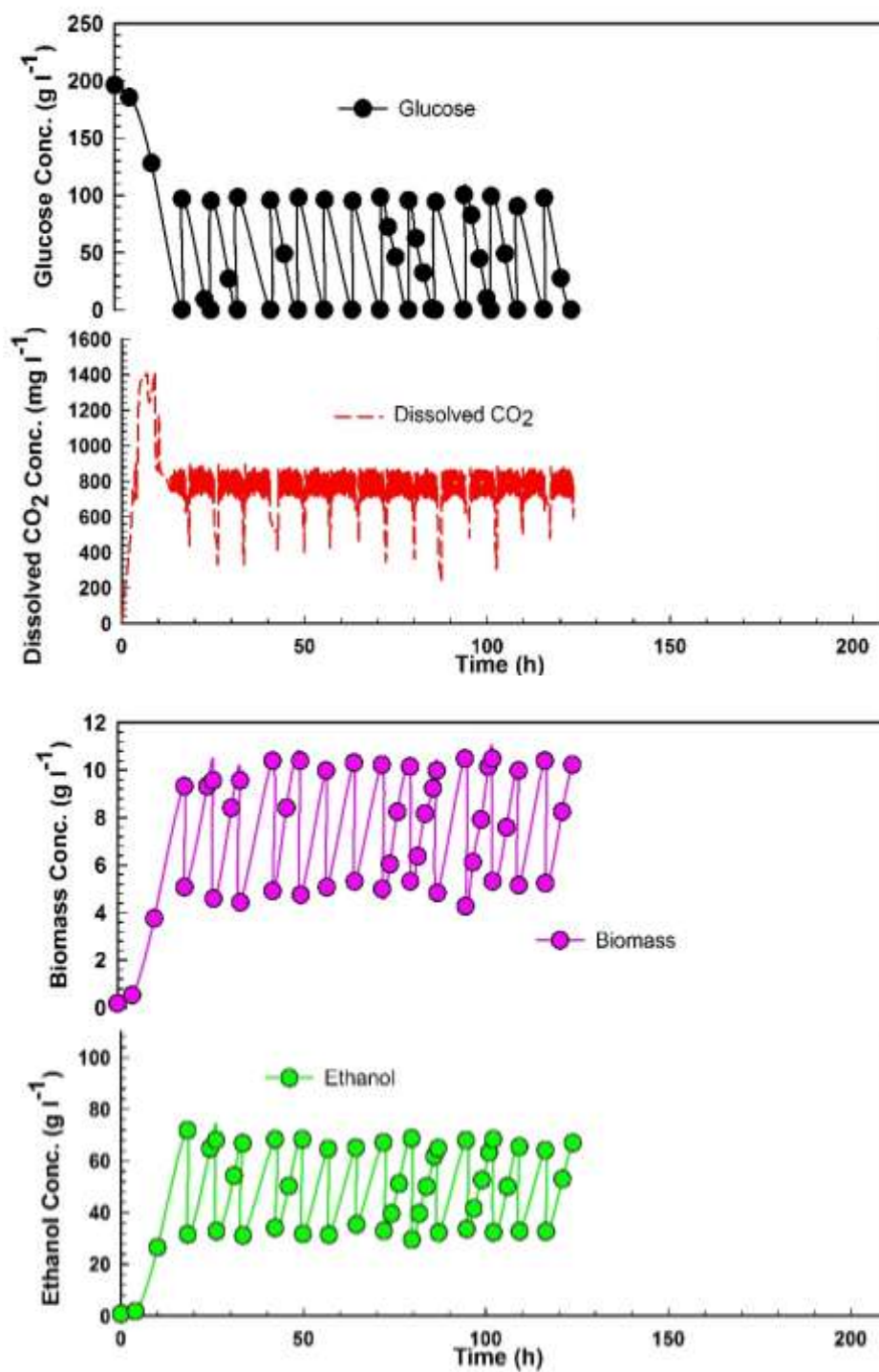


Figure A1.6 Raw data of $\sim 200 \text{ g glucose l}^{-1}$ feeding concentration DCO_2 control at 750 mg l^{-1} level by using independent feeding method

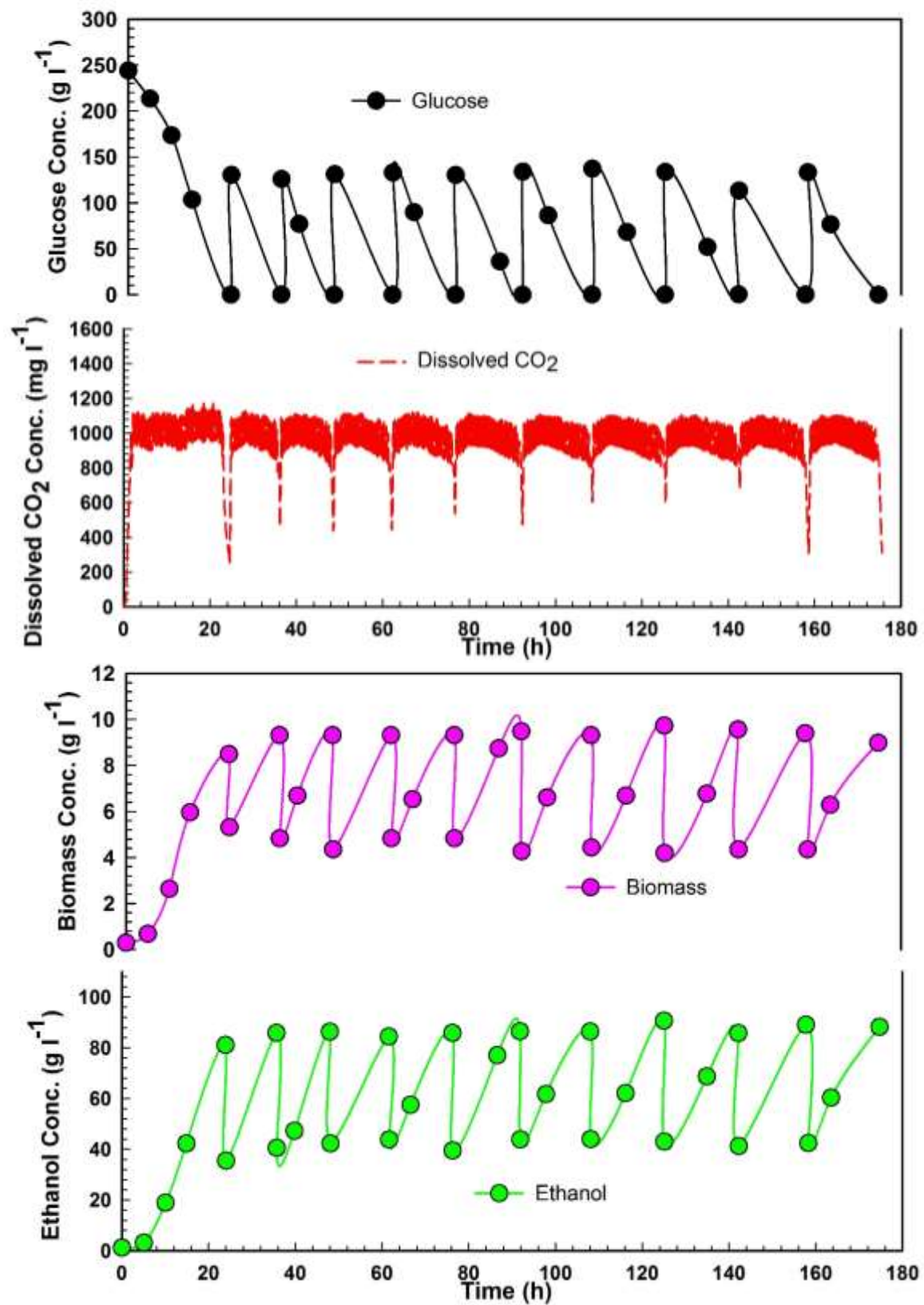


Figure A1.7 Raw data of $\sim 250 \text{ g glucose l}^{-1}$ feeding concentration DCO_2 control at 1000 mg l^{-1} level by using independent feeding method

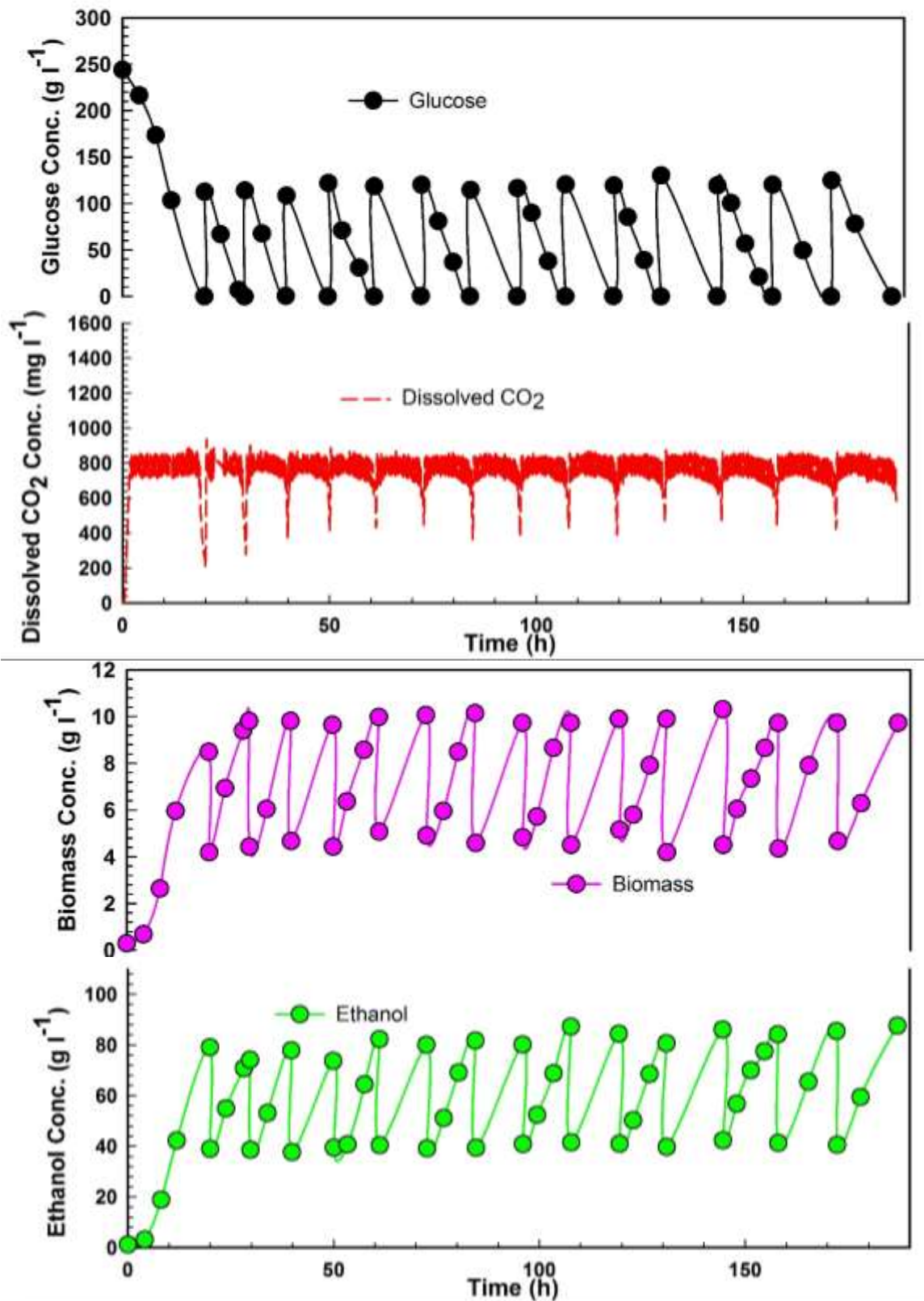


Figure A1.8 Raw data of ~250 g glucose l⁻¹ feeding concentration DCO₂ control at 750 mg l⁻¹ level by using independent feeding method

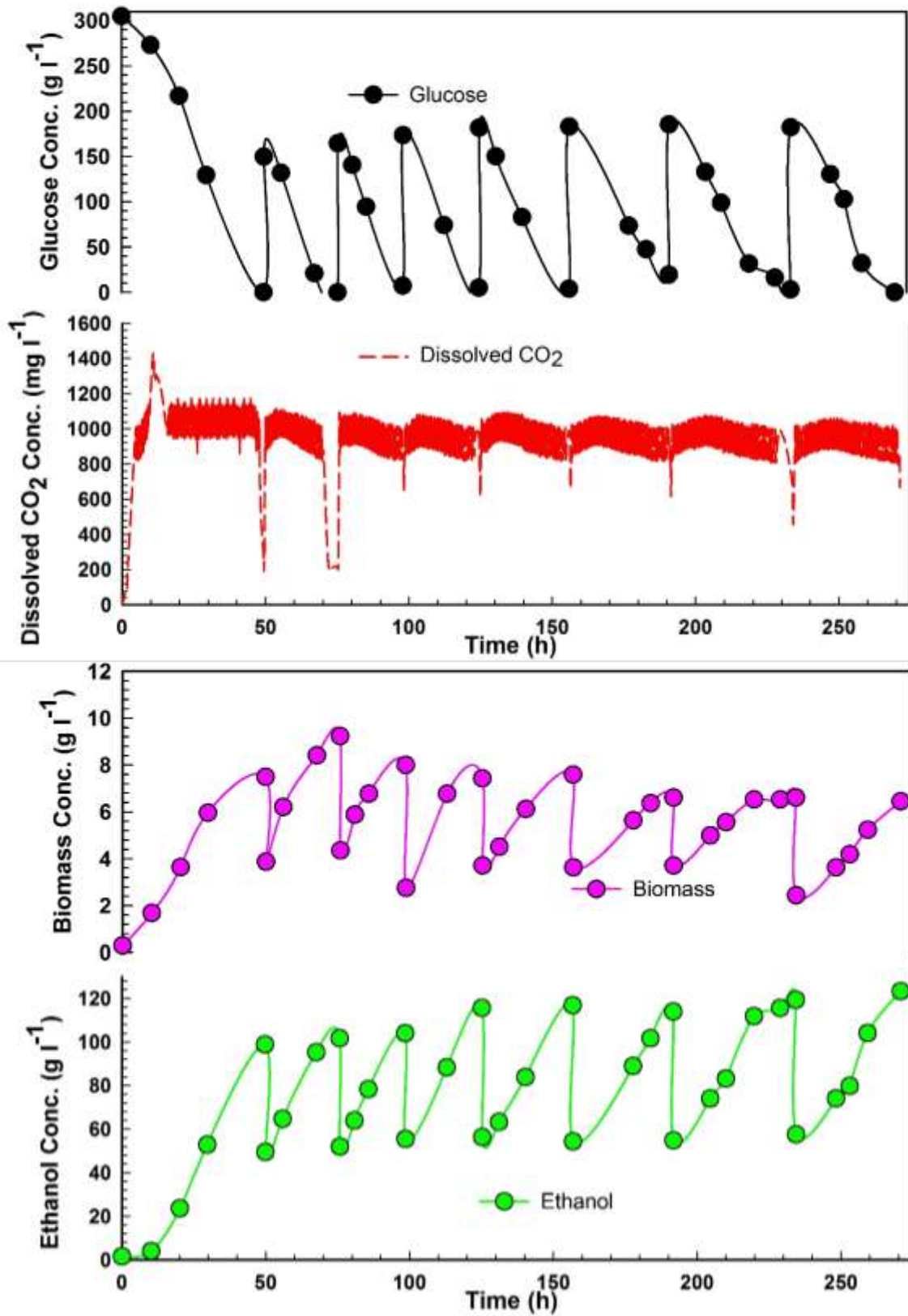


Figure A1.9 Raw data of ~300 g glucose l⁻¹ feeding concentration DCO₂ control at 1000 mg l⁻¹ level by using independent feeding method

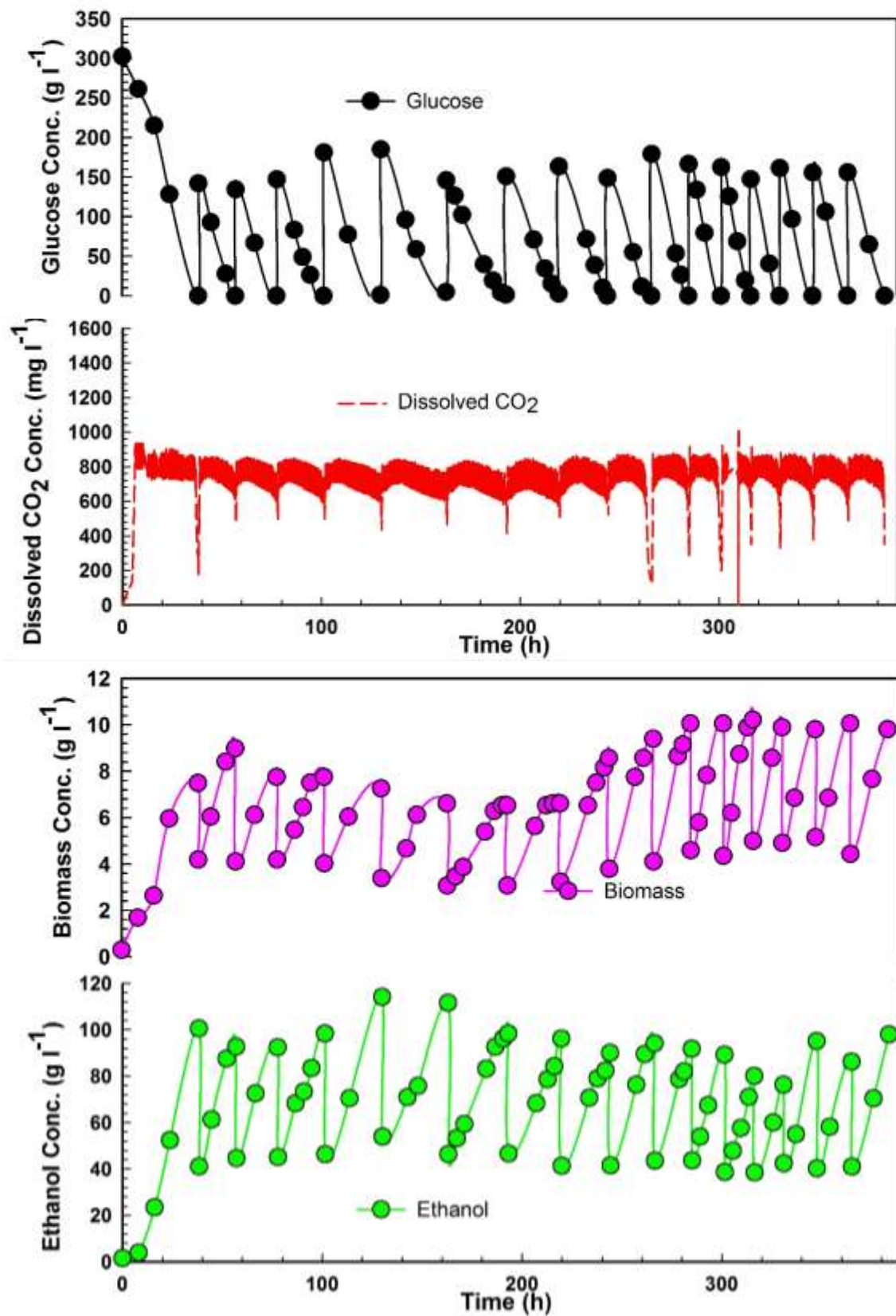


Figure A1.10 Raw data of $\sim 300 \text{ g glucose l}^{-1}$ feeding concentration DCO_2 control at 750 mg l^{-1} level by using independent feeding method

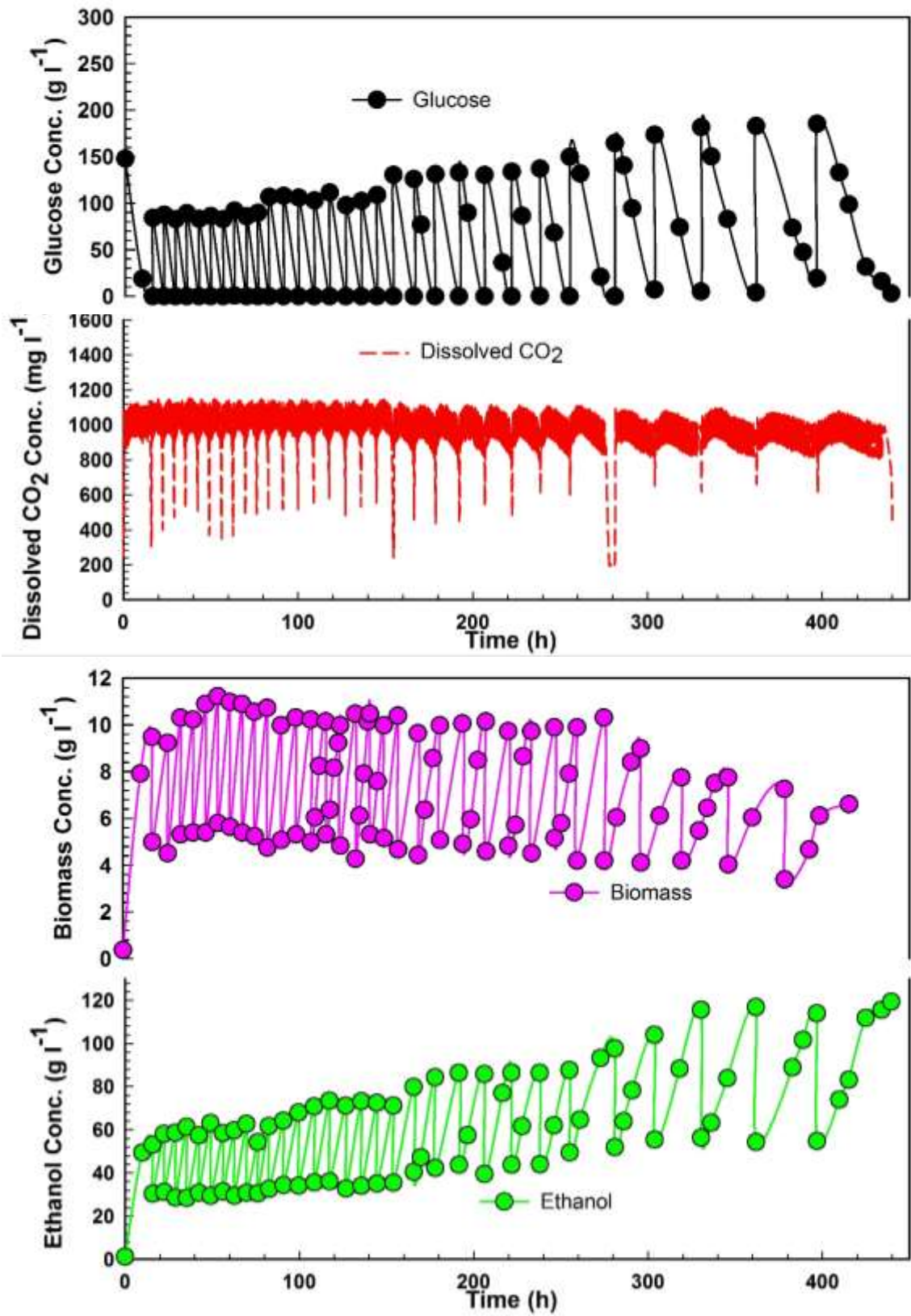


Figure A1.11 Raw data of DCO_2 control at 1000 mg l^{-1} level by using continuous feeding method

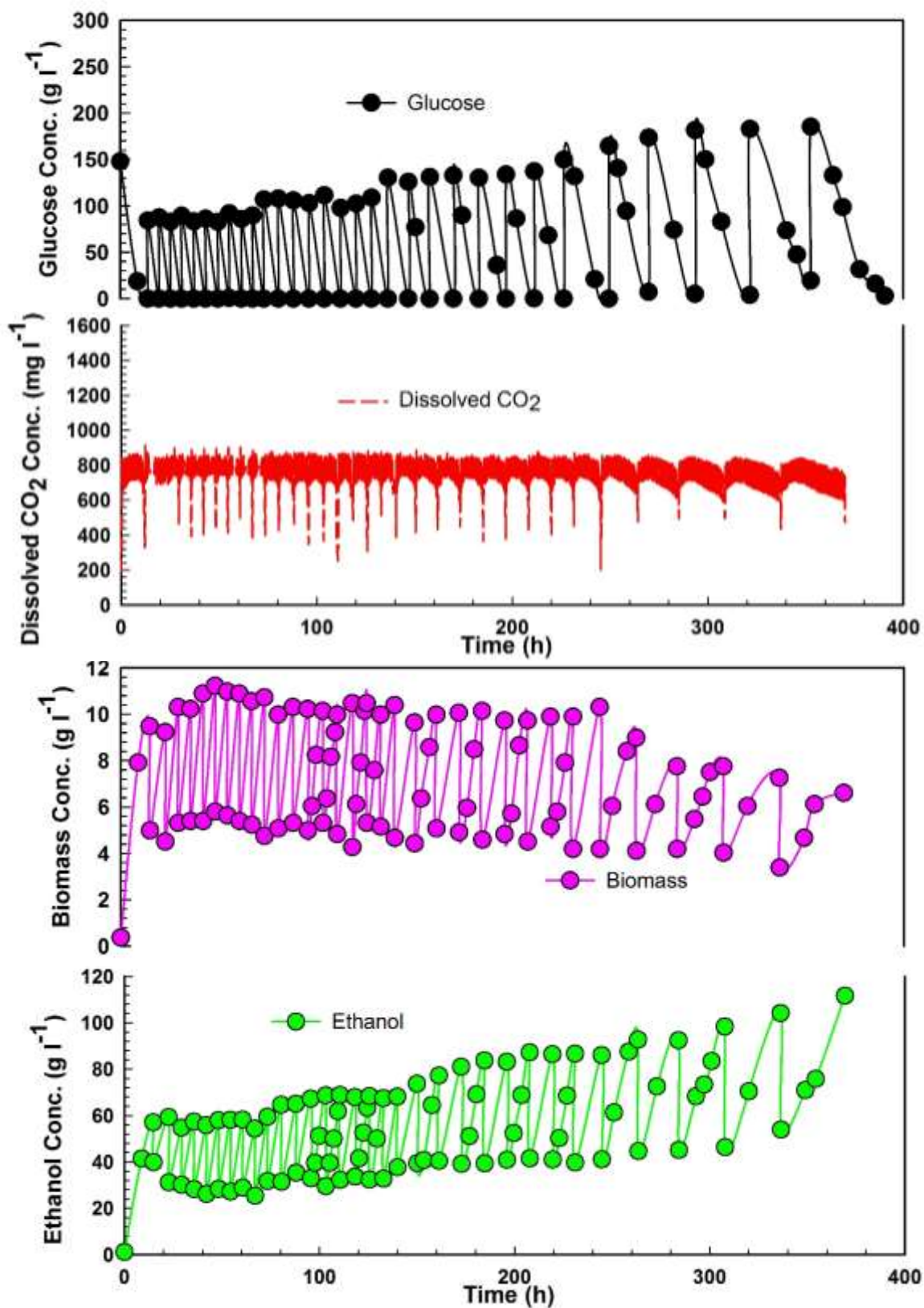


Figure A1.12 Raw data of DCO_2 control at 750 mg l^{-1} level by using continuous feeding method

A2-Calibration curves

The calibration curve of biomass was established using colorimeter (as shown in Subsection 3.5.2) and shown in Figure A2.1. This calibration figure described the relationship between OD (a°) and concentration ($g\ l^{-1}$), and its corresponding equation and regression coefficient was also shown in the figure.

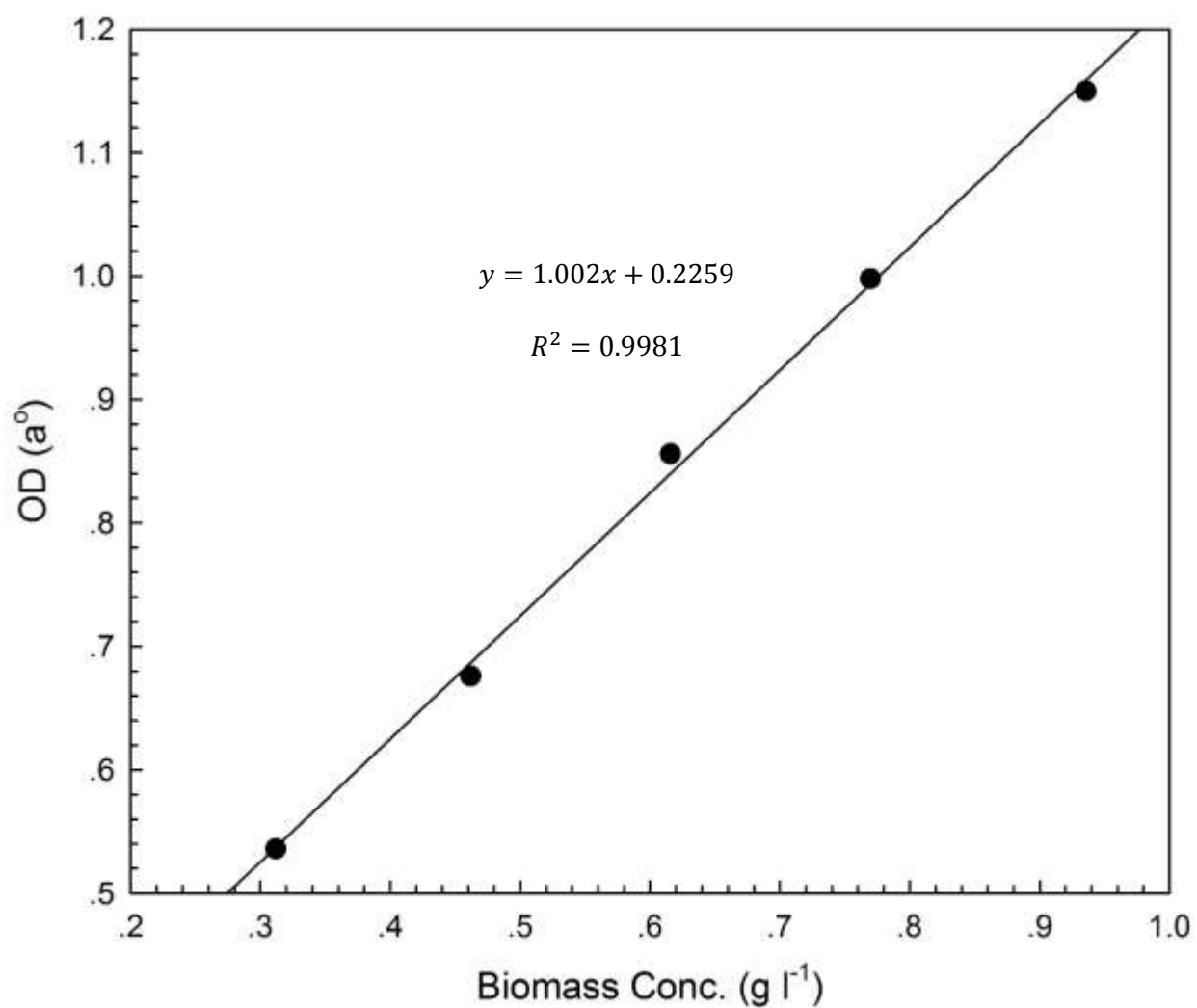


Figure A2.13 Calibration curve for biomass

The calibration curves of glucose, ethanol and glycerol were established using HPLC (as shown in Subsection 3.5.2) and shown in Figure A2.2, A2.3 and A2.4, respectively. These three calibration figures described the relationship between area ($\mu\text{S}\cdot\text{min}$) and concentration (g l^{-1}), and their corresponding equations and regression coefficients were also shown in the figures.

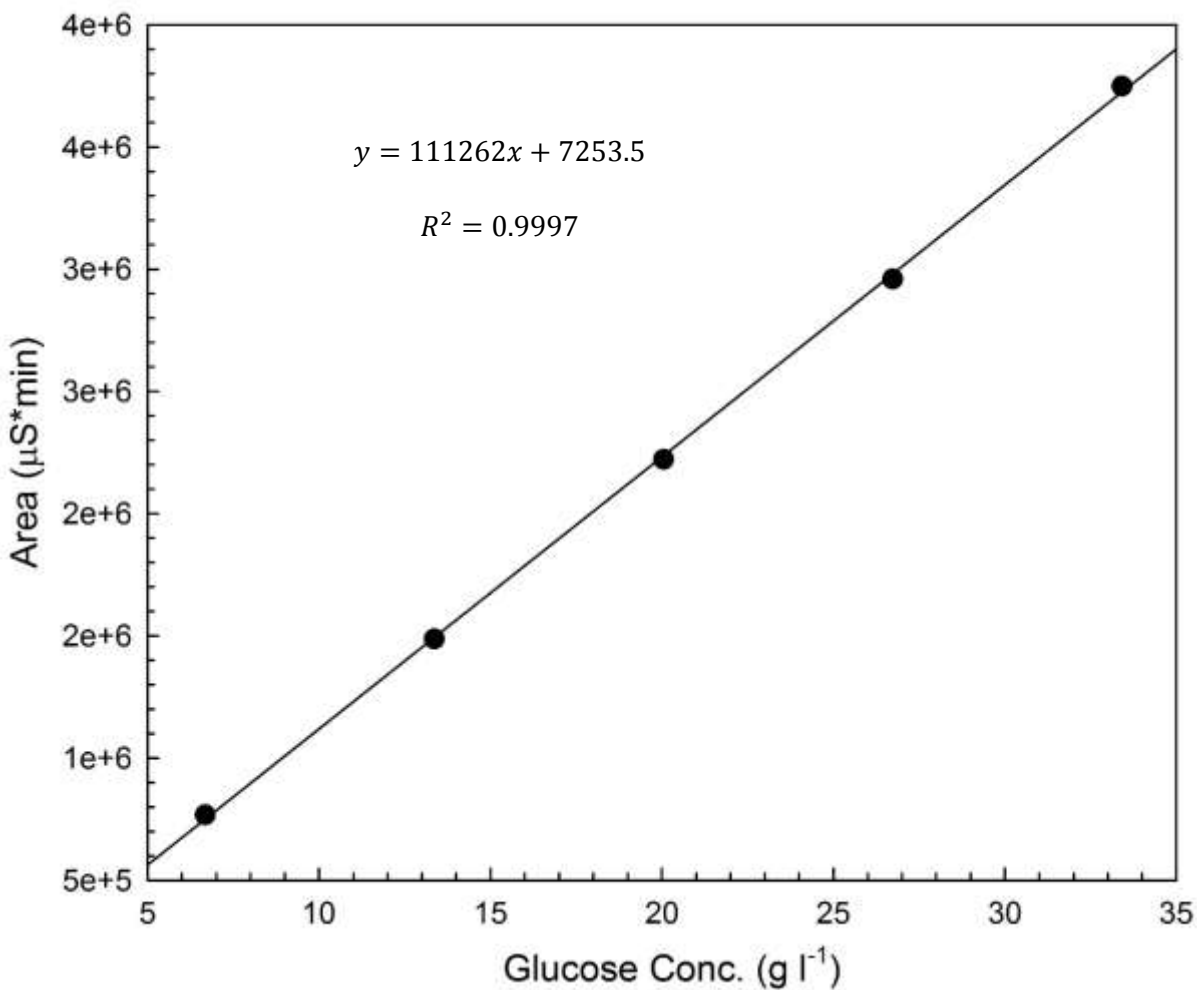


Figure A2.2 Calibration curve for glucose

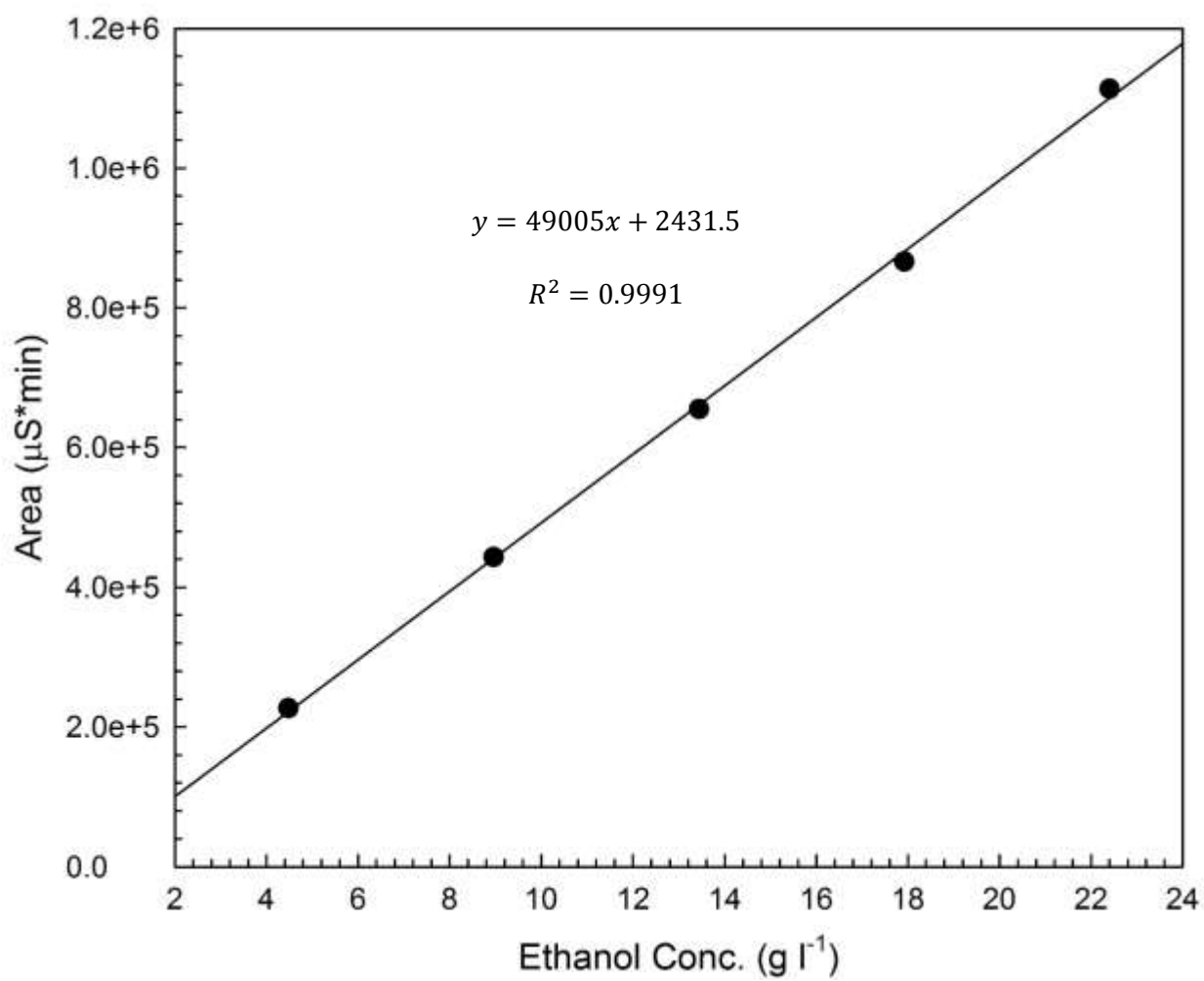


Figure A2.3 Calibration curve for ethanol

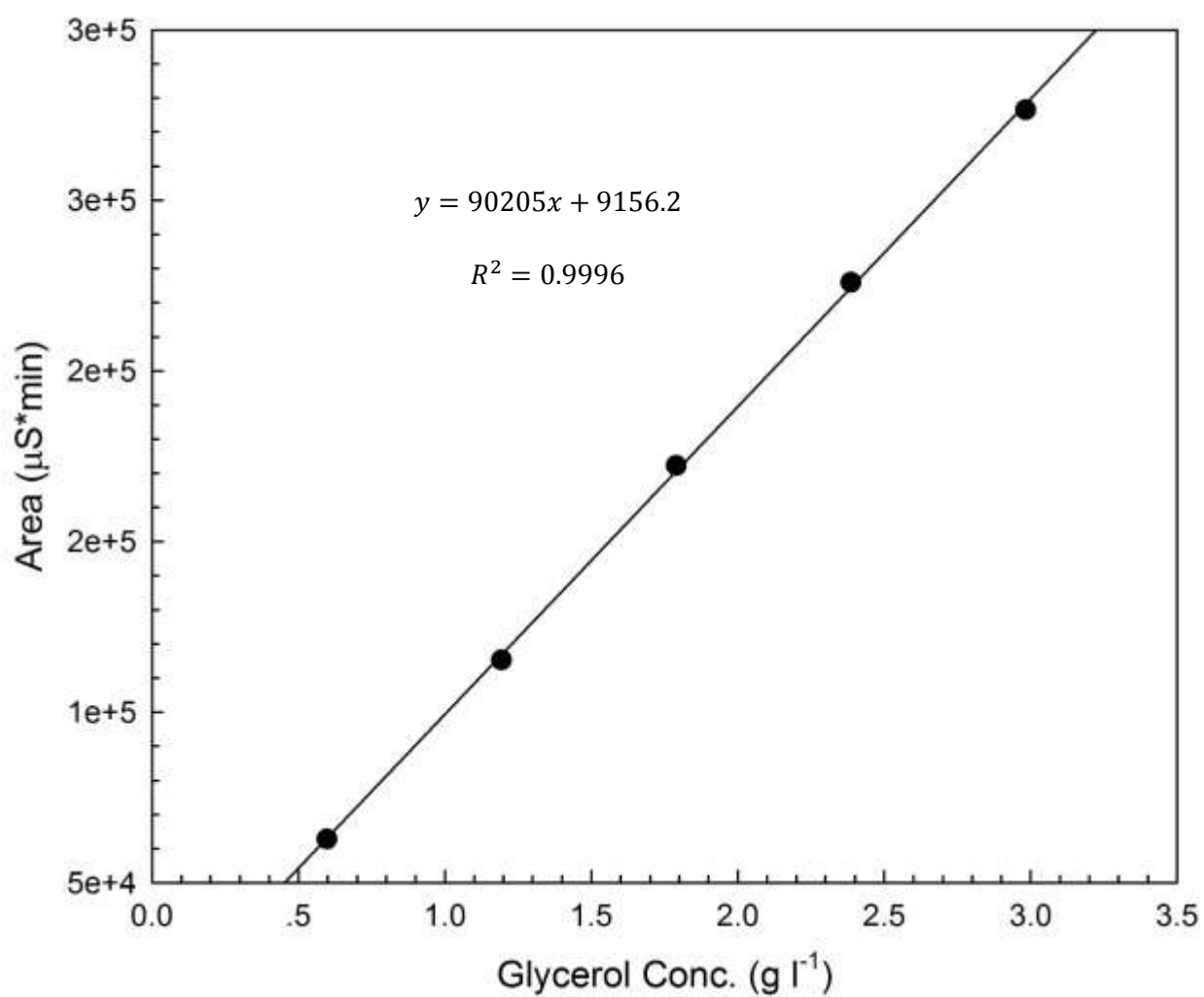


Figure A2.4 Calibration curve for glycerol

APPENDIX B

B1.1 sample calculation for Figure 4.6

Condition: with ~150 g glucose l⁻¹ feeding concentration in the absence of DCO₂ control

$$M_{tcg} = \frac{C_g}{180 \text{ g mol}^{-1}} \times 6 \times \frac{1}{T_f} = \frac{81.86}{180 \text{ g mol}^{-1}} \times 6 \times \frac{1}{11.3} = 0.241 \text{ mol h}^{-1} \text{ l}^{-1}$$

$$M_{tce} = \frac{C_e}{46 \text{ g mol}^{-1}} \times 2 \times \frac{1}{2T_f} = \frac{74.58}{46 \text{ g mol}^{-1}} \times 2 \times \frac{1}{2 \times 11.3} = 0.143 \text{ mol h}^{-1} \text{ l}^{-1}$$

$$M_{tcc} = \frac{C_e}{46 \text{ g mol}^{-1}} \times \frac{1}{2T_f} = \frac{M_{ce}}{2} = \frac{2.432}{2} = 0.0716 \text{ mol h}^{-1} \text{ l}^{-1}$$

$$M_{tcgly} = \frac{C_{gly}}{92 \text{ g mol}^{-1}} \times 3 \times \frac{1}{2T_f} = \frac{4.55}{92 \text{ g mol}^{-1}} \times 3 \times \frac{1}{2 \times 11.3} = 0.00984 \text{ mol h}^{-1} \text{ l}^{-1}$$

$$M_{tcb} = \frac{C_{cb}}{27.6 \text{ g mol}^{-1}} \times \frac{1}{2T_f} = \frac{3.2}{27.6 \text{ g mol}^{-1}} \times \frac{1}{2 \times 11.3} = 0.0105 \text{ mol h}^{-1} \text{ l}^{-1}$$

$$M_{tco} = M_{tcg} - M_{tce} - M_{tcc} - M_{tcgly} - M_{tcb} = 0.241 - 0.143 - 0.0716 - 0.00984 = 0.006 \text{ mol h}^{-1} \text{ l}^{-1}$$

$$\%M_{tce} = \frac{M_{tce}}{M_{tcg}} = \frac{0.143}{0.241} = 0.5941 = 59.4\%$$

$$\%M_{tcc} = \frac{M_{tcc}}{M_{tcg}} = \frac{0.0716}{0.241} = 0.2971 = 29.7\%$$

$$\%M_{tcgly} = \frac{M_{tcgly}}{M_{tcg}} = \frac{0.00984}{0.241} = 0.0273 = 4.1\%$$

$$\%M_{tcb} = \frac{M_{tcb}}{M_{tcg}} = \frac{0.0105}{0.241} = 0.0815 = 4.3\%$$

$$\%M_{tco} = \frac{M_{tco}}{M_{tcg}} = \frac{0.006}{0.241} = 0.0248 = 2.5\%$$

B1.2 sample calculation for Table 4.3

Condition: $C_e = 30 \text{ g l}^{-1}$

$$T_{sf1} = e^{0.0317 \times C_e} = e^{0.0317 \times 30} = 2.59 (h)$$

$$T_{sf2} = 1.304 \times e^{0.0274 \times C_e} = 1.304 \times e^{0.0274 \times 30} = 2.97(h)$$

$$\text{Difference} = \frac{|T_{sf1} - T_{sf2}|}{\max(T_{sf1}, T_{sf2})} = \frac{|2.59 - 2.97|}{2.97} = 0.1275 = 12.75\%$$

B1.3 Sample calculation for Table 4.4

$$R_{Eb} = \frac{C_e}{T_f} = \frac{187.30}{130} = 1.44 \text{ (} gh^{-1}l^{-1} \text{)}$$

$$R_{ER} = \frac{C_e}{2 \times T_f} = \frac{74.6}{11.3} = 3.30 \text{ (} gh^{-1}l^{-1} \text{)}$$

B1.4 Sample calculation for Table 4.5

$$R_{Ec} = C_e \times D = 51.15 \times 0.34 = 17.39 \text{ (g h}^{-1}\text{l}^{-1}\text{)}$$

B1.5 Sample calculation for Table 4.6

Condition: ~150 g glucose l⁻¹ in the absence of DCO₂ control

$$G_c = \frac{T_w}{T_f + T_d} \times V_w \times C_g = \frac{7290}{11.3 + 2} \times 10^5 \times 89.3 = 4895 \times 10^6 g$$

$$B_p = \frac{T_w}{T_f + T_d} \times \frac{V_w}{2} \times C_b = \frac{7290}{11.3 + 2} \times \frac{10^5}{2} \times 3.2 = 2221 \times 10^6 g$$

$$E_p = \frac{T_w}{T_f + T_d} \times \frac{V_w}{2} \times C_e = \frac{7290}{11.3 + 2} \times \frac{10^5}{2} \times 74.6 = 96 \times 10^6 g$$